Abstract Book

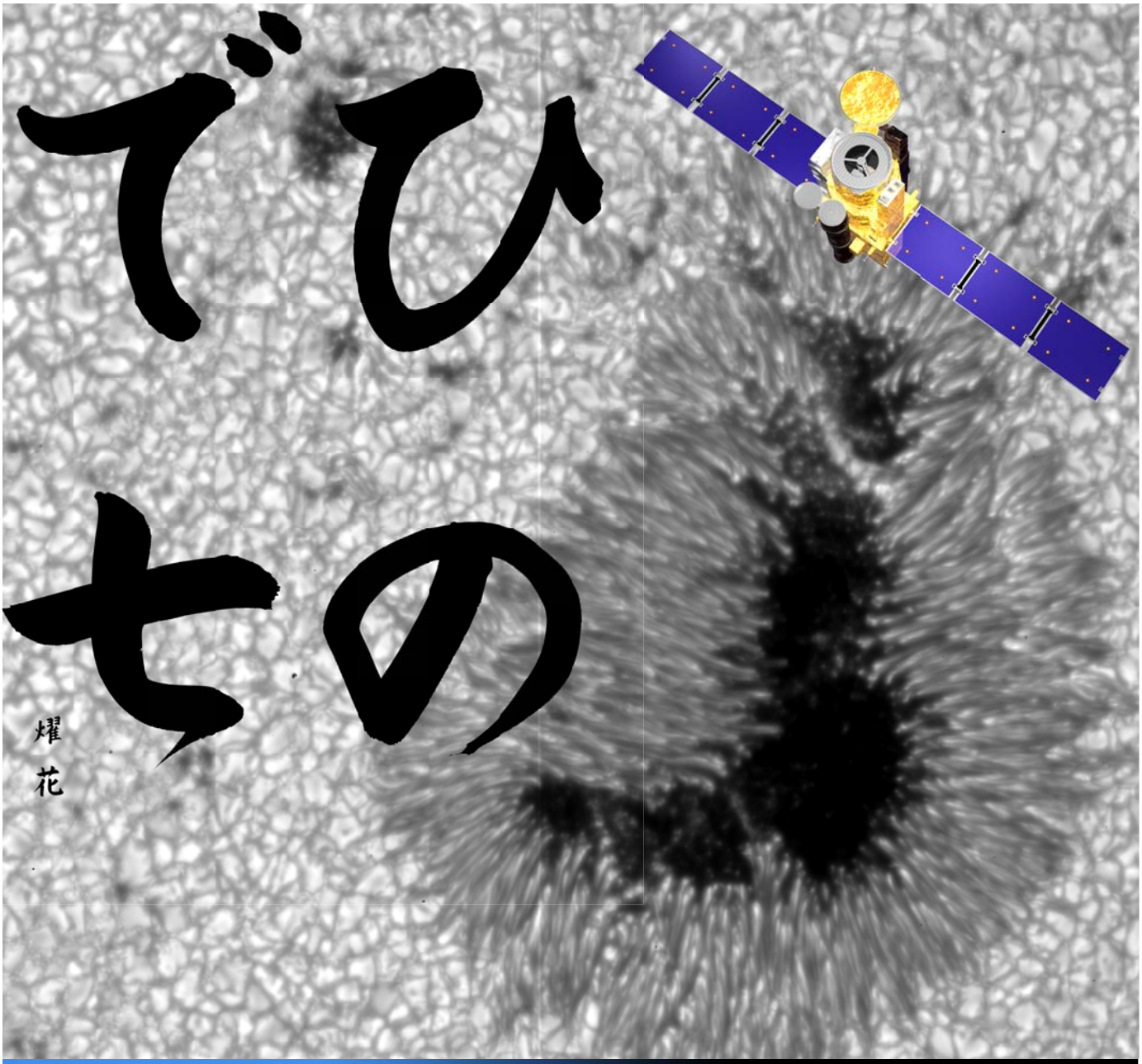

The 3rd NAOJ symposium

The Seventh Hinode Science Meeting

Takayama Japan

12-15 November 2013

http://www.kwasan.kyoto-u.ac.jp/hinode-7/

THE 3RD NAOJ SYMPOSIUM

THE SEVENTH HINODE SCIENCE MEETING (HINODE-7)

TAKAYAMA JAPAN, 12-15 NOVEMBER 2013

Scientific Organizing Committee

K. Shibata (chair), K. Kusano (co-chair), G. Aulanier, T. Berger, J. Chae, L. Green, H. Hara, H. Isobe, D. Longcope, T. Sakao, J. Schmelz, H. Socas-Navarro, Y. Yan

Local Organizing Committee

K. Ichimoto, S. Nagata, A. Asai, M. Hagino, A. Hillier, T. T. Ishii, T. Kawate, K. Nishida, D. Nogami, A. Oi, S. Ueno, T. Sakurai, T. Watanabe, T. Shimizu, S. Masuda, S. Nozawa, T. Yokoyama

Supporting Staff

G. Kimura, Y. Nakatani, M. Katoda, N. Kaneda, S. Shirakawa

Jointly hosted by

Kwasan and Hida Observatories, Kyoto University

National Astronomical Observatory of Japan

Japan Aerospace Exploration Agency

Sponsored by

The meeting is partially supported by the JSPS Core-to-Core Program 22001 "Center for Magnetic Self-Organization in Laboratory and Astrophysical Plasmas (CMSO)" as the Eighth CMSO Seminar.

Takayama City

Gifu Prefecture

主催：京都大学理学研究科附属天文台、自然科学研究機構国立天文台
共催：宇宙航空研究開発機構宇宙科学研究所
後援：高山市（コンベンション開催支援補助金）、
岐阜県（イベント・コンベンション誘致推進事業費補助金）

Hinode is a Japanese mission developed and launched by ISAS/JAXA, with NAOJ as domestic partner and NASA and STFC (UK) as international partners. It is operated by these agencies in co-operation with ESA and NSC (Norway).

Table of Contents

Overview

	10 Nov (Sun)	11 Nov (Mon)	12 Nov (Tue)	13 Nov (Wed)	14 Nov (Thu)	15 Nov (Fri)	16 Nov (Sat)	
9:30								
9:45			Registration	S2-I-02	S4-C-03	**(Session 7)**		
10:00					S4-C-04	S7-I-01		
				S2-I-03	S4-C-05	S7-I-02		
10:30			Opening		S4-C-06			
			(Session 1)	S2-C-04	S4-I-02	S7-C-01		
11:00			S1-I-01	S2-C-05		S7-C-02		
			S1-C-01	**(Session 3)**	S4-C-07	S7-C-03		
11:30			S1-I-02	S3-I-01	S4-C-08	Summary (Prof. Priest)		
				S3-C-01	S4-C-09			
12:00			lunch	lunch	lunch	lunch		
13:15			S1-C-02	S3-C-02	S4-I-03		CLASP meeting (closed)	Takayama Public event
	SWG meeting (closed)	Solar-C meeting	S1-C-03	S3-C-03				
13:45			S1-I-03	S3-C-04	S4-C10			
				S3-I-02	S4-C11			
14:15			S1-C-04		S4-C12			
14:30			S1-C-05	S3-C-05	coffee & poster			
14:45			S1-C-06	S3-C-06				
15:00			coffee & poster	coffee & poster	**(Session 5)** S5-I-01	Excursion (13:00-)		
16:00			S1-C-07	S3-C-07	S5-C-01			
			S1-C-08	S3-C-08	S5-C-02			
16:30			S1-C-09	S3-C-09	S5-C-03			
			(Session 2)	S3-C-10	**(Session 6)**			
17:00			S2-I-01	**(Session 4)**	S6-I-01			
			S2-C-01	S4-I-01	S6-C-01			
17:30			S2-C-02	S4-C-01	S6-C-02			
			S2-C-03	S4-C-02	S6-C-03			
18:00		Welcome reception (18:00-)		Conference dinner (19:00-)				
evening								
	10 Nov (Sun)	11 Nov (Mon)	12 Nov (Tue)	13 Nov (Wed)	14 Nov (Thu)	15 Nov (Fri)	16 Nov (Sat)	

Social Activities

☀ 11 Nov (Mon) 18:00-: Welcome reception

☀ 13 Nov (Wed) 19:00-: Conference dinner @Matsurinomori

Shuttle buses (conference venue - "Matsurinomori") are arranged. "Matsurinomori" is located within 10-minute walking distance of the conference venue (see a map).

☀ Excursion

!! Only for people who will go to KAMIOKANDE !!

You must **sign** beside your name on the list of people who will enter the mine, otherwise you will not be allowed to enter. This list will be placed near the reception desk.
Please be sure to sign the list by18:00 on the 14 Nov (Thu).
At the time you sign the list, please take a copy of the instructions for entering the mine. It is necessary for you to read these instructions before you arrive at KAMIOKANDE.
(People who will go to Hida Obs. do not have to sign any list at the reception desk.)

The participants who will go to Hida Obs will travel there by four buses and the participants who will go to KAMIOKANDE will travel there by two buses.
All the buses will leave the conference venue at 13:00 on 15 Nov (Fri), so, **please be sure to gather at conference venue bus stop by 12:50**.

On the 15 Nov (Fri), the passenger lists for each bus will be displayed at the reception desk.
Please check the list to confirm on which bus you will be riding and be sure to get on that bus.
*At Hida Obs, participants will be divided into four groups and be taken on a tour around telescopes.
*At KAMIOKANDE, participants will be divided into two groups and be taken on a tour of the facility.
All the passengers on the same bus will be treated as a single group for their respective tour.

There will be NO space to put large luggage on the buses for the excursion.
In addition, after the excursion, the buses will go directly to Takayama Station, without returning to the conference venue, where the excursion will end at around 18:00.
Therefore, participants should leave any large luggage at their hotel or in a locker at Takayama Station on the morning of 15 Nov.
!! Please do not bring large luggage to the conference venue on that day. !!

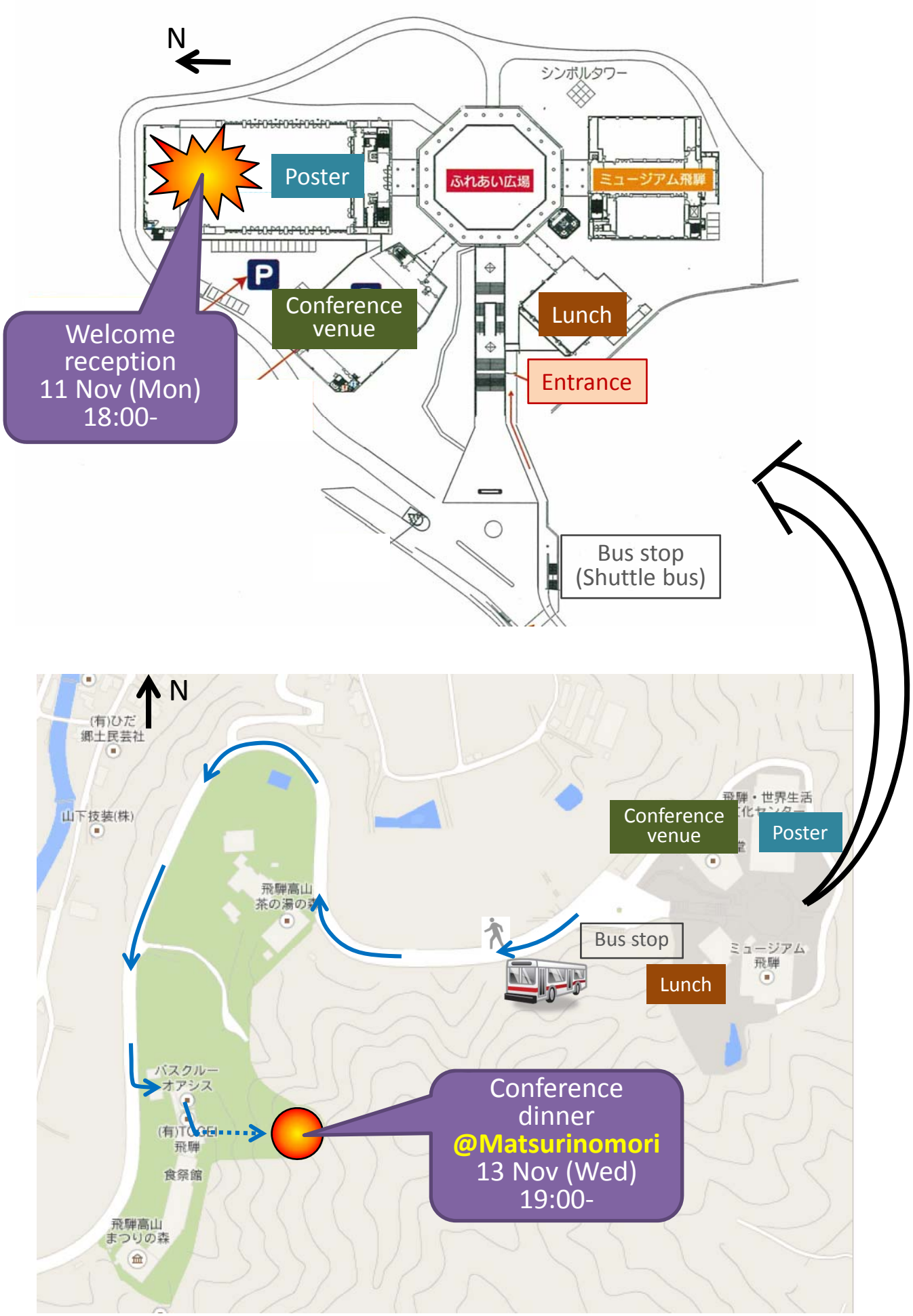
N
シンボルタワー
ふれあい広場
ミュージアム飛騨
Poster
Conference venue
Lunch
Entrance
Welcome reception
11 Nov (Mon)
18:00-
Bus stop
(Shuttle bus)
N
(有)ひだ郷土民芸社
山下技装(株)
飛騨高山茶の湯の家
Conference venue
Poster
Bus stop
Lunch
ミュージアム飛騨
バスクルーオアシス
飛騨
食祭館
飛騨高山まつりの森
Conference dinner
@Matsurinomori
13 Nov (Wed)
19:00-

Solar-C Science Meeting

11 November (Monday)

Time	Presenter	Title
		Registration
10:00-		*Opening Address*
Session 1. Solar-C mission proposal - critaical review		
10:05-	Tetsuya Watanabe (NAOJ)	*Mission Goals*
10:25-	Kiyoshi Ichimoto (Kyoto Univ)	*SUVIT*
10:45-	Taro Sakao (JAXA) / Jonathan Cirtain (NASA)	*XIT*
11:05-	Toshifumi Shimizu (JAXA)	*EUVST*
Session 2. Science impacts and implications from new observations - chromospheric - lower transition-region dynamics		
11:25-	Bart De Pontieu (LMSAL)	*IRIS*
12:05-	Jongchul Chae (Seoul Univ)	*BBSO/FIS*
		Lunch
- high res. magnetic fields		
14:00-	Achim Gandorfer (MPS)	*SUNRISE*
14:30-	C.V. Martinez-Pillet (NSO)	*ATST/EST*
- high res. TR-coronal dynamics		
15:00-	Amy R Winebarger (NASA)	*HI-C*
		Coffee
- Mg 280nm observation		
15:40-	Mats Carlsson (Oslo Univ)	*IRIS Observation*
16:00-	Yoshinori Suematsu (NAOJ)	*Technical Prospect*
16:20-		*Discussion*
Session 3. Discussion - space weather		
17:00-	Carolus J Schrijver (LMSAL)	
17:20-	Kanya Kusano (Nagoya Univ)	
17:40-		*Discussion*
18:00		***Adjournment***

Hinode-7 Meeting

12 November (Tuesday)

Chair	Time	Presenter	Title
	9:30-10:30		*Registration*
	10:30-10:45	Kazunari Shibata	*Welcoming Remarks*
		Session 1. Magnetic Fields and Solar Cycle	
T. Sakurai	10:45-11:15	Steven H. Saar Invited S1-I-01	*On Longterm Behavior of Quieter Aspects of the Sun, Quiet Stars, and Magnetic Minima*
	11:15-11:30	Luis Bellot Rubio Contributed S1-C-01	*AN OCEAN OF INCLINED MAGNETIC FIELDS IN THE VERY QUIET SUN*
	11:30-12:00	Hideyuki Hotta Invited S1-I-02	*Current status of understanding about solar global convection*
	12:00-13:15		***Lunch***
	13:15-13:30	Dibyendu Nandi Contributed S1-C-02	*Towards Solar Cycle Predictions: Recent Advances in Modelling and Observations*
	13:30-13:45	Daikou Shiota Contributed S1-C-03	*Magnetic evolution at over 70 degrees latitude during the polarity reversal*
	13:45-14:15	Hiroko Watanabe Invited S1-I-03	*Observations of fine scale structures and dynamics in sunspots*
T. Yokoyama	14:15-14:30	Ada Ortiz-Carbonell Contributed S1-C-04	*Emergence of granular-sized magnetic bubbles through the solar atmosphere.*
	14:30-14:45	Sanja Danilovic Contributed S1-C-05	*2D inversions of weak internetwork spectropolarimetric signals*
	14:45-15:00	Andreas Lagg Contributed S1-C-06	*A granular light bridge observed by Hinode: evidence for naked granules*
	15:00-16:00		***Coffee & Poster***
	16:00-16:15	David Buehler Contributed S1-C-07	*Properties of solar plage from a spatially coupled inversion of Hinode SP data*
	16:15-16:30	David Orozco Suarez Contributed S1-C-08	*Determining the magnetic field vector in quiescent prominence threads*
	16:30-16:45	Yukio Katsukawa Contributed S1-C-09	*Implication of the magnetic power spectra derived with the Hinode SP*
		Session 2. Atmospheric and Interior Couplings	
H. Hara	16:45-17:15	Alan M. Title Invited S2-I-01	*Overview of IRIS First Observations*
	17:15-17:30	Ted Tarbell Contributed S2-C-01	*First Results from Coordinated Observing with IRIS, Hinode, and Ground-Based Observatories*
	17:30-17:45	Andrew S. Hillier Contributed S2-C-02	*Determination of Prominence Plasma β from the Dynamics of Rising Plumes*
	17:45-18:00	Elena Dzifcakova Contributed S2-C-03	*Effect of Kappa-distributions on the Temperature Structure of the Prominence-Corona Transition Region*

13 November (Wednesday)

Chair	Time	Presenter	Title
	Session 2. Atmospheric and Interior Couplings		
H. Isobe	9:45-10:15	Shin Toriumi Invited S2-I-02	*Observations and Modelings of the Solar Flux Emergence*
	10:15-10:45	Etienne Pariat Invited S2-I-03	*Chromospheric and coronal jets: triggering and driving processes*
	10:45-11:00	Irina N. Kitiashvili Contributed S2-C-04	*Small-Scale Plasma Eruptions Driven by Magnetic Vortex Tubes*
	11:00-11:15	Mark Cheung Contributed S2-C-05	*Observations of Recurrent Coronal Jets by IRIS, Hinode and SDO*
	Session 3. Coronal Heating and Solar Wind Acceleration		
	11:15-11:45	Harry P. Warren Invited S3-I-01	*The Observation and Modeling of Active Region Emission: Constraints from Hinode*
	11:45-12:00	Philippe A. Bourdin Contributed S3-C-01	*Coronal loops above an active region - observation versus model*
	12:00-13:15		***Lunch***
T. Sakao	13:15-13:30	Vasyl Yurchyshyn Contributed S3-C-02	*High-Resolution Observations of Chromospheric Activity Associated with Small-Scale Emerging Flux in near Sunspot Regions*
	13:30-13:45	Shinsuke Takasao Contributed S3-C-03	*Relation among low atmospheric reconnection, shock formation and chromospheric jets*
	13:45-14:00	Tiago M. D. Pereira Contributed S3-C-04	*An IRIS look at spicules*
	14:00-14:30	Ineke De Moortel Invited S3-I-02	*Recent advances in theory and modelling of coronal wave heating*
	14:30-14:45	Jiansen He Contributed S3-C-05	*Quasi-periodic slow waves and intermittent high-speed outflows unified in a kinetic scenario*
	14:45-15:00	Paola Testa Contributed S3-C-06	*Observing coronal nanoflares in active region moss, with Hi-C and IRIS*
	15:00-16:00		***Coffee & Poster***
Y. Yan	16:00-16:15	Viggo H. Hansteen Contributed S3-C-07	*IRIS observations of transition region unresolved fine structure*
	16:15-16:30	Peter R. Young Contributed S3-C-08	*Dark jets in coronal holes*
	16:30-16:45	Valentyna Abramenko Contributed S3-C-09	*Characteristic Length of Energy-containing Structures at the Base of a Coronal Hole*
	16:45-17:00	Hwanhee Lee Contributed S3-C10	*Magnetic configurations responsible for the coronal heating and the solar wind*
	Session 4. Flares and Coronal Mass Ejections		
	17:00-17:30	Helen E. Mason Invited S4-I-01	*The Evolution of Small Solar Flares Observed with Hinode and SDO (AIA and EVE)*
	17:30-17:45	Sabrina L. Savage Contributed S4-C-01	*Coordinated observations of X-ray and high-resolution EUV active region dynamics*
	17:45-18:00	Louise Harra Contributed S4-C-02	*The location of non-thermal velocity in the early phases of large flares - revealing pre-eruption flux ropes*

14 November (Thursday)

Chair	Time	Presenter	Title
	Session 4. Flares and Coronal Mass Ejections		
G. Aulanier	9:45-10:00	Edward E. DeLuca Contributed S4-C-03	*An MHD Model of a Solar Eruption Starting from NLFFF Initial Conditions*
	10:00-10:15	Miho Janvier Contributed S4-C-04	*Evolution of electric currents and their connection with the 2011 February 15 X-class flare ribbons*
	10:15-10:30	Toshifumi Shimizu Contributed S4-C-05	*High speed photospheric flows observed around polarity inversion lines of a delta-type sunspot*
	10:30-10:45	Hyungmin Park Contributed S4-C-06	*A solar flare observed by Fast Imaging Solar Spectrograph*
	10:45-11:15	Naoto Nishizuka Invited S4-I-02	*Nonlinear Fragmentation of Flare Current Sheets*
	11:15-11:30	David E. McKenzie Contributed S4-C-07	*Spatially Resolved Measurements of Turbulence in the Flare Reconnection Region*
	11:30-11:45	Hirohisa Hara Contributed S4-C-08	*Spectroscopy at the Site of Magnetic Reconnection in the X-class Solar Flare on 2013 May 15*
	11:45-12:00	Kathy Reeves Contributed S4-C-09	*Thermal Structure of Supra-arcade Downflows and Flare Plasma Sheets*
	12:00-13:15		***Lunch***
K. Shibata	13:15-13:45	Jun Lin Invited S4-I-03	*Review on Current Sheets in CME development*
	13:45-14:00	David R. Williams Contributed S4-C10	*The topology of supersonic outflows in a filament eruption*
	14:00-14:15	David Long Contributed S4-C11	*Measuring the Magnetic Field Strength of the Quiet Solar Corona Using "EIT Waves"*
	14:15-14:30	Shin-nosuke Ishikawa Contributed S4-C12	*High-sensitivity hard X-ray solar observation with the FOXSI rocket*
	14:30-15:30		***Coffee & Poster***
K. Kusano	**Session 5. Space Weather and Space Climate**		
	15:30-16:00	Karel Schrijver Invited S5-I-01	*Upper limit for solar flare energies*
	16:00-16:15	J. L. Culhane Contributed S5-C-01	*Active Region Upflow Plasma: Does it Reach the near-Earth Environment?*
	16:15-16:30	Bruce T. Tsurutani Contributed S5-C2	*Extreme Interplanetary Shocks/Coronal Mass Ejections and Consequences for the Magnetosphere and Earth*
	16:30-16:45	Fusa Miyake Contributed S5-C3	*Rapid events in the carbon-14 content of tree-rings*
	Session 6. Solar-Stellar Connection		
	16:45-17:15	Hiroyuki Maehara Invited S6-I-01	*Superflares on solar-type stars*
	17:15-17:30	Allan Sacha Brun Contributed S6-C-01	*Convection and Dynamo Action in Solar-like stars*
	17:30-17:45	Petr Heinzel Contributed S6-C-02	*Hinode helps us to understand the nature of stellar flares*
	17:45-18:00	Takeru K. Suzuki Contributed S6-C-03	*Saturation of Stellar Winds from Young Suns*

15 November (Friday)

Chair	Time	Presenter	Title
	Session 7. Future Problems and Observations		
Y. Suematsu	9:45-10:15	Br T. Welsch Invited S7-I-01	*A New Analysis of Photospheric Fields and Flows*
	10:15-10:45	Valentin Martinez-Pillet Invited S7-I-02	*On the need of high-res/small-FOV vs. large-FOV magnetograms*
	10:45-11:00	David H. Brooks Contributed S7-C-01	*Resolving Loops in the Solar Corona: Lessons from EIS, AIA, and Hi-C.*
	11:10-11:15	Ryohko Ishikawa Contributed S7-C-02	*New diagnostic tool for magnetic fields in low- β plasma: CLASP*
	11:15-11:30	Alexander Kosovichev Contributed S7-C-03	*First Results of Coordinated Observations from Hinode, IRIS and New Solar Telescope*
	11:30-12:00	Eric R. Priest	*Conference Summary*
	12:00-12:10	Kiyoshi Ichimoto	*Closing Remarks*

Adjourn

List of Posters

Session 1. Magnetic Fields and Solar Cycle

ID	Presenter	Title
S1- P- 01	Y. Masada	*Large-scale Magnetic Field and Alpha-square Dynamo Wave in Turbulent Convective Dynamo Simulation*
S1- P- 02	J. Hao	*Solar cycle variation of helicity characteristics*
S1- P- 03	B. W. Lites	*THE SOLAR CYCLE DEPENDENCE OF THE WEAKEST INTERNETWORK FLUX*
S1- P- 04	V. K. VERMA	*On Long-Term Period of North-South Asymmetry of Solar Phenomena*
S1- P- 05	D. Shukuya	*Study on Asymmetry of Solar Polar Field Reversal between the North and South Hemisphere*
S1- P- 06	M. Gosic	*Temporal evolution of the quiet Sun magnetic fields inside supergranular cells*
S1- P- 07	L. Kleint	*Emission above sunspot umbrae*
S1- P- 08	J. de la Cruz Rodriguez	*Physical properties of a sunspot chromosphere with umbral flashes*
S1- P- 09	J. Jurcak	*Evolution of penumbral filaments in forming sunspot*
S1- P- 10	S. K. Tiwari	*Structure of sunspot penumbral filaments as obtained by spatially coupled inversion of Hinode (SOT/SP) data*
S1- P- 11	S. Esteban Pozuelo	*Temporal evolution of the velocity of lateral downflows in sunspot's penumbra*
S1- P- 12	V. Bommier	*Magnetometry from HINODE/SOT/SP data: solving the fundamental ambiguity from the 6301/6302 line pair inversion*
S1- P- 13	A. J. Kaithakkal	*The Association of Polar Faculae with Polar Magnetic Patches Examined with Hinode/SOT-SP Observations*
S1- P- 14	Y. Suematsu	*Study of 3D Fine-Scale Structure and Dynamics of Solar Polar Faculae*
S1- P- 15	G. B. Scharmer	*SST/CRISP observations of penumbral convective flows in the Fe I 5576 and 6301/6302 lines*
S1- P- 16	Y. Iida	*Displacement of patch structures and its insight to magnetic flux transport in magneto-convection system*
S1- P- 17	S. Thonhofer	*Parallelization of the SIR Code for the investigation of the dynamics of magnetic flux tubes*
S1- P- 18	D. Utz	*The evolution of important magnetic bright point parameters*
S1- P- 19	H. Iijima	*Kinetic and magnetic power spectra in the supergranular-scale convection studied by three-dimensional radiative magnetohydrodynamic simulations*
S1- P- 20	G. Vissers	*Center-to-limb variation in Ellerman bombs observed in Halpha and 1700 A*
S1- P- 21	L. Rouppe van der Voort	*Small-scale dynamic fibrils in sunspot chromospheres*
S1- P- 22	R. A. Shine	*Hinode/SOT and IRIS observations of Sunspot and Chromospheric Oscillations*
S1- P- 23	I. Piantschitsch	*Simulation of the dynamics of small scale magnetic fields in the lower solar atmosphere in regards of the atmospheric heating problem*
S1- P- 24	O. Steiner	*Recent RMHD simulations with CO5BOLD*
S1- P- 25	B. Lemmerer	*Detection and analysis of small scale convective patterns observed with Hinode compared to RHD simulations*
S1- P- 26	R. Kano	*Relation between magnetic fields and horizontal velocity in an active region*

S1- P- 27	M.	van Noort	*Very strong magnetic fields in supersonic downflows*
S1- P- 28	T.	Fukuoka	*The photospheric magnetic field measurement with Tandem Etalon Magnetogprah (TEC) of SMART telescope at Hida Observatory*
S1- P- 29	K.	Otsuji	*Statistical Analysis of Current Helicity Using Hinode/SOT SP Data*
S1- P- 30	G.	Giono	*Spatially Resolved images of the Corona and EUV & UV Irradiance Variability*
S1- P- 31	M. L.	DeRosa	*How Spatial Resolution in Boundary Data Affects Coronal Magnetic Field Extrapolations*
S1- P- 32	L. A.	Rachmeler	*Transition from two helmet streamers into a coronal pseudostreamer*
S1- P- 33	K.	Iwai	*Measurements of Coronal and Chromospheric Magnetic Fields using Polarization Observations by the Nobeyama Radioheliograph*
S1- P- 34	Y.	Tanaka	*Longitudinal structure of the polar field reversal and decadal trend of the sunspot's gyroresonance emissions in 17 GHz*

Session 2. Atmospheric and Interior Couplings

ID		Presenter	Title
S2- P- 01	M.	Carlsson	*First Comparison between IRIS Data and Numerical Models*
S2- P- 02	B.	Rathore	*Diagnostic potential of CII lines for NASA/SMEX mission IRIS.*
S2- P- 03	J.	Leenaarts	*The formation of the Mg II h&k lines in the solar atmosphere*
S2- P- 04	T.	Van Doorsselaere	*Forward modelling of solar atmospheric structures and their oscillations*
S2- P- 05	O.	Steiner	*Revealing the nature of magnetic halos and shadows with numerical 3D-MHD simulations*
S2- P- 06	S.	Shelyag	*Spectropolarimetric signatures of photospheric intergranular vortices*
S2- P- 07	P. S.	Cally	*Coupling Interior and Atmosphere through Active Regions*
S2- P- 08	R.	Morton	*Observations of the excitation and damping of Alfvenic waves throughout the solar atmosphere*
S2- P- 09	A. S.	Hillier	*A statistical study of prominence oscillations: Evidence for photospheric motions as the transverse wave driver in a quiescent prominence*
S2- P- 10	E.	Dzifcakova	*Kappa-distributions and the Differential Emission Measure of Active Regions*
S2- P- 11	R.	Soler	*Seismic inference of physical parameters in solar prominences using observations of their fine structure oscillations*
S2- P- 12	R.	Kitai	*Morphological study of penumbral formation*
S2- P- 13	S.	Wedemeyer	*Magnetic tornadoes on the Sun*
S2- P- 14	R. A.	Maurya	*Changes in High Degree p-mode parameters with Magnetic and Flare Activities*
S2- P- 15	R. F.	Pinto	*Solar wind and coronal rotation during an activity cycle.*
S2- P- 16	F.	Chen	*A coupled model for the formation of active region corona*
S2- P- 17	S.	Nozawa	*Relationship between satellite anomalies and space weather*
S2- P- 18	A.	Ohkawa	*Analysis of Sunspot oscillations observed with DST/Hida*
S2- P- 19	S.	Sawada	*Magnetic field of active region filaments observed with DST/Hida*

S2- P- 20	Y.	Kato	*Simultaneous multi-line observation of Ellerman bombs using the DST in Hida observatory*
S2- P- 21	R.	Sato	*Numerical study on the generation of waves by asymmetrical magnetic reconnection*
S2- P- 22	B.	Fleck	*On the Signature of Waves and Oscillations in IRIS Observations*

Session 3. Coronal Heating and Solar Wind Acceleration

ID		Presenter	Title
S3- P- 01	B.	De Pontieu	*First IRIS observations of lower solar atmospheric activity*
S3- P- 02	H.-H.	Lin	*The formation of the OI 135.56 nm and CI 135.58 nm lines in solar atmosphere*
S3- P- 03	J.	Okamoto	*Hinode-IRIS observations of prominences*
S3- P- 04	J.-P.	Wuelser	*Initial Calibration and Performance of the IRIS Instrument*
S3- P- 05	Y.	Kato	*Chromospheric and Coronal Wave Generation in the Network Magnetic Elements Through the Magnetic Pumping*
S3- P- 06	H.	Skogsrud	*Torsional motion of spicules*
S3- P- 07	N.	Kitagawa	*Spatial and temporal correspondence between enhanced blue wing observed with Hinode/EIS and propagating disturbances in fan loops seen in AIA images*
S3- P- 08	S.	UeNo	*Report of Cooperative Observations between Hida Observatory & Hinode Satellite (HOP0012, 0075, 0128)*
S3- P- 09	T. P.	Golding	*Non-equilibrium helium ionization and its effects on the He II 304 and He I 10830 lines*
S3- P- 10	K.-S.	Lee	*Spectroscopic properties of a dark lane and a cool loop in a limb active region observed by Hinode/EIS*
S3- P- 11	S.	Parenti	*Off-limb hot thermal structure of AR 11459*
S3- P- 12	M.	Asgari-Targhi	*Observational signatures of Alfven Wave Turbulence*
S3- P- 13	I.	Arregui	*How to determine the physical parameters that govern wave dissipation time and spatial scales*
S3- P- 14	B. N.	Dwivedi	*On the Signature of Alfven Wave Dissipation in the Localized Coronal Funnel as a Source of Nascent Solar Wind*
S3- P- 15	R.	Morton	*Hi-C and AIA observations of transverse magnetohydrodynamic waves in active*
S3- P- 16	A. R.	Winebarger	*Fine-scale Fluctuations in the Corona observed with Hi-C*
S3- P- 17	H.	Peter	*Structure of solar coronal loops: from miniature to large-scale*
S3- P- 18	H.	Peter	*Constant cross section of loops in the solar corona*
S3- P- 19	V.	Joulin	*Distributions of energy of EUV bright points in the solar corona*
S3- P- 20	K.	Olluri	*Synthezided spectra of optically thin emission lines produced by the Bifrost stellar atmosphere code*
S3- P- 21	T.	Yokoyama	*Magnetothermal Instability in the Solar Atmosphere*
S3- P- 22	T.	van Wettum	*The response of the corona to different heating mechanisms.*
S3- P- 23	E.	Dzifcakova	*Synthetic spectra for the kappa-distributions using modified CHIANTI*

S3- P- 24	P.	Antolin	*Forward modelling of MHD kink oscillations in the solar corona*
S3- P- 25	C.	Guennou	*Can the Differential Emission Measure diagnostic be used to constrain the timescale of energy deposition in the corona?*
S3- P- 26	M.	Weber	*What DEM Analysis Can and Cannot Tell Us*
S3- P- 27	M.	Hahn	*Quantification of the Energy Dissipated by Alfven Waves in a Polar Coronal Hole*
S3- P- 28	M.	Hahn	*Anisotropic Ion Temperatures, Non-Thermal Velocities, and Doppler Shifts in a Coronal Hole*
S3- P- 29	P.	Kayshap	*On the Coronal Reconnection Height and Hot Jet Formation in the North Polar Coronal Hole (NPCH) as Observed by Hinode/EIS*
S3- P- 30	T.	Suda	*Double-thread structure of spicules generated by magnetic reconnection*

Session 4. Flares and Coronal Mass Ejections

ID	Presenter		Title
S4- P- 01	V. H.	Hansteen	*`Realistic' 3D simulations of a small flare resulting from flux emergence*
S4- P- 02	T.	Kaneko	*MHD Simulation of Filament Formation by Thermal Instability*
S4- P- 03	T.	Kaneko	*MHD Simulation of Plasma Eruption by Interaction between Emerging Flux and Coronal Arcade Field*
S4- P- 04	T.	Nakabo	*Simulation study of magnetic reconnection in high magnetic Reynolds number plasmas*
S4- P- 05	R. F.	Pinto	*Thermal x-ray emission in flaring coronal loops*
S4- P- 06	K.	Nishida	*The Role of a Flux Rope Ejection in Three-dimensional Magnetohydrodynamic Simulation of a Solar Flare*
S4- P- 07	L.	Ni	*Reconnection in partially ionized plasma with radiation cooling]{Fast magnetic reconnection with multiple plasmoids applied in the partially ionized plasma*
S4- P- 08	S.	Wang	*Analysis on Mechanisms of Reconnection Rate Enhancement in 3D MHD simulation of a Current Sheet*
S4- P- 09	T.	Shimizu	*Three-dimensional instability of spontaneous fast magnetic reconnection in solar flares*
S4- P- 10	A.	Berlicki	*Ellerman bombs - physical parameters derived from high-resolution multiline spectroscopic observations*
S4- P- 11	A. R.	Kobelski	*Modeling Active Region Transient Brightenings observed with XRT to Constrain the Heating Function of Active Regions*
S4- P- 12	Y.	Bamba	*Comparison between Hinode/SOT and SDO/HMI, AIA data for the study of solar flare trigger processes*
S4- P- 13	S.	Imada	*Coronal Behaviors before the Large Flare Onset*
S4- P- 14	N.	Sako	*An energetics study of X-ray jets*
S4- P- 15	A.	Savcheva	*A New Catalog of Sigmoidal Active Regions: Statistical Properties and Evolutionary Histories*
S4- P- 16	P.	Heinzel	*Prominence visibility in soft X-rays using Hinode XRT observations*
S4- P- 17	H.-S.	Yu	*Are Jets CMEs? The Jet Response Mass Loading of Solar Wind Plasma*
S4- P- 18	G. A.	Doschek	*Solar Flare Observations with EIS*
S4- P- 19	M.	Kasuga	*Calibration on EIS Instrumental Width from Observations and Its Application*

S4- P- 20	Y.	Matsui	*Simultaneous observation of high temperature cusp loops and bi-directional inflow in the limb flare with Hinode/EIS and SDO/AIA*
S4- P- 21	T.	Watanabe	*Hot Reconnection Outflows Associated to an X-class Flare*
S4- P- 22	Y.	Li	*The EUV Late Phase of Solar Flares: Additional Heating or Cooling Signature?*
S4- P- 23	V. K.	Verma	*On M2.2 Solar Flare and CMEs Observed on 26 November, 2000 from NOAA AR 9236*
S4- P- 24	V. K.	VERMA	*On Classification of Solar Coronal Mass Ejections Observed by LASCO/SOHO during period 1996-2011*
S4- P- 25	R. A.	Maurya	*SDO/AIA Observations of a Spotless Two-ribbon Flare and associated Sympathetic Flare*
S4- P- 26	J.	Dudik	*Slipping flare loops observed by SDO/AIA and the slipping magnetic reconnection*
S4- P- 27	M .V.	Gutierrez	*A 3-Dimensional View of the Filament Eruption and Coronal Mass Ejection Associated with the 2011 March 8 Solar Flare*
S4- P- 28	N. V.	Nitta	*Magnetic reconnection rate in eruptive and non-eruptive events as calculated with flare ribbons*
S4- P- 29	A.	Reva	*CME Observations with TESIS EUV Telescopes and LASCO C2 Coronograph*
S4- P- 30	X.	Wang	*The maximum energy particles accelerated by the CME-driven shock*
S4- P- 31	I. G.	Hannah	*The energetics of microflares observed with Hinode, RHESSI and SDO*
S4- P- 32	I. G.	Hannah	*EM maps of hot ribbons during the rise phase of a flare*
S4- P- 33	F.	Rubio da Costa	*Combining simulations of radiative hydrodynamics and particle acceleration to model solar flares*
S4- P- 34	K.	Watanabe	*White-Light Emission and related Particle Acceleration Phenomena in an X1.8-class Flare on 2012 October 23*
S4- P- 35	G. S.	Kerr	*Properties of the optical sources in the 15th February 2011 solar flare*
S4- P- 36	Y.	Shen	*Sequential Filament Oscillations Caused by An Invisible Moreton Wave*
S4- P- 37	M.	Yamaguchi	*Statistical Study of Filament Eruptions and Moreton Waves Observed by the Flare Monitoring Telescope at Hida Observatory, Kyoto University*
S4- P- 38	S.	Masuda	*Microwave and X-ray observations of an X-class flare on 13 May 2013*
S4- P- 39	T.	Kawate	*The origin of nonthermal electrons in solar flares*
S4- P- 40	J.	He	*Three kinds of MHD waves excited around flare due to impact of reconnection-induced plasmoids into ambient plasma*
S4- P- 41	E. G.	Kupriyanova	*Long-period oscillations of solar flare emissions*
S4- P- 42	F.	Farnik	*The Spectrometer Telescope for Imaging X-rays (STIX) onboard Solar Orbiter*
S4- P- 43	T.	Takahashi	*Investigation of shock nature of an EUV wave using a prominence activation*

Session 5. Space Weather and Space Climate

ID	Presenter		Title
S5- P- 02	S.	Kameda	*Mercury observed by Hinode SOT*
S5- P- 03	D.	Baker	*FIP bias in a sigmoidal active region-coronal hole complex*
S5- P- 04	D.	Baker	*What can we deduce from the 3D geometry of AR upflows?*

S5- P- 05	D.	Baker	*Active Region Upflow Plasma: How can it escape from below a closed helmet streamer?*
S5- P- 06	Y.	Hada	*Diagnosing flare productive active regions using EUV images for space*
S5- P- 07	S.	Imajo	*Dayside ionospheric equivalent current system of Pi 2 pulsations*
S5- P- 08	H.	Matsushita	*Space weather research using MAGDAS/CPMN data*

Session 6. Solar-Stellar Connection

ID		Presenter	Title
S6- P- 01	P.	Testa	*The thermal structure of the quiet Sun coronal emission*
S6- P- 02	M.	Kanao	*SOT BFI plate scale re-calibration on June 2012 Venus transit event*
S6- P- 03	M.	Wedemeyer	*From high-resolution observations and models of the Sun towards cool stars*
S6- P- 04	S. H.	Saar	*Flare Rates for Solar-like Stars in the One Gigayear Year Old Kepler Cluster NGC 6811, With Implications for the Sun*
S6- P- 05	S. H.	Saar	*More Evidence HD 3651 May be in a Maunder-like Magnetic Minimum*
S6- P- 06	S. H.	Saar	*Differential Rotation at One Gigayear: Rotational Period Changes in Kepler Cluster NGC 6811*
S6- P- 07	T.	Shibayama	*Superflares on Solar Type Stars Observed with Kepler*
S6- P- 08	Y.	Notsu	*High Dispersion Spectroscopy of Solar-Type Stars showing Superflares*
S6- P- 09	S.	Notsu	*High-Dispersion Spectroscopy of the Superflare Star KIC6934317*
S6- P- 10	A. D.	Kawamura	*3D test particle simulation of ISM Oxygen interacting with Heliosphere for IBEX observations*

Session 7. Future Problems and Observations

ID		Presenter	Title
S7- P- 01	A.	Sainz Dalda	*Refining SOT/SP Measurements of Photospheric Magnetic Field By A Two-Step Deconvolution-Inversion Method*
S7- P- 02	S.	Gunar	*Synthetic high-resolution prominence observations*
S7- P- 03	K.	Yoshimura	*Useful methods for coalignment calibration; from the experiences of XRT calibration*
S7- P- 04	S. H.	Saar	*Empirical Corrections for the Small Light Leak in Hinode XRT*
S7- P- 05	N. E.	Hurlburt	*IRIS data products and distribution*
S7- P- 06	Y.	Kato	*Detecting chromospheric magneto-acoustic body wave near the MBPs by using Mg II h&k lines*
S7- P- 07	M.	Goto	*Analytical solution of the Hanle effect in view of CLASP and future polarimetric solar studies*
S7- P- 08	N.	Narukage	*UV spectropolarimeter design for precise polarization measurement with 0.1% accuracy*
S7- P- 09	J.	Stepan	*Polarization of the Lyman-alpha line of hydrogen in multi-thread models of quiescent solar prominences*
S7- P- 10	C.	Bethge	*The Center for Advanced Solar Spectro-Polarimetric Data Analysis (CASSDA)*
S7- P- 11	S.	Bogachev	*The Solar EUV telescopes for the Arka mission*

S7- P- 12	L.	Teriaca	*LEMUR/EUVST: the spectrograph for the Solar C mission*
S7- P- 13	D.	Nandi	*Solar Hyper-spectral Imaging Polarimeter (SHIP): A Novel Instrument Concept for Near-simultaneous Polarimetric Imaging of the Solar Corona*
S7- P- 14	J.	Trujillo Bueno	*Our Gateway to the Magnetism of the Chromosphere-Corona Transition Region*
S7- P- 15	K.	Ichimoto	*Attempts for high spatial resolution at Hida observatory and future coordination with Hinode*
S7- P- 16	T.	Anan	*Magnetic field and electric field of a surge with a spectropolarimetric observation in HI Paschen lines*
S7- P- 17	M.	Hagino	*Development of a universal tunable filter for future space and ground observations*
S7- P- 18	A.	Oi	*The magnetic and velocity field structure of the sunspot chromosphere*
S7- P- 19	S.	Abe	*An Investigation of coronal mass ejections and EUV waves for space weather forecasting*
S7- P- 20	K.	Suto	*Study of automatic observation system for compact solar telescope*
S7- P- 21	K.	Yaji	*Coordinated observations for High School Students as Hinode EPO Activity*
S7- P- 22	N.	Mouri	*Development of the Mobile Spectrograph for Educational Observation*

Hinode-7

Session 1

Magnetic Fields and Solar Cycle

On Longterm Behavior of Quieter Aspects of the Sun, Quiet Stars, and Magnetic Minima

Abstract Author(s): Steven H. Saar

Institution(s): Harvard-Smithsonian Center for Astrophysics

Presentation: S1-I-01

Abstract

I review work on the temporal, spatial, and thermal variability of quieter aspects of the Sun. I focus in particular on X-ray brightpoints, the ubiquitous tiny kernels of activity seen throughout the solar cycle. Long-term behavior of bright points has been studiedwith SOHO, and can now be extended with Hinode and AIA. I combine this with work work on inactive solar-like stars, to build a picture of what the outer atmosphere of Sun might have been like in a Maunder-like magnetic minimum.

Hinode-7
Session 1: Magnetic Fields and Solar Cycle

AN OCEAN OF INCLINED MAGNETIC FIELDS IN THE VERY QUIET SUN

Abstract Author(s): Luis Bellot Rubio

Institution(s): Instituto de Astrofisica de Andalucia (CSIC)

Presentation: S1-C-01

Abstract

Using Hinode measurements, we demonstrate that linear polarization signals occur nearly everywhere in the quiet Sun internetwork. As the noise level is reduced, up to 70% of the area covered by the observations show clear Stokes Q or U signals. The mere presence of linear polarization implies that internetwork fields are very inclined, as suggested by other studies. We determine the distributions of field strength, inclination, azimuth, and filling factor by inverting pixels with Stokes Q or U amplitudes of at least 4.5 times the noise level. These signals, which account for more than 50% of the field of view, allow a very precise determination of the vector magnetic field to be made. At the highest angular resolution to date, our results confirm that internetwork fields are weak and highly inclined, but not completely horizontal nor isotropically distributed. We suggest that these fields are the ones traced by Hanle measurements, now detectable through the Zeeman effect thanks to the superb spatial resolution of the Hinode spectropolarimeter.

Hinode-7
Session 1: Magnetic Fields and Solar Cycle

Current status of understanding about solar global convection

Abstract Author(s): Hideyuki Hotta

Institution(s): University of Tokyo

Presentation: S1-I-02

Abstract

We present a summary of recent progress in the 3-D hydrodynamic and MHD simulations of solar global convection. The solar global convection, the angular momentum transport, and its dynamo action have been investigated using the anelastic approximation implemented in several numerical codes in order to avoid the severe limitation in the time step by the sound wave (e.g. Miesch et al. 2008). These studies provide a lot of great insights of the maintenance of the differential rotation, the meridional flow and the large-scale magnetic field. The next important challenge is the inclusion of the near surface layer, i.e. the study on the connection between the large-scale convection in the deeper layer and the small-scale (granulation- and supergranulation-scale) one in the near surface layer, for the unified understanding of the solar convection zone. The problems for this issue are that resolving the small-scale convection requires the large number of grids and that the anelastic approximation does not hold in the near surface layer. In order to overcome these, we adopt another method, the reduced speed of sound technique(RSST), which significantly reduces the computational cost. This method enables us to approach the real solar surface without loosing the importance physical processes and reproduce the small-scale convection using the high resolution. We also show the result using newly developed numerical code with the RSST, which resolves the supergranulation-scale convection in the global domain with the higher upper boundary at 0.99Rsun. We find that this small-scale downflow plumes penetrate deeper layer to some extent and excite the small-scale turbulence there.

Towards Solar Cycle Predictions: Recent Advances in Modelling and Observations

Abstract Author(s): Dibyendu Nandi

Institution(s): CESSI, IISER Kolkata

Presentation: S1-C-02

Abstract

Forecasting the amplitude of future solar cycles is important for mitigating the adverse impacts of space weather on our technologies based in space and on Earth. However, reliable solar cycle forecasting is still not possible due to a number of uncertainties regarding the theoretical basis of the solar cycle itself. For the ongoing solar cycle 24, no early consensus was achieved by the NOAA-NASA International Solar Cycle Prediction Panel and official forecasts were revised multiple times. In this talk, I will take stock of the lessons learnt from attempts to forecast solar cycle 24 and review the convergence in recent dynamo modelling results and polar field observations that may lead to more accurate solar cycle predictions.

Hinode-7
Session 1: Magnetic Fields and Solar Cycle

Magnetic evolution at over 70 degrees latitude during the polarity reversal

Abstract Author(s): Daikou Shiota, Masumi Shimojo, Anjali John K., Nobuharu Sako, Saku Tsuneta

Institution(s): Solar-Terrestrial Environment Laboratory, Nagoya University, National Astronomical Observatory of Japan , ISAS/JAXA

Presentation: S1-C-03

Abstract

The magnetic field in the Sun's polar region is a key ingredient of the solar dynamo mechanism because the polar field strength at a solar minimum has a correlation with solar activity of the following cycle. The evolution processes of the polar field (its polarity reversal and its build-up after the reversal) are thought to be caused by magnetic flux transport due to meridional flow and diffusion by turbulent convection. Nevertheless, our understanding of the meridional flow and diffusion near the pole is still poor because of many difficulties for magnetic observation in such a region.

The polar observations of Hinode revealed the fine distribution of the polar magnetic fields, and have been continued from 2008 to understand the polar magnetic evolution in a solar cycle. The series of the high quality vector magnetograms obtained with the SOT-SP aboard Hinode revealed the position of the polarity reversal front (the polarity inversion line of radial component). By the magnetic field distributions of the whole north polar region observed in Jan. and Sep. of 2012, the polarity reversal front moved from 59 to 68 degrees latitude. The proceeding speed is 5 m s^{-1}.

We planned the observation of the whole north polar region in this September. The observation will reveal the behavior of the polarity reversal front over 70 degrees latitude, and the result might enable us to infer the meridional flow pattern near the pole during the polarity reversal.

In contrast to the north polar region, the magnetic field distribution of the south polar region in March 2013 showed that the whole observed region ($>\sim$67 degree latitude) has ample positive fields and that the polarity reversal front is still located out of the region.

Hinode-7
Session 1: Magnetic Fields and Solar Cycle

Observations of fine scale structures and dynamics in sunspots

Abstract Author(s): Hiroko Watanabe

Institution(s): Kyoto University

Presentation: S1-I-03

Abstract

Sunspots are the regions of intense magnetic field concentration that appear dark on the solar surface. Because of its strong magnetic field, sunspots are the source of many active phenomena on the Sun, such as the flares and the coronal mass ejections. Astronomers have been keenly observed the sunspots from hundreds of years ago. Hinode satellite opens a new era to the study of sunspots, because of its high spatial resolution and temporal stability. Fine scale structures in and around the sunspots, such as umbral dots, light bridges, penumbral filaments, moving magnetic features, have become one of the hottest topics in the solar physics. We found upflow inside umbral dots and confined downflowing regions outside of them (Bharti et al. 2007, Ortiz et al. 2010, Watanabe et al. 2012). These kinetic properties match the picture from numerical simulations on magneto-convective phenomena. Umbral dots and penumbral filaments should have a common origin, because there is an intermediate transition observed as an inward migration of penumbral grains. We still do not know whether there is a relation between umbral dots and chromospheric umbral flashes, and so needs richer multi spectral observation in the near future. The precursor of penumbral formation was found in the chromosphere (Shimizu et al. 2012). It has been proved that the magnetic field configuration in the chromosphere plays an important role on the onset of the field reconfiguration, both on the observational and theoretical viewpoint (Rempel 2012, Watanabe et al. 2013 in preparation). I will review recent highlights on the observation of fine scale structures in sunspots mainly by the Hinode but also by other satellites. Also I will introduce some numerical models that explain the mechanism of these phenomena.

Hinode-7
Session 1: Magnetic Fields and Solar Cycle

Emergence of granular-sized magnetic bubbles through the solar atmosphere.

Abstract Author(s): Ada Ortiz-Carbonell, Luis Bellot Rubio, Viggo Hansteen, Jaime de la Cruz Rodriguez, Luc Rouppe van der Voort

Institution(s): Institute of Theoretical Astrophysics, University of Oslo, Instituto de Astrofisica de Andalucia (CSIC) , Institute of Theoretical Astrophysics, University of Oslo , Deparment of Physics and Astronomy, Uppsala University , Institute of Theoretical Astrophysics, University of Oslo

Presentation: S1-C-04

Abstract

We study a granular-sized magnetic flux emergence event that occurred in NOAA 11024 in July 2009. The observations were made with the CRISP spectropolarimeter at the Swedish 1 m Solar Telescope achieving a spatial resolution of 0.14". Simultaneous full Stokes observations of the two photospheric Fe I lines at 630.2 nm and the chromospheric Ca II 854.2 nm line allow us to describe in detail the emergence process across the solar atmosphere. We report here on 3D semi-spherical bubble events, where instead of simple magnetic footpoints, we observe complex semi-circular feet straddling a few granules. Several phenomena occur simultaneously, namely, abnormal granulation, separation of opposite-polarity legs, and brightenings at chromospheric heights. However, the most characteristic signature is the observation of a dark bubble in filtergrams taken in the wings of the Ca II 854.2 nm line. There is a clear coincidence between the emergence of horizontal magnetic field patches and the formation of the dark bubble. We can infer how the bubble rises through the solar atmosphere as we see it progressing from the wings to the core of Ca I 854.2 nm. In the photosphere, the magnetic bubble shows mean upward Doppler velocities of 2 km/s and expands at a horizontal speed of 4 km/s. To aid the interpretation of the observations, we carry out 3D numerical simulations of the evolution of a horizontal magnetic flux tube injected in the convection zone, using the Bifrost code. The computational domain spans from the upper convection zone to the lower corona. In the modeled chromosphere, the rising flux tube produces a large, cool, magnetized bubble. We compare this bubble with the observed ones and find excellent agreement, including similar field strengths and velocity signals in the photosphere and chromosphere, ascent speeds, expansion velocities, temperature deficits, and lifetimes.

2D inversions of weak internetwork spectropolarimetric signals

Abstract Author(s): Sanja Danilovic

Institution(s): Max Planck Institute for Solar System Research

Presentation: S1-C-05

Abstract

Properties of the internetwork field have so far been determined based on only a small fraction of pixels that show high enough signal-to-noise ratio. Because of its unique way of accumulating information, the new spatially coupled (2D) inversion technique performs more robustly. The technique proved to be efficient in recovering the high spatial frequencies up to the diffraction limit and thus revealing the solar atmosphere in more detail than before. Here we test it on different synthetic snapshots produced with MURaM code. The best inversion strategy is then applied on the quietest regions observed by Hinode/SP. The results show the highest average magnetic flux density retrieved thus far. The observed power spectra are in agreement with power spectra retrieved from the MHD simulations.

Hinode-7
Session 1: Magnetic Fields and Solar Cycle

A granular light bridge observed by Hinode: evidence for naked granules

Abstract Author(s): Andreas Lagg, Sami K. Solanki, Michiel van Noort

Institution(s): Max Planck Institute for Solar System Research, Max Planck Institute for Solar System Research, Katlenburg-Lindau, Germany , Max Planck Institute for Solar System Research, Katlenburg-Lindau, Germany

Presentation: S1-C-06

Abstract

We present the atmospheric structure of a granular light bridge derived from spatially coupled inversions of data obtained with the spectropolarimeter of Hinode SOT. Several light bridges separating the umbra of AR10926 contain granular cells with properties similar to that of a quiet Sun granule, but with some distinct differences: The magnetic field exhibits a clear cusp-like shape in the higher layers, the downflows at the boundary to the umbra are cooler than in the intergranular lanes of the quiet Sun, and they exceed velocities of 10 km/s. The granule center in the deepest layer is basically field free. We interpret these characteristics of light bridge granules as being due to the presence of the Wilson depressed umbra next to it. This exposes the otherwise buried sides of the granules, in particular the downflow lanes, extending the visible downflow path length and allowing for an efficient radiative cooling of the granule towards the umbra. These effects together are proposed to explain the observed high downflow speeds. Hints of opposite polarity field near the footpoints of these fast downflows may be explained by umbral field being dragged down by the downflowing material.

Hinode-7
Session 1: Magnetic Fields and Solar Cycle

Properties of solar plage from a spatially coupled inversion of Hinode SP data

Abstract Author(s): David Buehler, Andreas Lagg, Sami Solanki, Michiel van Noort

Institution(s): Max Planck Insitute for Solar System Research, Max Planck Institute for Solar System Research , Max Planck Institute for Solar System Research , Max Planck Institute for Solar System Research

Presentation: S1-C-07

Abstract

The properties of magnetic features composing a plage region in the vicinity of a sunspot were investigated at high spatial resolution. Stokes spectra of the 630nm line pair recorded by the spectropolarimeter aboard Hinode were inverted using an extended version of the SPINOR code. The code preformed a spatially coupled inversion of the Stokes spectra using three $\log(\tau)$ nodes in optical depth. No magnetic filling factors was employed. The analysis of the inversion results reveals that the plage is composed of magnetic flux concentrations (MFCs) with typical field strengths of 1490G at $\log(\tau)$=-0.9 and inclinations between 10-15 degrees in all three $\log(\tau)$ nodes. Whilst the gas inside magnetic flux concentrations is typically at rest, the majority of MFCs were surrounded by a ring of downflows with typical values of 1-3km/s. The MFCs expand with forming magnetic canopies composed of weaker and more inclined magnetic fields. The expansion of the magnetic field and temperature stratification of MFCs with optical depth is in good agreement with a thin flux tube model. Within the downflow rings of MFCs small magnetic patches of opposite polarity to that of the main MFC were identified, which are predominantly situated beneath the canopy of its main MFC. We found evidence for a strong broadening of the Stokes profiles in MFCs (expressed by a microturbulence in the inversion). This indicates the presence of strong unresolved velocities.

Hinode-7
Session 1: Magnetic Fields and Solar Cycle

Determining the magnetic field vector in quiescent prominence threads

Abstract Author(s): David Orozco Suarez, Andres Asensio Ramos, Antonio J. Diaz, Javier Trujillo Bueno

Institution(s): Instituto de Astrofisica de Canarias

Presentation: S1-C-08

Abstract

Hinode has dramatically increased our knowledge on the fine scale structuring and dynamics of prominences through state-of-the-art high spatial resolution filter imaging. However, direct determination of the magnetic field vector in prominences is still limited to ground-based observations in spectral lines whose Stokes profiles are produced by atomic level polarization and the join action of the Zeeman and Hanle effects. In this contribution we show ground-based observations of a quiescent hedgerow prominence taken in the He I 1083.0 nm triplet with the Tenerife Infrared Polarimeter attached to he German Vacuum Tower Telescope (VTT) at the Observatorio del Teide (Tenerife; Canary Islands; Spain). The data consist of a prominence map showing vertical threads and a slit time series that recorded the evolution of prominence threads. We show how to infer the strength and orientation of the magnetic field vector in the prominence plasma from the analysis and interpretation of the polarization signals using the Hazel inversion code. We present the results of our inversions, i.e, the strength and orientation of the magnetic field vector across the prominence and in prominence threads. We also show how to complement the Hazel inversions with prominence seismology techniques. Since the time series data shows damped oscillations we can use this information to constraint the magnetic field strengths. These spectropolarimetric observations are of particular interest for Solar-C since this telescope plans to observe this spectral multiplet at unprecedented spatial and temporal resolutions from the space.

Hinode-7
Session 1: Magnetic Fields and Solar Cycle

Implication of the magnetic power spectra derived with the Hinode SP

Abstract Author(s): Yukio Katsukawa, David Orozco Suarez

Institution(s): National Astronomical Observatory of Japan, Instituto de Astrofisica de Canarias

Presentation: S1-C-09

Abstract

We can quantify spatial power spectra of the surface velocities and magnetic fields at the granular and subgranular scales using two-dimensional maps taken with the Hinode SP. The power spectra provide an insight on what kind of magnetic structures are important in the total magnetic energy budget. It is especially important to determine whether the power-law indices of the magnetic power spectra is larger or smaller than -1. If the power spectra are stepper than -1, the total magnetic energy mainly comes from the large-scale (i.e. granular scale) power. If less steep than -1, on the other hand, the small-scale power is more important. The magnetic power spectra derived with the Hinode SP have a peak at 700 $\sim$ 800 km in internetwork regions, and drops toward the small scale with the power-law index of $\sim$-1.3, which suggests that the granular scale structures are more important than the small-scale fields in the total magnetic energy budget. It is also demonstrated that the kinetic power spectra are steeper than the magnetic ones at the subgranular scale in the internetwork regions, and the power-law indices differ by about 2. The relationship between the kinetic and magnetic power spectra can be simply explained if magnetic fields are passively advected by convective motion and their structures are created by velocity shear. This result implies that when the kinetic power spectrum is steeper than -3, which is the case for the ones derived with the Hinode SP, the convective motion makes the magnetic power spectrum steeper than the power-law index of -1, where the granular-scale structures are dominant.

Hinode-7
Session 1: Magnetic Fields and Solar Cycle

Large-scale Magnetic Field and Alpha-square Dynamo Wave in Turbulent Convective Dynamo Simulation

Abstract Author(s): Youhei Masada, Takayoshi Sano

Institution(s): Department of Computational Science, Kobe University

Presentation: S1-P-01

Abstract

Magnetic dynamo action by turbulent penetrative convection is studied by means of local Cartesian box simulation. We find that large-scale horizontal magnetic field is spontaneously organized in the convection zone. It shows cyclic oscillations with the period of 200 τ_{cv}, where τ_{cv} is the convective turnover time. Since there is no mean flow developed in the simulation, the large-scale magnetic field should be maintained by α^2-type dynamo mechanism. The up-down asymmetry in the convective motion, which is caused by the rotation and stratification, would generate mean kinetic helicity, yielding the large-scale dynamo. For the deeper understanding of the dynamo mechanism, we construct one-dimensional mean-field model with adopting α-effect and turbulent diffusion (α and η_t) directly computed from the convective dynamo simulation. The quenching effects due to magnetic helicity on α and η_t are self-consistently taken into account. We demonstrate, for the first time, that the large-scale dynamo by turbulent convection is "quantitatively" reproduced by the mean-field model. The oscillation pattern of the mean magnetic field is interpreted as propagating α^2-dynamo wave. The cycle period is then controlled by "quenched" turbulent diffusion. Our findings strongly suggest that α^2-type dynamo process plays a crucial role in generating the oscillating large-scale magnetic field in solar and stellar interiors.

Solar cycle variation of helicity characteristics

Abstract Author(s): Juan Hao, Mei Zhang

Institution(s): National Astronomical Observatories, Chinese Academy of Sciences, Key Laboratory of Solar Activity, National Astronomical Observatory, Chinese Academy of Sciences, Datun Road A20, Chaoyang District, Beijing 100012, China

Presentation: S1-P-02

Abstract

In this talk we present our study on solar cycle variation of helicity characteristics using a sample of all active regions observed by SP/Hinode up to June 2012. We first confirmed our previous finding that the usual hemispheric helicity sign rule is not followed in the descending phase of solar cycle 23 and is followed in the ascending phase of solar cycle 24, with a further finding that the later phase of solar cycle 24 shows an even stronger evidence to follow the usual hemispheric helicity sign rule. We also checked our previous finding that the strong and weak magnetic fields possess opposite helicity signs and found that this rule is not followed in the later phase of solar cycle 24. This means that this helicity character also possesses a solar cycle variation, in addition to the solar cycle variation of the usual hemispheric helicity sign rule, and there is a roughly 2-years time delay between these two.

Hinode-7
Session 1: Magnetic Fields and Solar Cycle

THE SOLAR CYCLE DEPENDENCE OF THE WEAKEST INTERNETWORK FLUX

Abstract Author(s): Bruce W. Lites

Institution(s): HAO/NCAR

Presentation: S1-P-03

Abstract

In a prior analysis using 45 data sets measured with the Hinode/SOT Spectro-Polarimeter (SP) during 2007, Lites (2011, ApJ 737, p. 52) examined the weakest components of the internetwork flux and their possible association with the stronger, larger scale flux of the quiet Sun. No association of the weakest mixed-polarity flux to the stronger, larger-scale flux patterns. Also, the weakest flux remained very nearly equally balanced between positive and negative flux, even in quiet Sun regions that had significant overall flux imbalance. The observed behavior of these data taken near the minimum of the solar cycle suggests that this weak flux arises from a local, small-scale dynamo process. A local, small-scale dynamo should be independent from the large-scale dynamo of the solar cycle. In the present study, we examine the SP "irradiance data" taken in identical fashion every month since late 2008. In all, 990 separate SP maps were processed. Each month these data span the full range of solar latitude from pole-to-pole. We look for solar-cycle signatures of the weakest components of the magnetic flux as a function of both time and solar latitude. As expected for a local small-scale dynamo process, the preliminary examination of the data shows no visible patterns that would suggest an association of the weakest flux with solar activity. On the other hand, the weak transverse (horizontal) flux appears to increase in the activity belt as the solar cycle rises, suggesting possibly the solar cycle flux produces a canopy of magnetic field.

On Long-Term Period of North-South Asymmetry of Solar Phenomena

Abstract Author(s): V K. VERMA

Institution(s): Uttarakhand State Application Center

Presentation: S1-P-04

Abstract

The long-term behavior of North-South (N-S) asymmetry related to solar activity phenomena are investigated. In the investigation we have used sunspots area data (1821-2013), flare index data (1936-2012) and solar active prominences (1957-2013) data for various solar cycles. The statistical technique was used check the validity of asymmetry. Earlier Verma (1992, 1993, and 2009) reported long-term cyclic period 11 solar cycles in N-S asymmetry and also predicted that the N-S asymmetry of solar activity phenomena during solar cycles 21, 22, 23 and 24 will be south dominated and the N-S asymmetry will shift to north hemisphere in solar cycle 25. The present study shows that the N-S asymmetry during solar cycles 22 and 23 were southern dominated as predicted by Verma (1992). The initial years (2008-2012) of solar cycle 24th are showing southern domination and tend to confirm the result of Verma (1992). The 11 solar cycles periodic behavior of the Sun may be related to internal structure of the Sun. The result of this study may be helpful to understand long-term helioseismic phenomena and dynamo models of the Sun which are based on the magnetic fields related to solar active regions.

References:

Verma, V.K. (1992) ASP Conference Series, 27, 429.
Verma, V. K. (1993) APJ, 403, 797.
Verma, V.K. (2009) ASP Conference Series, 416, 483.

Hinode-7
Session 1: Magnetic Fields and Solar Cycle

Study on Asymmetry of Solar Polar Field Reversal between the North and South Hemisphere

Abstract Author(s): Daishi Shukuya, Kanya Kusano

Institution(s): STEL, Nagoya University

Presentation: S1-P-05

Abstract

It is known that solar polar magnetic field at one pole reverses following that on the other pole. This time difference of the polarity reversals between the poles was first noted by Babcock (1959) from the very first observation of polar field. Recently, it was confirmed by detailed observations with the HINODE satellite (Shiota et al. 2012). However, the mechanisms of hemispheric asymmetry in polarity reversal are still open to be revealed.

In this paper, we study the asymmetric feature of the solar dynamo based on the flux transport dynamo model (Chatterjee et al. 2004) to explain the time difference of the polarity reversals. We carried out the mean field dynamo simulations using the updated SURYA code which was developed originally by Choudhuri and his collaborators (2004). We decomposed the symmetric and asymmetric components of magnetic field, which correspond respectively to the quadrupole and dipole-like components (Nishikawa and Kusano 2008), and analyzed the phase relation between them. As a result, we found that the two components are mixed even if the dipole-like component is predominant and that the two components spontaneously form 90 or -90 degree out of phase oscillation. The solutions with 90 and -90 degree out of phase oscillation make the different attracters of dynamo solutions. Based on the results, we found that the time difference of the polarity reversals can be explained by the out of phase relation between the different components of dynamo solution.

We also analyzed the polar magnetic field data observed by Wilcox Solar Observatory using the same decomposition technique of magnetic field to compare the simulation results and the observation.

Temporal evolution of the quiet Sun magnetic fields inside supergranular cells

Abstract Author(s): Milan Gosic

Institution(s): Milan Gosic

Presentation: S1-P-06

Abstract

Small scale magnetic fields in the quiet Sun are transient magnetic concentrations distributed all over the solar surface. Their origin and contribution to the solar activity is still unclear. To investigate magnetic concentrations at small scales we are using long time data sequences obtained with the NFI on board Hinode. These data sets are characterized with high spatial resolution (0.16 arcsec/pixel), cadence (90 s) and the highest magnetograms sensitivity ever achieved (6 Mx/cm^2). In several continuous measurements of up to 40 hours, we track magnetic features manually and automatically from their appearance to disappearance. We derive their physical properties and analyse how magnetic flux vary as a function of time and radial distance from the center of the supergranule. Using this unique data sets, we determine the flux appearance rate in the solar photosphere and discuss about origin of internetwork magnetic fields.

Emission above sunspot umbrae

Abstract Author(s): Lucia Kleint, Alberto Sainz Dalda, IRIS TEAM

Institution(s): LMSAL / BAER Institute, Stanford Lockheed Institute for Space Research, LMSAL / BAER Institute

Presentation: S1-P-07

Abstract

The newly launched IRIS spacecraft provides us with an unprecedented view of sunspots in the upper layers of the solar atmosphere, especially in the highly dynamic transition region. We find bright emission ribbons above the umbrae of several sunspots, even during relatively low solar activity. These emission ribbons resemble flare ribbons and with IRIS' high spatial resolution, locations of enhanced heating inside the ribbon can be identified. Similar features were investigated with Hinode and IBIS in lower atmospheric layers in the unusual AR 11302 in September 2011, during phases where flare activity was high. We propose a scenario that may explain both observations, giving us a three-dimensional picture of heating above sunspots.

Physical properties of a sunspot chromosphere with umbral flashes

Abstract Author(s): Jaime de la Cruz Rodriguez, Luc Rouppe van der Voort, Hector Socas-Navarro, Michiel van Noort

Institution(s): Uppsala University, University of Oslo , Instituto de Astrofi?sica de Canarias , Max-Planck Institute for Solar System Research

Presentation: S1-P-08

Abstract

We present new high-resolution spectro-polarimetric Ca II 8542 observations of umbral flashes in sunspots. At nearly 0.18", and spanning about one hour of continuous observation, this is the most detailed dataset published thus far at such wavelength. Our study involves both LTE and non-LTE inversions (but includes also a weak field analysis as a sanity check) to quantify temperatures, mass flows and the full magnetic field vector geometry. We confirm earlier reports that UFs have very fine structure with hot and cool material intermixed at sub-arcsecond scales. The shock front is roughly 1000 K hotter than the surrounding material. We do not observe significant fluctuations of the field in the umbra. In the penumbra, however, the passage of the running penumbral waves alter the magnetic field strength by some 200 G (peak-to-peak amplitude) but it does not change the field orientation.

Evolution of penumbral filaments in forming sunspot

Abstract Author(s): Jan Jurcak, Nazaret Bello Gonzalez, Reza Rezaei, Rolf Schlichenmaier

Institution(s): Astronomical Institute AS CR, Kiepenheuer-Institut fur Sonnenphysik, Schoneckstr. 6, 79104 Freiburg, Germany , Kiepenheuer-Institut fur Sonnenphysik, Schoneckstr. 6, 79104 Freiburg, Germany , Kiepenheuer-Institut fur Sonnenphysik, Schoneckstr. 6, 79104 Freiburg, Germany

Presentation: S1-P-09

Abstract

We analyse formation of penumbral filaments with respect to the magnetic field configuration in active region NOAA 11024. We use spectropolarimetric data obtained by the GFPI instrument attached to the German VTT and by the Hinode satellite. The preliminary results suggest that the penumbral filaments form on the umbra/quiet Sun boundary when the magnetic field inclination is higher than 50 degrees (with respect to the local normal line). During the penumbra evolution, the heads of the filaments protrude deeper into umbra, i.e., towards stronger and more vertical magnetic field. In some segments of the developing penumbra, this inward motion is obvious and stops when the heads of the filaments reach regions with vertical component of magnetic field of 1900 G. This value is comparable to the one found for umbra/penumbra boundaries in developed sunspots.

Hinode-7
Session 1: Magnetic Fields and Solar Cycle

Structure of sunspot penumbral filaments as obtained by spatially coupled inversion of Hinode (SOT/SP) data

Abstract Author(s): Sanjiv Kumar Tiwari, Michiel van Noort, Andreas Lagg, Sami K. Solanki

Institution(s): Max-Planck Institute for Solar System Research, Max Planck Institute for Solar System Research, Max Planck Institute for Solar System Research, Max Planck Institute for Solar System Research

Presentation: S1-P-10

Abstract

The sunspot penumbra is composed of copious thin, radially elongated filaments. These filaments are responsible for heat transport in the penumbra but their structure is still not clear. We have utilized the inversion code SPINOR, in its spatially coupled mode, to obtain the height stratification of thermal, magnetic and velocity parameters of a sunspot observed nearly at solar disc center by SOT/SP onboard Hinode. The new technique, spatially coupled inversion, can resolve fine structures up to the diffraction limit of the telescope. The inversion output allowed us to identify and isolate a number of filaments from all parts of the sunspot penumbra. Filaments of different sizes show very similar thermal, magnetic, and velocity patterns in all parts of the sunspot penumbra except for a difference in the temperature at the tails of outer penumbral filaments, them being hotter in comparison to that of the inner ones. To reveal the common physical properties to all of them and reduce the fluctuations in the surroundings, we averaged all the selected filaments. The averaged filament displays upflows with upward directed field at the heads, downflows with downward directed field at the tails, and upflows continuing along the filament axis for more than half of its length with lateral downflows along its sides. The upflowing gas is hotter than the downflowing gas. Magnetic field strength in the bulk of the filament is of the order of 1 kG. We, for the first time, present a rather complete picture of the sunspot penumbral filaments. Our illustration is consistent with penumbral filaments being magneto-convective cells, in line with recent MHD simulations. In addition, we also investigate the nature of the Evershed flow in penumbral filaments of several sunspots observed at different solar disc positions by SOT/SP.

Hinode-7
Session 1: Magnetic Fields and Solar Cycle

Temporal evolution of the velocity of lateral downflows in sunspot's penumbra

Abstract Author(s): Sara Esteban Pozuelo, Luis Ramon Bellot Rubio, Jaime de la Cruz Rodriguez

Institution(s): Instituto de Astrofisica de Andalucia (IAA - CSIC)

Presentation: S1-P-11

Abstract

The brightness of the sunspot's penumbra is a challenging issue. Many theoretical models have tried to illustrate how matter moves in a strongly magnetized medium where convective transport must be inhibited. 3D MHD simulations have shown a convective driven mechanism. And, observational analysis have corroborated it detecting downflows at the edges of the filaments using deconvolved spectropolarimetric data. Deconvolution was needed because it was thought that straylight contamination disables to detect lateral downflows. Recently, Tiwari et al. (2013) have also found them making use of spectropolarimetric data obtained by SOT/SP on board the Hinode spacecraft.

We have detected downflows at the rims of penumbral filaments using a temporal sequence of high-resolution spectropolarimetric data without deconvolution. We can observe how they evolve and some of them move together with blueshifted filaments. Thanks to the image quality, our goal is to study the temporal velocity behavior of these downflows. For this purpose, the used data were obtained with CRISP at the SST of a sunspot located close to the center of the solar disk. In order to calculate the LOS velocity in deeper layers, we have applied the bisector technique to the intensity profiles of Fe I 6173 A. Besides, we have deconvolved our data to be able to compare our study to those performed previously. Downflows observed in undeconvolved data are enfatized in deconvolved ones. Thence, downflow appearing is not only due to deconvolve data.

Hinode-7
Session 1: Magnetic Fields and Solar Cycle

Magnetometry from HINODE/SOT/SP data: solving the fundamental ambiguity from the 6301/6302 line pair inversion

Abstract Author(s): Veronique Bommier

Institution(s): LESIA, Observatoire de Paris

Presentation: S1-P-12

Abstract

Following Khomenko & Collados (2007), the two Fe I 6301.5 and 6302.5 A lines are similarly formed with a spatially constant formation depth difference. Faurobert et al. (2009) achieved a direct measurement of this difference by Fourier phase shift analysis of HINODE/SOT/SP data. We applied the UNNOFIT Milne-Eddington inversion (Bommier et al., 2007) to the two lines separately, determining the field vector at each formation depth. These field vectors are ambiguous in the so-called 180 ° azimuthal or fundamental ambiguity, where two field vectors symmetrical with respect to the line-of-sight have identical Zeeman effect signature and cannot be discriminated. Advantage is taken from the formation depth difference to solve the ambiguity by minimizing |divB| derived from the line pair observation. We applied the ME0 code by Metcalf et al., in which we replaced the extrapolated vertical dependence by the observed one. 23 examples of resolved maps can be seen at http://lesia.obspm.fr/perso/veronique-bommier/, concerning isolated sunspots as well as more complex active regions. Once the ambiguity is solved at the two different depths, it is possible to derive the current density full vector, and in particular its horizontal component, which remains inaccessible to single line observations like for instance the ones of SDO/HMI. We will present the main features of the horizontal current component as we observe it in the 23 maps. When doing this resolution, we were faced with the very surprising feature that the horizontal magnetic field gradient is of 0.3 G/km whereas the vertical one is of 3 G/km in sunspots, a feature confirmed in the literature, leading to a non-zero |divB|. We guessed that this difference is a consequence of the strong stratification of the solar surface, and we propose that the non-zero |divB| is the result of a plasma effect, the Debye shielding made anisotropic by the stratification.

The Association of Polar Faculae with Polar Magnetic Patches Examined with Hinode/SOT-SP Observations

Abstract Author(s): Anjali John Kaithakkal, Yoshinori Suematsu, Masashito Kubo, Daikou Shiota, Saku Tsuneta

Institution(s): SOKENDAI, NAOJ, NAOJ, NAOJ , STEL,Nagoya University, ISAS/JAXA

Presentation: S1-P-13

Abstract

Polar faculae are bright, small-scale features in the polar region of the Sun. They are observed with concentrations of magnetic fields. Previous studies have shown that the number of polar faculae follows an 11 year cycle that is anti-correlated with the sunspot cycle. The aim of this study is to understand the magnetic properties of polar faculae, which are generally associated with the polar magnetic patches. We analyzed data of the north polar region taken by the Hinode/SOT spectropolarimeter (SP) in September 2007. Accurate measurements of vector magnetic fields at high spatial resolution by Hinode/SP for the first time allow us to compare polar faculae with the associated magnetic fields in detail. The continuum intensity map is corrected for limb darkening to identify the faculae by their relative brightness. There are many patchy magnetic field structures in the polar region and thresholds on both size and intensity for the patches are applied to identify polar faculae pixels. The definition of magnetic patches is the same as in Shiota et al. (2012 ApJ). We find that: (1) The polar faculae are embedded in nearly all magnetic patches with fluxes greater than 10^{18} Mx, while magnetic patches without polar faculae dominate in the flux range below 10^{18} Mx. (2) The faculae are considerably smaller than their parent patches, and single magnetic patch contains single or multiple faculae. (3) The faculae in general have higher intrinsic magnetic field strengths than the surrounding regions within their parent patches. (4) Less than 20% of the total magnetic flux contributed by the large ($> 10^{18}$ Mx) field concentrations, which are known to be modulated by the solar cycle, is accounted for by the associated polar faculae.

Hinode-7
Session 1: Magnetic Fields and Solar Cycle

Study of 3D Fine-Scale Structure and Dynamics of Solar Polar Faculae

Abstract Author(s): Yoshinori Suematsu, Anjali John Kaithakkal

Institution(s): National Astronomical Observatory of Japan

Presentation: S1-P-14

Abstract

The three dimensional fine-scale structure and dynamics of solar polar faculae were studied using Hinode/SOT filtergraphic observations at polar regions in G-band, Ca II H and H-alpha line. To elucidate finer scale structure of the faculae, we improved time series of images from G-band and Ca II H by applying a super-resolution technique to derive structures finer than the diffraction-limit of the SOT. As a result, much thinner structures of close to 0.1 arcsec are being revealed and the faculae appear as a cluster of thin tapered tube-like structures; individual size is about 0.2 x 0.5 arcsec, reaching the maximum closer mid-way to the limb, are likely projected on the limb-side neighboring granules with center-ward dark lanes in G-band. Typical lifetime of each facular elements is about five minutes, showing side-way motion during the life. Corresponding bright fine elongated structures are seen in Ca II H, although such structures are more numerous and therefore there does not always exist one-to-one correspondense of Ca II H bright structures with the G-band facular elements. In H-alpha, fibril structure emanating limb-ward from the faulae and Ca II H bright regions. Those facts imply that the polar faculae appear in the root of intense vertically-oriented thin magnetic flux tubes. We give detailed characteristics of fine-scale structure and dynamics of the polar faculae, discussing about the hot-wall flux tube model to interpret them.

SST/CRISP observations of penumbral convective flows in the Fe I 5576 and 6301/6302 lines

Abstract Author(s): Goran B. Scharmer, Jaime de la Cruz Rodriguez

Institution(s): Institute for Solar Physics of Stockholm University

Presentation: S1-P-15

Abstract

We report on convective flows in a sunspot penumbra observed with SST/ CRISP at a spatial resolution of 0.15 arcsec in the Fe I 5576 and 6301/6302 lines. The data are processed with MOMFBD image reconstruction and are compensated for straylight. Using NICOLE inversions allowing for line-of-sight gradients in the atmospheric properties, we unveil signatures of convective flows, opposite polarity field and Evershed flows in magnetic intra-spines. These flow properties are consistent with the convective gap model proposed in 2006 and recent simulations by Rempel et al.

Hinode-7
Session 1: Magnetic Fields and Solar Cycle

Displacement of patch structures and its insight to magnetic flux transport in magneto-convection system

Abstract Author(s): Yusuke Iida

Institution(s): ISAS/JAXA

Presentation: S1-P-16

Abstract

Spatial displacement of patch structure on the solar surface in several quiet regions is investigated based on auto-tracking technique in this presentation.

Magento-convection system on the solar surface is important not only as energy storage of various solar activities but also as an actual example of magneto-convection. One important issue is how magnetic flux is transported there. One of the critical characters for the description is the dependence of mean-square distance on the elapsed time. Our aim in this study is to investigate it by using SOT/FG magnetograms and to obtain description of flux transport on the solar surface.

Several sets of quiet region magnetograms are used in this study. In each data set, number of tracked patches is enough for statistical study, more than 40000 in the longest date set. The obtained dependence of mean-square distance of patches on time show a different character above and below the point of L$\sim$ 10^4 km. Below that scale, it has a power-law dependence with an index of $\sim$ -1.4, namely super-diffusion scheme. However, in the larger scale, the power-law dependence becomes ~ -0.6, namely sub-diffusion scheme. These characters can be explained by the network flow pattern qualitatively. Below the network scale, patch is transported by constant flow ($\sim$ 0.3km s^{-1}) from center of network cell to edge of the cell addition to the large ($\sim$ 1km s^{-1}) perturbing flow of granulation. On the other hand, above the network scale, patches experience the trapping around flow conjunction point, which makes displacement of patch shorter than that only by diffusion motion.

In the presentation, I will make further discussion about the dependence on flux imbalance.

Hinode-7
Session 1: Magnetic Fields and Solar Cycle

Parallelization of the SIR Code for the investigation of the dynamics of magnetic flux tubes

Abstract Author(s): Stefan Thonhofer, Luis Bellot Rubio, Dominik Utz, Arnold Hanslmeier, Isabell Piantschitsch, Jurgen Pauritsch, Birgit Lemmerer

Institution(s): Instituto de Astrofisica de Andalucia and University of Graz, Instituto de Astrofisica de Andalucia, Granada, Spain, IGAM/Institute of Physics, University of Graz, Austria, IGAM/Institute of Physics, University of Graz, Austria, IGAM/Institute of Physics, University of Graz, Austria, IGAM/Institute of Physics, University of Graz, Austria, IGAM/Institute of Physics, University of Graz, Austria

Presentation: S1-P-17

Abstract

A high-resolution 3-dimensional model of the magnetic field configuration in the solar photosphere is essential for the investigation of magnetic flux tubes. In order to study their dynamic behavior it is furthermore necessary to observe them over a sufficiently long time range. The SIR Code is an advanced inversion code that retrieves physical quantities, e.g. the magnetic field or the line-of-sight velocity, from Stokes profiles. In order to improve the runtime performance we parallelized the SIR Code using an established message-passing system. This enables us to invert a large number of spectropolarimetric images in an efficient way. Based on these inversion results we investigate the properties of selected flux tubes. We focus on the temporal evolution of the stratification of the line-of-sight velocity in order to observe shock fronts ascending from flux tubes which have already been found in simulations.

Hinode-7
Session 1: Magnetic Fields and Solar Cycle

The evolution of important magnetic bright point parameters

Abstract Author(s): Dominik Utz, Jose Carlos del Toro Iniesta, Luis Bellot Rubio, Jan Jurcak, Stefan Thonhofer, Isabell Piantschitsch, Birgit Lemmerer, Arnold Hanslmeier

Institution(s): IGAM/Institute of Physics, Karl Franzens University Graz, Instituto de Astrofisica de Andalucia, CSIC, Granada, Instituto de Astrofisica de Andalucia, CSIC, Granada, Astronomical Institute, Academy of Sciences of the Czech Republic, IGAM/Institute of Physics, Karl Franzens University of Graz, IGAM/Institute of Physics, Karl Franzens University of Graz, IGAM/Institute of Physics, Karl Franzens University of Graz, IGAM/Institute of Physics, Karl Franzens University of Graz

Presentation: S1-P-18

Abstract

The activity of the Sun is caused by its ever changing magnetic fields. The stronger and more extended ones have played a key-role in solar research over the last centuries. Due to newly installed ground-based and space-borne telescopes (such as NST, Hinode, Sunrise), it became possible to study fields on ever smaller scales reaching nowadays down to hundreds of km in diameter and making it possible to resolve single flux tubes.

Good candidates for isolated magnetic flux tubes are so-called magnetic bright points (MBPs). These features have been studied exhaustively in the G-band since the 70's of the last century. Most of the past studies concentrated on purely photometric investigations and parameters like size and brightness. In the current study we will use the Hinode/SP and Sunrise/IMaX instruments to investigate spectro-polarimetric data. Therefore we can apply inversion codes such as SIR or Merlin on these data sets and retrieve plasma physical parameters such as temperature and the vector magnetic field. We study the temporal evolution of these important parameters of MBPs to shed more light on the physics of MBPs and especially what happens during their evolution (coupling of plasma flows and magnetic field characteristics).

Hinode-7
Session 1: Magnetic Fields and Solar Cycle

Kinetic and magnetic power spectra in the supergranular-scale convection studied by three-dimensional radiative magnetohydrodynamic simulations

Abstract Author(s): Haruhisa Iijima, Takaaki Yokoyama

Institution(s): The University of Tokyo

Presentation: S1-P-19

Abstract

We use three-dimensional magneto-convection simulation to investigate the possible mechanism of the magnetic network and supergranulation. The simulation includes gray radiative transfer and realistic equation of state. Those described below is our preliminary results. The numerical box size is 100x100x20 Mm^3. The uniform vertical magnetic field of 10 G is introduced on the relaxed non-magnetic simulation for the initial condition. The network-like structure of vertical magnetic field appears near the photosphere. The horizontal power spectrum of the vertical magnetic field has a peak around the wave length of 25 Mm. The spectral peak of horizontal magnetic field appears at shorter wave length of 1 Mm. The network magnetic field becomes sufficiently strong so that it affects the velocity field. The horizontal velocity spectrum is enhanced near the supergranular-scale compared with the weak magnetic field case (initial magnetic field strength of 0.1 G).

Hinode-7
Session 1: Magnetic Fields and Solar Cycle

Center-to-limb variation in Ellerman bombs observed in Halpha and 1700 A

Abstract Author(s): Gregal Vissers, Luc Rouppe van der Voort, Rob Rutten

Institution(s): Institute of Theoretical Astrophysics, Oslo, Institute of Theoretical Astrophysics, University of Oslo , Institute of Theoretical Astrophysics, University of Oslo

Presentation: S1-P-20

Abstract

We present a study of transient events known as Ellerman bombs using high-resolution imaging spectroscopy in Halpha from the CRisp Imaging SpectroPolarimeter (CRISP) at the Swedish 1-m Solar Telescope (SST) and simultaneous imaging in the 1700 A channel from the Atmospheric Imaging Assembly (AIA) on the Solar Dynamics Observatory (SDO). The Ellerman bombs show up at regular bright points outlining magnetic network in the observed active regions, but flare upward with much larger brightness and distinct jet morphology, which becomes more pronounced with increasing limbward view of the data. Their morphology and occurrence location with respect to the underlying magnetic field are indicative of reconnection.

We apply an automated detection algorithm that selects Ellerman bomb candidates in both Halpha and 1700 A based on brightness, size and lifetime constraints. We investigate the center-to-limb variation in observed Ellerman bomb properties and present statistics on their lifetimes, sizes, elongation and brightness as function of viewing angle. Even though not all Ellerman bombs detected in Halpha are recovered in the AIA 1700 A data, our results suggest that the latter may be used for full-disk monitoring of Ellerman bomb occurrence and, consequently, of small-scale reconnection in emerging active regions.

Hinode-7
Session 1: Magnetic Fields and Solar Cycle

Small-scale dynamic fibrils in sunspot chromospheres

Abstract Author(s): Luc Rouppe van der Voort, Jaime de la Cruz Rodriguez

Institution(s): University of Oslo, Uppsala University

Presentation: S1-P-21

Abstract

Sunspot chromospheres display vigorous oscillatory signature when observed in chromospheric diagnostics like the strong Ca II lines and H-alpha. New high resolution SST/CRISP observations reveal the ubiquitous presence of small-scale periodic jets that move up and down. Their widths are often less than 0.5 arcsec and they display clear parabolic trajectories in space-time diagrams. The maximum extension of the top of the jets is lowest in the umbra, a few hundred 100 km, and progressively longer further away from the umbra in the penumbra, with the longest more than 1000 km. These jets resemble dynamic fibrils found in plage regions but at smaller extensions. LTE inversion of spectro-polarimetric Ca II 8542 observations allow for a comparison of the magnetic field inclination and properties of the small-scale jets. There is a clear correlation for the spatially longer, long-period jets to be located in regions with more horizontal magnetic fields. This is a direct observational confirmation of the mechanism of long-period waves propagating along inclined magnetic fields into the solar chromosphere. This mechanism was identified earlier as the driver of dynamic fibrils in plage and mottles.

Hinode-7
Session 1: Magnetic Fields and Solar Cycle

Hinode/SOT and IRIS observations of Sunspot and Chromospheric Oscillations

Abstract Author(s): Richard Alan Shine, Alan M Title

Institution(s): LMSAL, LMSAL

Presentation: S1-P-22

Abstract

The Ca H filter on the SOT/FPP instrument on Hinode shows the well known types of chromosperic and sunspot oscillations including umbral flashes and running penumbral waves. With the recent launch of the Interface Region Imaging Spectrograph (IRIS) in June 2013, we can now also study these with Mg II, C II, and Si IV imaging and spectra in these and additional nearby lines. Although some of the types of oscillations seen in the IRIS data are familiar from groundbased and other spacebased observations, the detail is remarkable and the spectra provide additional physical attribues of the solar plasma. Together with Hinode data from the photosphere and chromosphere, they provide information on the origin and propogation of local oscillations and their relationship to photospheric and chromospheric features. We review earlier results from Hinode and present some early examples of IRIS data including planned co-spatial/temporal Hinode/IRIS sets.

This work was supported by NASA contract NNM07AA01C.

Hinode-7
Session 1: Magnetic Fields and Solar Cycle

Simulation of the dynamics of small scale magnetic fields in the lower solar atmosphere in regards of the atmospheric heating problem

Abstract Author(s): Isabell Piantschitsch, Stefan Thonhofer, Dominik Utz, Arnold Hanslmeier, Jurgen Pauritsch, Miroslav Barta, Birgit Lemmerer

Institution(s): Universitatsplatz 5, 8010 Graz, Austria

Presentation: S1-P-23

Abstract

To the present day there is no complete understanding why the upper layers of the sun, i.e. chromosphere, transition region and corona, possess higher temperatures than the surface of the sun. Therefore, there must be some sort of heating mechanism which keeps up these high temperatures. In the literature we encounter two different basic concepts which are capable of explaining this behaviour, namely wave heating and heating by reconnection. One possible source for these heating processes is the dynamics of small scale magnetic fields in the photosphere. These dynamic processes can cause different forms of magnetohydrodynamic (MHD) waves which propagate into the chromosphere and/or lead to reconnection. In order to describe and explain the movements of these magnetic fields and their effects in the chromosphere numerical simulations regarding the required region of the sun are essential. For that purpose we apply the Total Variation Diminishing (TVD) Lax-Friedrichs method do develop a parallelized numerical two- fluid MHD code which performs a 2.5D simulation of the above described dynamic processes and which includes the effects of ion-neutral collisions, ionisation/recombination, thermal/resistive diffusivity and collisional/resistive heating. Furthermore, the results of the simulations will be compared to Hinode SOT/SP data to get useful information concerning the atmospheric heating problem.

Recent RMHD simulations with CO5BOLD

Abstract Author(s): Oskar Steiner

Institution(s): Kiepenheuer-Institut

Presentation: S1-P-24

Abstract

We have carried out new, explorative high-resolution simulations on solar and stellar 'box-in-a-star' models with the CO5BOLD code. This poster presents a few aspects on these latest runs.

Hinode-7
Session 1: Magnetic Fields and Solar Cycle

Detection and analysis of small scale convective patterns observed with Hinode compared to RHD simulations

Abstract Author(s): Birgit Lemmerer, Dominik Utz, Arnold Hanslmeier, Astrid Veronig, Stefan Thonhofer, Hannes Grimm-Strele

Institution(s): IGAM-Kanzelhoehe Observatory Institute of Physics, University of Graz

Presentation: S1-P-25

Abstract

New results from high resolution solar granulation observations reveal the existence of a subpopulation of small granular structures on scales below 600 km in diameter, which strongly contribute to the total area of granules. These small convective cells are located in the intergranular lanes, predominantly forming chains and clusters.We developed an automated image segmentation algorithm specifically adapted to observations obtained from the Hinode spacecraft as well as to high resolution simulations for the identification and tracking of granules. The resulting segmentation masks are applied to continuum images and Dopplergrams as well as to physical quantities provided by the simulation. A new clustering algorithm was developed in order to study the alignment of small granular cells. We found that small granules make a distinct contribution to the total area of granules and form clusters of chain-like alignments. These cells exhibit on average lower intensities and their intensity distribution deviates from a normal distribution, as known for larger granules.

Relation between magnetic fields and horizontal velocity in an active region

Abstract Author(s): Ryouhei Kano, Kohei Ueda, Saku Tsuneta

Institution(s): National Astronomical Observatory of Japan

Presentation: S1-P-26

Abstract

We investigate the photospheric properties (vector magnetic fields and horizontal velocity) in a well-developed active region, NOAA AR 10978, by using the Hinode Solar Optical Telescope (SOT), especially for discussing what makes coronal loops so different in temperature from "warm loops" (1–2 MK) observed in EUV wavelengths to "hot loops" (>3 MK) in X-rays. We found that outside sunspots the magnetic filling factor in network varies with location, and anti-correlated with the horizontal random velocity. If we accept that the observed magnetic features consist of unresolved magnetic flux tubes, this anti-correlation can be explained well by the ensemble average of the flux-tube motion driven by small-scale random flows. The observed data are consistent with the flux tube of ∼77 km, and the flow at ∼ 2.6 km/s with its spatial scale of ∼ 120 km. We also found that outside sunspots there is no significant difference between warm and hot loops either in the magnetic properties except the inclination or in the horizontal random velocity at their footpoints, which are identified with the Hinode X-ray Telescope (XRT) and the Transition Region and Coronal Explorer (TRACE). The energy flux injected into the coronal loops by the observed photospheric motion of the magnetic fields is evaluated to be 2×10^6 erg/s/cm^2, which is the same for both warm and hot loops. This suggests that coronal situation (e.g. loop length) plays more important role for making a variety of temperature in coronal loops than the photospheric parameters.

Very strong magnetic fields in supersonic downflows

Abstract Author(s): Michiel van Noort, Andreas Lagg, Sanjiv Tiwari, Sami Solanki

Institution(s): Max Planck Institute for solar system research, Max-Planck institute for Solar system research, Max-Planck institute for Solar system research

Presentation: S1-P-27

Abstract

We applied the spatially coupled SPINOR inversion code to Hinode SP scans of two separate sunspots to obtain a simplified, height-stratified atmosphere of both. A statistical analyisis of the penumbral downflows in both sunspots shows a clear relation between downflow velocity and magnetic field strength in the downflow regions. The fastest and largest downflows are found on the outer edge of the penumbra and contain magnetic fields with a field strength in excess of that found in the sunspot umbra. This result is in good qualitative and quantitative agreement with the downflows found in a recent MHD simulation of a sunspot. A small number of very fast downflows was found in the inverted atmospheres that were not present in the MHD simulation. A detailed analysis of these downflows showed that they are associated with external patches of magnetic field, that they are long-lived and that they show signs of heating in the upper photosphere. These downflows were found to be highly supersonic and appear to contain magnetic fields with a field strength in excess of 7kG.

Hinode-7
Session 1: Magnetic Fields and Solar Cycle

The photospheric magnetic field measurement with Tandem Etalon Magnetogprah (TEC) of SMART telescope at Hida Observatory

Abstract Author(s): Takatoshi Fukuoka, Shin'ichi Nagata, Kiyoshi Ichimoto

Institution(s): Kyoto University

Presentation: S1-P-28

Abstract

The Tandem Etalon Magnetograph (TEM) consists of two Fabry Perot filters, two CCD camera with 30fps frame rate, rotating waveplate and polarizing beam splitter. We can obtain the Stokes profile of Fe I 6302.5A with this instrument. We have compared the Stokes maps obtained with TEM and that with Helioseismic and Magnetic Imager (HMI) onboard Solar Dynamic Observatory (SDO). We found that photometric accuracy of the Stokes map of TEM deduced from the 20 sec duration reaches to 3×10^{-4}, and confirmed this was better than that of HMI/SDO. Now, we are developing the Stokes Inversion code for TEM. The code is besed on that of Narrow band Filter Instrument (NFI) equipped in Solar Optical Telescope (SOT) onboard Hinode. In this paper, we discuss the optimization of the inversion code by using the simulation based on Millen Edington atmosphere mode, also we compare the observations with TEM, SOT/SP, and SDO/HMI.

Hinode-7
Session 1: Magnetic Fields and Solar Cycle

Statistical Analysis of Current Helicity Using Hinode/SOT SP Data

Abstract Author(s): Kenichi Otsuji, Takashi Sakurai, Kirill Kuzanyan

Institution(s): National Astronomical Observatory of Japan Solar Observatory

Presentation: S1-P-29

Abstract

We performed a statistical study on the current helicity of solar active regions observed with the Spectro-Polarimeter (SP) of Hinode Solar Optical Telescope (SOT). Current helicity is an observational proxy of mean magnetic helicity in solar active regions (Zhang et al. 2012) and generally negative in the northern hemisphere and positive in the southern hemisphere. Hagino and Sakurai (2005) pointed out that this hemispheric sign rule may be violated at the beginning of solar cycles.

In our study, we used SOT SP data obtained from 2006 to 2012. To compare our result to the ground-based observational study, we calculated the current helicity using several different magnetic field strength ranges and seeing parameters. We found that the current helicity follows the normal hemispheric sign rule when the weak magnetic strength range is considered and no seeing effect is adopted. On the other hand, the pattern of current helicity fluctuates and violates the hemispheric sign rule when the larger magnetic field range is considered and the seeing effect (image deterioration) is introduced by smoothing the data. Furthermore, we found a tendency that the weak and inclined field obeys and the strong and vertical field violates the hemispheric sign rule. These results suggest that the ground-based observations are not directly comparable to the SOT SP data but are regarded as filtered subsets of SOT SP (true) data, in considering the seeing deterioration and field range restriction.

Spatially Resolved images of the Corona and EUV & UV Irradiance Variability

Abstract Author(s): G. Giono, J. Zender, R. Kariyappa, S.T. Kumara, V. Delouille, L. Dame, J-F. Hochedez, V. Cerbeeck, B. Mampaey

Institution(s): NAOJ, European Space Research and Technology Center (ESTEC), Noordwijk, The Netherlands, Indian Institute of Astrophysics, Bangalore 560034, India, Indian Institute of Astrophysics, Bangalore 560034, India, Royal Observatory of Belgium, Circular Avenue 3, 1180 Brussels, Belgium, LATMOS, 11 boulevard d'Alembert, 78280 Guyancourt, France, LATMOS, 11 boulevard d'Alembert, 78280 Guyancourt, France, Royal Observatory of Belgium, Circular Avenue 3, 1180 Brussels, Belgium, Royal Observatory of Belgium, Circular Avenue 3, 1180 Brussels, Belgium

Presentation: S1-P-30

Abstract

The Sun is the primary source of energy responsible for governing both the weather and climate of Earth. For that reason alone one would expect that changes in the amount and type of energy Earth received from the Sun could alter weather and climate on the Earth. The variations in the EUV & UV irradiance are produced by surface manifestation of solar magnetic activity. Considering the variations in the solar EUV & UV flux may cause significant changes in the Earth's climate, understanding the physical origin of EUV & UV irradiance changes is an extremely important issue in Solar and Space Physics.

In our work we studied coronal features (active regions, quiet Sun and coronal holes) observed with EUV telescopes AIA onboard SDO (NASA) and SWAP onboard PROBA2 (ESA). We tracked these features from January 2011 to December 2012 using the Spatial Possibilistic Clustering Algorithm (SPoCA) developed at the Royal Observatory of Belgium. This software produces segmentation map for each AIA images used during the two years period. Maps were then used to extract the intensity & filling factors (area) of the coronal features from AIA & SWAP images. We compared the intensity received by the EUV telescopes for each coronal features with full-disk irradiance measurements at the same wavelength from LYRA radiometer onboard the PROBA2 spacecraft.We found that active regions have a great impact on the irradiance fluctuation, having the highest correlation coefficient of the coronal features to the total irradiance measured by LYRA. However the quiet Sun appears to be the greatest contributor to the solar irradiance, with up to 63% of total intensity value. We also find that area of the features is highly variable suggesting that their area has to be taken into account in the irradiance models, in addition to their intensity variations.

How Spatial Resolution in Boundary Data Affects Coronal Magnetic Field Extrapolations

Abstract Author(s): Marc L. DeRosa, Michael S. Wheatland

Institution(s): Lockheed Martin Solar and Astrophysics Laboratory, School of Physics, University of Sydney, Sydney, Australia

Presentation: S1-P-31

Abstract

Previous investigations into the determination of nonlinear force-free fields (NLFFFs) of the solar corona had uncovered several factors that affected the ability to obtain reliable results. Of these factors, the effects due to the spatial resolution of the photospheric vector magnetogram boundary data were hypothesized to be significant, due to the apparent fine-scale nature of vertical currents present in high-resolution vector data. Here, we test this hypothesis by performing extrapolations of the coronal magnetic field overlying AR10978 of December 2007, using high-resolution polarization spectra from the spectropolarimeter on Hinode-SOT in normal-map mode that have been rebinned by various factors prior to being inverted into vector magnetograms. We illustrate the effects of such binning, which ranges from a factor of 1 (0.16" pixels, i.e., native normal-map resolution) to 16 (2.56" pixels), by intercomparing the resulting field models using these binned boundary data, and discussing the ramifications for current and future instrumentation (e.g., SDO/HMI and Solar-C).

Transition from two helmet streamers into a coronal pseudostreamer

Abstract Author(s): Laurel A. Rachmeler, Daniel B. Seaton, Christian W. Bethge, Sarah J. Platten, Anthony R. Yeates

Institution(s): Royal Observatory of Belgium

Presentation: S1-P-32

Abstract

Both pseudostreamers and helmet streamers have been studied at length, and we present the first known analysis that connects the two into a single magnetic structure. A helmet streamer occurs at the boundary between open field regions of opposite polarity, resulting in a coronal current sheet which is usually seen above a filament channel. Pseudostreamers are similar in that they occur at the boundary between two open field regions, but in this case the field is of the same polarity. Large-scale pseudostreamers are usually seen above a pair of roughly parallel filament channels. We present an observation of two long-lived filament channels that converge such that initially on the solar limb two helmet streamers are seen, which transition into a pseudostreamer at a later time due to the disappearance of open field between the two filaments. This single magnetic structure is relatively static in time such that the transition is spatial rather than temporal. We use a range of observations, including the PROBA2/SWAP EUV imager and CoMP coronal polarization to support our analysis of the structure.

Measurements of Coronal and Chromospheric Magnetic Fields using Polarization Observations by the Nobeyama Radioheliograph

Abstract Author(s): Kazumasa Iwai, Kiyoto Shibasaki

Institution(s): Nobeyama Solar Radio Observatory, National Astronomical Observatory of Japan, Nobeyama Solar Radio Observatory, National Astronomical Observatory of Japan

Presentation: S1-P-33

Abstract

The magnetic field of the solar atmosphere is an important clue to understanding and forecasting many solar phenomena such as flares and coronal mass ejections. In magnetized plasma, ordinary and extraordinary modes of the radio free-free emission have different optical depths. Hence, the radio circular polarization observation enables us to derive the longitudinal component of the magnetic field. In this study, we have derived coronal and chromospheric magnetic fields from circular polarization observations by Nobeyama Radioheliograph (NoRH).

NoRH observes the full solar disk every 1 second at 17 GHz (intensity and circular polarization) and 34 GHz (intensity). We observed an active region on April 13, 2012. The observed degree of circular polarization was between 0.5 % and 1.7 %. The magnetic fields are derived from the observed radio circular polarization and the spectral index of the brightness temperature. The ratio of the observed radio magnetic field and the corresponding photospheric magnetic field is about 0.2 to 0.5 at the center of the active region.

The observed radio magnetic fields contain both the coronal and chromospheric components. We assume that the solar atmosphere observed in the microwave range has two components: the optically thin corona and the optically thick chromosphere. At the edge of the active region, radio circular polarization is observed even though the corresponding magnetic field at the photosphere is almost 0 G. On the other hand, the location of the observed radio circular polarization corresponds to that of the coronal loop structures. Therefore, we can assume that there is almost no chromospheric circularly polarized component there and derive the pure coronal magnetic field strength. At the center of the active region, the chromospheric and coronal components cannot be separated, and the derived magnetic field is emission-measure weighted.

Longitudinal structure of the polar field reversal and decadal trend of the sunspot's gyroresonance emissions in 17 GHz

Abstract Author(s): Yuki Tanaka, Hiroko Watanabe, Tomoko Kawate, Kiyoshi Ichimoto, Kiyoto Shibasaki, Kenichi Otsuji, Takehiro Miyagoshi

Institution(s): Kyoto University, Kyoto University, Kyoto University, Kyoto University, Nobeyama Radio Observatory, NAOJ, NAOJ, JAMSTEC

Presentation: S1-P-34

Abstract

The polar magnetic field is recognized as a fundamental ingredient of the solar activity cycle, and its strength at the minimum phase of the solar activity is found to be correlated with the strength of the following solar cycle. Therefore the details of process of the polar field reversal is of particular interest for understanding the mechanism of the solar magnetic cycle and its prediction. The butterfly diagram made from solar magnetograms demonstrates the poleward migration of magnetic flux, which eventually causes the reversal of polar magnetic field in Sun's 11-year cycle. Since usual butterfly diagram is made by integrating synoptic maps in longitude, any information about longitudinal distribution of magnetic field are lost. But, according to Ichimoto et al. 1985 or Berdyugina et al. 2006, it is known that there are characteristics structures of solar activity in longitudinal direction. We investigate the longitudinal structure in transportation of polar magnetic fields by using ' special ' butterfly diagrams for longitudinal segments and time series of pole-on view maps of magnetic field. As a result, we found an evidence of ' active longitudes ' in transportation of polar magnetic fields in solar cycle 23 and 24. Furthermore, we investigated the long term variation of the sunspot's magnetic flux by using the gyroresonance emissions in 17GHz recorded at the Nobeyama Radio Heliograph for past 20 years. We found that the occurrence of strong gyroresonance emission is significantly enhanced in the later phase of cycle 23 and it is far diminished in cycle 24. These results may provide a new insight for the recent peculiar behavior of the solar activity.

Hinode-7

Session 2

Atmospheric and Interior Couplings

Hinode-7
Session 2: Atmospheric and Interior Couplings

Overview of IRIS First Observations

Abstract Author(s): Alan M Title, the IRIS Team

Institution(s): LMSAL

Presentation: S2-I-01

Abstract

The Interface Region Imaging Spectrometer (IRIS) was launched in June, 2013, and underwent successful commissioning in July and August. Observations for the initial science plan began in late August. This talk will give an overview of the first observations of the chromosphere, transition region and corona in quiet sun, coronal holes, active regions, sunspots, filaments and prominences.

First Results from Coordinated Observing with IRIS, Hinode, and Ground-Based Observatories

Abstract Author(s): Ted Tarbell, the IRIS Team

Institution(s): LMSAL

Presentation: S2-C-01

Abstract

The NASA Small Explorer Interface Region Imaging Spectrometer (IRIS) was launched in June, 2013, and underwent successful commissioning in July and August. IRIS obtains UV spectra and images with high spatial resolution (0.33 arcsec) and high time cadence (1 sec) of the chromosphere and transition region of the Sun. It does not measure magnetic fields, and so the mission plans from the beginning have included coordination with other observatories to provide these, as well as additional coverage of chromospheric and coronal images and spectra. Coordinated observing with Hinode and with ground-based observatories, including Big Bear, the National Solar Observatory, and the Swedish Solar Telescope on La Palma, began in August. An extended campaign with SST from late August through early October (HOP 236) has been scheduled, performed by LMSAL and Oslo Co-I's. In these campaigns, Hinode SOT provides photospheric magnetic fields with high resolution and sensitivity, and the ground-based observatories provide chromospheric magnetic field measurements (and other images) in Ca II 8542 and/or He I 10830. IRIS performs observations from its initial observing plan on a variety of solar targets, and the other observatories follow its lead. This talk will describe some of these coordinated campaigns and first scientific results from them.

Hinode-7
Session 2: Atmospheric and Interior Couplings

Determination of Prominence Plasma β from the Dynamics of Rising Plumes

Abstract Author(s): Andrew Stephen Hillier, Richard Hillier, Durgesh Tripathi

Institution(s): Kwasan Observatory, Kyoto University; Department of Aeronautics, Imperial College; Inter-University Centre for Astronomy and Astrophysics

Presentation: S2-C-02

Abstract

Observations by the Hinode satellite show in great detail the dynamics of rising plumes, dark in chromospheric lines, in quiescent prominences that propagate from large ($\sim$10 Mm) bubbles that form at the base of the prominences. These plumes present a very interesting opportunity to study magnetohydrodynamic (MHD) phenomena in quiescent prominences, but obstacles still remain. One of the biggest issues is that of the magnetic field strength, which is not easily measurable in prominences. In this paper we present a method that may be used to determine a prominence's plasma β when rising plumes are observed. Using the classic fluid dynamic solution for flow around a circular cylinder with an MHD correction, the compression of the prominence material can be estimated. This has been successfully confirmed through simulations; application to a prominence gave an estimate of the plasma β as $\beta = 0.47 \pm 0.079$ to 1.13 $\pm$ 0.080 for the range $\gamma = 1.4 - 1.7$. Using this method it may be possible to estimate the plasma β of observed prominences, therefore helping our understanding of a prominence's dynamics in terms of MHD phenomena.

Effect of Kappa-distributions on the Temperature Structure of the Prominence-Corona Transition Region

Abstract Author(s): Elena Dzifcakova, Simon Mackovjak, Petr Heinzel, Jaroslav Dudik

Institution(s): Astronomical Institute Odrejov

Presentation: S2-C-03

Abstract

The prominence-corona transition region (PCTR), with a strong gradient of temperature and density, can allow to form a non-Maxwellian electron distribution with an enhanced number of particles in the high energy tail – the kappa-distribution. Generally, the kappa-distributions influence both the ionization and excitation equlibrium. The ionization peaks are wider and shifted to lower temperatures in comparison with the Maxwellian distribution. This behavior infuences also the shapes of DEM for PCTR derived from observed line intensities. The calculated DEM for kappa-distributions are flatter than for the Maxwellian distribution. An important consequence of the kappa-distribution presence is the formation of emission lines in much wider temperature ranges. The shifted maximum of contribution to the line emision in comparison with the Maxwellian distribution is usually present. The PCTR emission in SDO/AIA bands for the kappa-distributions is also calculated. The implications for the formation temperature of observed AIA band emissions are discussed.

Hinode-7
Session 2: Atmospheric and Interior Couplings

Observations and Modelings of the Solar Flux Emergence

Abstract Author(s): Shin Toriumi

Institution(s): Department of Earth and Planetary Science, University of Tokyo

Presentation: S2-I-02

Abstract

In a wide variety of magnetic activity phenomena in the Sun, flux emergence is one of the most prominent events. It is important to study flux emergence since this is the process that transports the magnetic flux from the deep interior to the upper atmosphere, creates active regions, and sometimes causes catastrophic flaring eruptions. Recent observations have revealed that flux emergence ranges from the formation of large-scale active regions including sunspots to the small-scale events observable only with advanced instruments such as Hinode/SOT, covering a very broad spectrum of scale involved. In addition, helioseismology may allow us to investigate the process even before the flux itself appears at the visible surface of the Sun. At the same time, recent developments in the numerical modeling of flux emergence opens the door to further understanding of the physical processes such as resistive and convective emergence. In this talk, we will review the observational and numerical progress in the field of flux emergence study and discuss what should be investigated in the future.

Hinode-7
Session 2: Atmospheric and Interior Couplings

Chromospheric and coronal jets: triggering and driving processes

Abstract Author(s): Etienne Pariat

Institution(s): LESIA, CNRS, Observatoire de Paris

Presentation: S2-I-03

Abstract

In the solar atmosphere, jet-like features are observed over a broad range of spatial, energy and temporal scales. Recent solar missions (e.g. Hinode, SDO ...) have recently provided ground breaking observations of these active events. While developing in sensitively different environments, both chromospheric and coronal jets present numerous morphological similarities, pointing to a common universal mechanism generating them. Recent numerical models have improved our understand the underlying physics of these dynamic events. In this present talk, I will detail the results of several recent observations and numerical experiments of the trigger of coronal jets. I will show that magnetic reconnection is the key process and I will discuss our curent understanding of the driving process of solar jets.

Small-Scale Plasma Eruptions Driven by Magnetic Vortex Tubes

Abstract Author(s): Irina N. Kitiashvili

Institution(s): Stanford University

Presentation: S2-C-04

Abstract

The solar surface is covered by high-speed jets transporting mass and energy into the solar corona and feeding the solar wind. The most prominent of these jets have been known as spicules. However, the mechanism initiating these eruption events is still unknown. Using realistic numerical simulations we find that small-scale eruptions are produced by ubiquitous magnetized vortex tubes generated by the Sun's turbulent convection in subsurface layers. The swirling vortex tubes (resembling tornadoes) penetrate into the solar atmosphere, capture and stretch background magnetic field, and push the surrounding material up, generating shocks. Our simulations reveal complicated high-speed flow patterns and thermodynamic and magnetic structure in the erupting vortex tubes. The main results are: (1) the eruptions are initiated in the subsurface layers and are driven by high-pressure gradients in the subphotosphere and photosphere and by the Lorentz force in the higher atmosphere layers; (2) the fluctuations in the vortex tubes penetrating into the chromosphere are quasi-periodic with a characteristic period of 2-5 minutes; and (3) the eruptions are highly non-uniform: the flows are predominantly downward in the vortex tube cores and upward in their surroundings; the plasma density and temperature vary significantly across the eruptions. We investigate the spectro-polarimetric characteristics of these eruptions for the Hinode Fe I 630.15 and 630.25 nm spectral lines, and attempt to detect these using the Hinode SP data.

Hinode-7
Session 2: Atmospheric and Interior Couplings

Observations of Recurrent Coronal Jets by IRIS, Hinode and SDO

Abstract Author(s): Mark CM Cheung, Katherine K Reeves, Theodore D Tarbell, Bart De Pontieu, Yixing Fu, Alan M Title

Institution(s): LMSAL, Smithsonian Astrophysical Observatory , Lockheed Martin Solar & Astrophysics Laboratory , Lockheed Martin Solar & Astrophysics Laboratory , University of California, Berkeley , Lockheed Martin Solar & Astrophysics Laboratory

Presentation: S2-C-05

Abstract

We report on the first IRIS observations of coronal jet initiation and evolution. Over a 5-hour period on July 21st 2013, recurrent coronal jets were observed by IRIS to emanate from NOAA AR 11793. In more than one instance, double-peaked FUV spectra probing plasma at transition region temperatures (∼100,000 K) show evidence of oppositely directed (Doppler) outflows exceeding +/- 100 km/s. This result is consistent with magnetic reconnection as the mechanism for coronal jet initiation. Simultaneous observations of the region by SDO and Hinode suggest possible causes of the recurrent jets to be one (or a combination of) emerging flux, footprint rotation and flux cancellation. Time-dependent data-driven simulations are used to investigate the plausibility of these driving mechanisms.

Hinode-7
Session 2: Atmospheric and Interior Couplings

First Comparison between IRIS Data and Numerical Models

Abstract Author(s): Mats Carlsson, Bart De Pontieu, Viggo Hansteen, Tiago Pereira, Jorrit Leenaarts, Boris Gudiksen, IRIS team

Institution(s): Institute of Theoretical Astrophysics, University of Oslo, Institute of Theoretical Astrophysics, University of Oslo, Institute of Theoretical Astrophysics, University of Oslo, Institute of Theoretical Astrophysics, University of Oslo, Institute of Theoretical Astrophysics, University of Oslo

Presentation: S2-P-01

Abstract

The enigmatic chromosphere is the transition between the solar surface and the eruptive outer solar atmosphere. The chromosphere harbours and constrains the mass and energy loading processes that define the heating of the corona, the acceleration and the composition of the solar wind, and the energetics and triggering of solar outbursts (filament eruptions, flares, coronal mass ejections).

The chromosphere is arguably the most difficult and least understood domain of solar physics. All at once it represents the transition from optically thick to thin radiation escape, from gas-pressure domination to magnetic-pressure domination, from neutral to ionised state, from MHD to plasma physics, and from near-equilibrium ("LTE") to non-equilibrium conditions.

IRIS provides a leap in observational capability of the chromospheric plasma with an unprecedented combination of high spatial, temporal and spectral resolution in lines with diagnostic information all the way from the photosphere to the upper transition region. To fully extract this information it is necessary to combine the observations with numerical simulations that include a realistic description of the complicated physics of the chromosphere.

In this talk, we will present the first comparision between IRIS data and such realistic simulations, spanning the solar atmosphere from the convection zone to the corona.

Hinode-7
Session 2: Atmospheric and Interior Couplings

Diagnostic potential of CII lines for NASA/SMEX mission IRIS.

Abstract Author(s): Bhavna Rathore, Mats Carlsson, Jorrit Leenaarts

Institution(s): Institute for theoritical astrophysics, Universitet i oslo

Presentation: S2-P-02

Abstract

The lines from singly ionized carbon around 1335 A··· are among the strongest lines in the far ultraviolet (FUV) region of the spectrum covered by the NASA/ SMEX mission Interface Region Imaging Spectrograph (IRIS). The diagnostic potential of these lines are therefore of great interest. In the present piece of work, we investigate the formation of these lines and what one can learn about the solar atmosphere from IRIS observations of them. We do this with the help of 3D modeling.

The formation of the Mg II h&k lines in the solar atmosphere

Abstract Author(s): Jorrit Leenaarts, Tiago Pereira, Mats Carlsson, Bart de Pontieu, Han Uitenbroek

Institution(s): University of Oslo, University of Oslo, University of Oslo, LMSAL , NSO

Presentation: S2-P-03

Abstract

NASA's Interface Region Imaging Spectrograph (IRIS) studies how the solar atmosphere is energized. IRIS contains an imaging spectrograph that covers the Mg II h&k lines as well as a slit-jaw imager centered at Mg II k. By combing in a snapshot of a dynamic 3D radiation-MHD model of the solar atmosphere with non-LTE radiative transfer, we investigate which diagnostic information about the atmosphere is contained in the synthetic line profiles. We find that the Mg II h&k lines are excellent probes of the very upper chromosphere just below the transition region, a height regime that is impossible to probe with other spectral lines. They also provide decent temperature and velocity diagnostics of the middle chromosphere. We apply these findings to Mg II spectra obtained with IRIS and discuss what this tells us about the structure of the chromosphere.

Hinode-7
Session 2: Atmospheric and Interior Couplings

Forward modelling of solar atmospheric structures and their oscillations

Abstract Author(s): Tom Van Doorsselaere, Patrick Antolin, Veronika Reznikova, Michael Moreels

Institution(s): KU Leuven

Presentation: S2-P-04

Abstract

The corona is optically thin, making the interpretation of observations non-trivial because of the superposition of foreground and background plasma. Forward modelling helps in this respect, by creating synthetic views from analytical and numerical models. In Leuven, we focus on the forward modelling of models for coronal oscillations. In particular, we pay attention to spectroscopic properties that could be measured with Hinode/EIS or IRIS. As a case study, we will present the forward modelling results for a sausage mode obtained with the FoMo code. Contrary to the intuition, the compressive sausage mode does not necessarily result in large intensity variations. In fact, the connection between observable spectral line properties (intensity, Doppler shift, broadening) and the actual plasma motion and compression depends strongly on the selected spectral line. We will make the contrast between the popular 171Å and 193Å iron lines.

Hinode-7
Session 2: Atmospheric and Interior Couplings

Revealing the nature of magnetic halos and shadows with numerical 3D-MHD simulations

Abstract Author(s): Oskar Steiner, Christian Nutto, Markus Roth

Institution(s): Kiepenheuer-Institut, Kiepenheuer-Institut fur Sonnenphysik

Presentation: S2-P-05

Abstract

We have carried out three-dimensional numerical simulations of magneto-acoustic wave propagation in a solar atmospheric model that is threaded by a complexly structured magnetic field, resembling a magnetic network element. Waves of 10 mHz frequency are artificially excited at the bottom of the simulation domain. On their way through the upper convection zone and through the photosphere and the chromosphere they become refracted and converted to different mode types. The power maps of the line-of-sight velocities of the upper photosphere and the lower chromosphere show clear signatures of the magnetic halo and the magnetic shadow: seams of enhanced and suppressed power surrounding magnetic network elements as known from observations. We conclude that the appearance of the halo and the shadow is linked to the mode conversion process and that power maps at these height levels result from the contribution of three different magneto-acoustic wave modes.

Spectropolarimetric signatures of photospheric intergranular vortices

Abstract Author(s): Sergiy Shelyag

Institution(s): Monash Centre for Astrophysics, Monash University, Australia

Presentation: S2-P-06

Abstract

Intergranular photospheric vortices, which have recently been discovered using simulations of photospheric magneto-convection, are a photospheric phenomenon that appears to be responsible for transport of energy from the solar interior through the solar atmosphere. The vortices are horizontal motions characterised by relatively short lifetimes and small spatial scales, which makes them difficult to detect and observe. I will demonstrate the physical properties and spectropolarimetric signatures of intergranular vortex motions and discuss the ways to observe them.

Coupling Interior and Atmosphere through Active Regions

Abstract Author(s): Paul S Cally, Hamed Moradi

Institution(s): Monash University, Monash University

Presentation: S2-P-07

Abstract

The Sun's interior oscillations, the p-modes, are normally trapped in a subsurface cavity, but behave very differently when they encounter an active region. The magnetic field turns them into a complex mixture of fast, slow, and Alfven waves through two different mode conversion processes. They then partially escape into the solar atmosphere and partially reflect to rejoin the internal wave field, with profound consequences for the local seismology. We present results of simulations that show substantial 'travel time' shifts that depend on magnetic field inclination and orientation, and are closely related to escaping acoustic and Alfvenic wave fluxes.

Hinode-7
Session 2: Atmospheric and Interior Couplings

Observations of the excitation and damping of Alfvenic waves throughout the solar atmosphere

Abstract Author(s): Richard Morton, Gary Verth, Andrew Hillier, Robertus Erdelyi

Institution(s): Northumbria University, Sheffield University, Kyoto University, Sheffield University

Presentation: S2-P-08

Abstract

Magnetohydrodynamic waves are thought to play a vital role in the transport of energy between the photosphere and corona in the Sun's quiescent atmosphere. To investigate the transport of Alfvenic wave energy provided by the MHD kink mode we exploit multi-instrument observations, finding that the chromospheric kink wave velocity power spectra contains the signature of horizontal photospheric motions. This provides strong evidence that these motions are the main driving mechanism for the observed incompressible modes. Crucially, the first comparison between chromospheric and coronal power spectra is provided, revealing transmission profiles that imply both enhanced and frequency-dependent damping of Alfvenic waves in the lower corona.

Hinode-7
Session 2: Atmospheric and Interior Couplings

A statistical study of prominence oscillations: Evidence for photospheric motions as the transverse wave driver in a quiescent prominence

Abstract Author(s): Andrew Stephen Hillier, Richard Morton, Robertus Erdelyi

Institution(s): Kwasan Observatory, Kyoto University; Mathematics and Information Science, Northumbria University; Solar Physics and Space Plasma Research Centre, University of Sheffield

Presentation: S2-P-09

Abstract

The launch of the Hinode satellite has allowed for seeing-free observations at high-resolution and high-cadence making it well suited to study the dynamics of quiescent prominences. In recent years it has become clear that quiescent prominences support small-amplitude transverse oscillations. These oscillations are often hypothesised as being driven by photospheric motions. However, the sample of waves taken in each earlier study has been small, which has not allowed firm conclusions to be made. We remedy this by providing a statistical study of transverse oscillations in vertical prominence threads. Over a three-hour period of observations it was possible to measure the properties of 3436 waves, finding periods from 50-6000 s with typical velocity amplitudes ranging between 0.2-12 km s^{-1}. The large number of observed waves allows for the derivation of the velocity power spectrum for the transverse waves. Significantly, the frequency dependence of the velocity power is consistent with the velocity power spectra generated from observations of the horizontal motions of magnetic elements in the photosphere. This provides the first strong piece of evidence that the prominence transverse waves are driven by photospheric motions.

Kappa-distributions and the Differential Emission Measure of Active Regions

Abstract Author(s): Elena Dzifcakova, Simon Mackovjak, Jaroslav Dudik

Institution(s): Astronomical Institute Odrejov

Presentation: S2-P-10

Abstract

We investigate the effect of the the non-Maxwellian kappa-distributions on the reconstructed differential emission measure (DEM) for the cores of three active regions observed by Hinode/EIS and listed in Warren et al. (2012). DEMs for kappa-distributions were calculated using two methods: the Withbroe-Sylwester method (Withbroe, 1975; Sylwester et al., 1980) and the regularization method (Hannah & Kontar, 2012). The results are compared with DEMs for the Maxwellian distribution. In general, the kappa-distributions widen and shift contribution functions for individual spectral lines. This behavior is reflected in the reconstructed DEMs and influences calculated temperature distribution of AR. The impact of the changes in DEM with the kappa-distributions for the physics of active region corona is discussed.

Seismic inference of physical parameters in solar prominences using observations of their fine structure oscillations

Abstract Author(s): Roberto Soler, Ramon Oliver, Jose Luis Ballester

Institution(s): University of the Balearic Islands

Presentation: S2-P-11

Abstract

Transverse oscillations of thin threads in solar prominences are frequently reported in high-resolution observations. The typical periods are in the range of 3 - 20 minutes and the oscillations are damped after few periods. Theoretically, the oscillations are interpreted as kink magnetohydrodynamic waves, while the mechanism responsible for the damping is most likely resonant conversion to Alfven waves. Here, we show that it is possible to use observational information of the fine structure oscillations in combination with theoretical models to infer some physical properties of the prominence plasma. In particular, the observed period can be used to estimate the Alfven velocity, whereas the plasma inhomogeneity length scale can be inferred from the ratio of the damping time to the period. Examples of the method are given using actual oscillations observed with Hinode.

Hinode-7
Session 2: Atmospheric and Interior Couplings

Morphological study of penumbral formation

Abstract Author(s): Reizaburo Kitai, Hiroko Watanabe, Ken'ichi Otsuji

Institution(s): Kyoto University, Kyoto University , NAOJ

Presentation: S2-P-12

Abstract

Penumbrae are known to be area of mainly horizontal magnetic field surrounding umbrae of relatively large and mature sunspots.

Rucklidge (1995) studied the energy flows in a model sunspot including the lateral energy flux from surrounding inclined magnetic field, and showed that sunspot MHD structure has two equilibrium states (pores and sunspots) and that the structure will change abruptly or transit from pore state to sunspot state when the inclination of surrounding magnetic field gets larger than a threshold value. Succeeding numerical simulations by Hurlburt and Rucklidge (2000) and Tildesley and Weiss (2004) led to the idea of magnetic pumping mechanism around sunspots. Cheung et al. (2010) and then Rempel et al. (2012) closely studied the necessary condition of chromospheric boundary conditions for extended penumbral formation.

Observationally, Shimizu et al. (2012) detected a case of penumbral formation, where appearance of chromospheric dark annular zone, which may correspond to horizontal magnetic field, precedes the formation of photospheric penumbra.

In this paper, we observationally studied the formation of penumbrae in NOAA10978, where several penumbral formations were observed in G-band images of SOT/Hinode. Thanks to the continuous observation by Hinode, we could morphologically follow the evolution of sunspots and found that there are several paths to the penumbral formation: (1) Active accumulation of magnetic flux, (2) Rapid EFR regions, (3) Appearance of twisted or rotating magnetic tubes. In all of these cases, magnetic fields are expected to sustain high inclination at the edges of flux tube concentration longer than the characteristic growth time of magnetic pumping.

Hinode-7
Session 2: Atmospheric and Interior Couplings

Magnetic tornadoes on the Sun

Abstract Author(s): Sven Wedemeyer

Institution(s): University of Oslo

Presentation: S2-P-13

Abstract

High-resolution observations with the Swedish 1-m Solar Telescope (SST) and the Solar Dynamics Observatory (SDO) reveal rotating magnetic field structures that extend from the solar surface into the chromosphere and even the corona. These so-called "magnetic tornadoes" are primarily detected as rings or spirals of rotating plasma in the Ca II 854.2 nm line core ("chromospheric swirls"). Detailed numerical simulations show that the observed chromospheric plasma motion is caused by the rotation of magnetic field structures, which again is driven by photospheric vortex flows at the footpoints of magnetic field structures. The magnetic field couples the atmospheric layers and mediates the rotation into the upper atmosphere. This mechanism may provide an alternative way of channeling energy into the upper solar atmosphere, although the details and the resulting net contribution to heating the solar corona have to be investigated further. Rotating magnetic field structures are also observed on larger spatial scales. The largest examples, here referred to as ' giant ' solar tornadoes are likely the rotating legs of solar prominences. New combined SST/SDO observations suggest that giant tornadoes may play a role in building up twist of magnetic field structures and may thus act as source of instability for prominences.

Changes in High Degree p-mode parameters with Magnetic and Flare Activities

Abstract Author(s): Ram Ajor Maurya

Institution(s): Seoul National University

Presentation: S2-P-14

Abstract

Solar energetic transients, e.g., flares, CMEs, etc., release large amount of energy which is expected to excite acoustic waves (p-modes) by exerting mechanical impulse of the thermal expansion of the flare on the photosphere. We study the p-mode properties of flaring and dormant active regions (ARs) to find association between flare and p-mode parameters. We compute the magnetic and flare activity indices of ARs using the line-of-sight magnetograms and GOES X-ray fluxes, respectively. The p-mode parameters are computed from the ring-diagram analysis. We correct p-mode parameters for magnetic field, filling factors and foreshortening by multiple linear-regression analysis. Our analysis of several flaring and dormant ARs observed during the Carrington rotations 1980-2109, showed strong association of mode parameters with magnetic and flare activities. We find that the mode parameters are contaminated by the geometrical effect. Mode amplitude decreases with angular distance from the solar disc centre. The mode width increases with magnetic activity while amplitude showed opposite relation due to mode absorption by the sunspot. After correcting modes due to all geometrical effects, magnetic activity and filling factor, we find that the modes amplitude, and mode energy increases with flare energy while width shows opposite relation.

Hinode-7
Session 2: Atmospheric and Interior Couplings

Solar wind and coronal rotation during an activity cycle.

Abstract Author(s): Rui F. Pinto, Sacha Brun

Institution(s): LESIA, Observatoire de Paris & AIM/SAp, CEA Saclay, AIM/Sap, CEA Saclay

Presentation: S2-P-15

Abstract

The properties of the solar wind flow are strongly affected by the time-varying strength and geometry of the global background magnetic field. The wind velocity and mass flux depend directly on the size and position of the wind sources at the surface. The angular momentum (torque) balance depends on how the differential surface rotation is transmitted upwards across the highly stratified chromospheric layers, and up to the corona along the magnetic field. We address these problems by performing numerical simulations coupling a kinematic dynamo code (STELEM) evolve in a 2.5D axisymmetric coronal MHD code (DIP) covering an 11 yr activity cycle. The latitudinal distribution of the calculated wind velocities agrees with in-situ (ULYSSES) and radio measurements (IPS). We found that the Alfven radii and the global Sun's mass loss rate vary considerably throughout the cycle (by a factor 4.5 and 1.6, respectively), leading to strong temporal modulations of the global angular momentum flux and magnetic braking torque. Finally, we point out directions to assess the effects of more transient phenomena on the global properties of the wind.

A coupled model for the formation of active region corona

Abstract Author(s): F. Chen, H. Peter, S. Bingert, R. Cameron, M. Schussler, M. C.M. Cheung

Institution(s): Max Planck Institute for Solar System Research, Katlenburg-Lindau, Germany

Presentation: S2-P-16

Abstract

We present the first model that couples the formation of an active region corona to a model of the emergence of a sunspot pair. This allows us to study when, where, and why active region loops form, and how they evolve. For this we use an existing 3D radiation MHD model of the emergence of an active region through the upper convection zone and the photosphere as a lower boundary for the coronal model. Our 3D MHD coronal model accounts for the braiding of the magnetic field lines which induces currents in the corona hating up the plasma, and allows us to synthesize the coronal emission for a direct comparison to observations. Starting with a basically field-free atmosphere we follow the flux emergence filling the corona with magnetic field. In this process numerous individually identifiable hot coronal loops form, which would be visible in EUV or X-ray observations with AIA or Hinode XRT. The temperature in the coronal loops reaches well above 1 MK, and the density in the model loops corresponds to actual observations. These loops develop quickly within only a few minutes. Initially appearing as a thin tube, an emerging coronal model loop rises and expands significantly in the horizontal direction. It finally fragments and develops into a system of multiple loops. We find that the footpoints of the loops are found where small patches of magnetic flux concentrations move into the sunspots. At these footpoints we find an increased upwards-directed Poynting flux that leads to the increased heating and formation of the loops. Overall, this model coupling the coronal evolution to a flux emergence simulation gives a comprehensive self-consistent view of the formation of an active region loop.

Relationship between satellite anomalies and space weather

Abstract Author(s): Satoshi Nozawa, Tetsuya Nagano, Susumu Tamaoki

Institution(s): Ibaraki University, Ibaraki University, Ibaraki University

Presentation: S2-P-17

Abstract

Geosynchronous satellite anomalies are occurred by the space weather phenomena. We examined three indexes of space weather. They are magneto-pause that balance solar wind and magnetosphere (GMC: Geosynchronous Magnetopause Crossing), DST index that indicated to magnetic storm and AE index that indicated to influx of energy from sun wind for magnetosphere. We looked at the effect DST index and AE index variation on satellites anomalies how we use ONMI2 1 hour data. DST index is examined between the frequency of satellites anomalies and magnetic storm occurred. AE index is integrate in day why examine between the frequency of satellites anomalies and influx of energy for magnetosphere growing value. The result is that the more the magnetopause is compressed, the more the frequency of satellites anomalies is increased exponentially. DST index the smaller value, the more frequency of satellites anomalies is increased exponentially. Integration AE index the more growth, the more frequency of satellites anomalies is increased. In addition, direct and indirect relationship between satellite anomaly occurrence and geomagnetic perturbations by solar wind are discussed.

Hinode-7
Session 2: Atmospheric and Interior Couplings

Analysis of Sunspot oscillations observed with DST/Hida

Abstract Author(s): Akihiro Ohkawa, Tetsu Anan, Kiyoshi Ichimoto, Satoru Ueno, Akihito Oi, Satoshi Nozawa, S Sawada

Institution(s): Ibaraki University, Kyoto University, Kyoto University, Kyoto University, Kyoto University, Ibaraki University, Ibaraki University

Presentation: S2-P-18

Abstract

Sunspot oscillation studies that repetitive brightenings and doppler velocity variations on sunspots went on over 40 years discovered by Beckers & Tallant (1969), while the research of the generation and the propagation of waves in the photosphere and the chromosphere has debated well (e.g., Lites 1992). However, it is unclear about magnetic field structures in the sunspot, in particular how is the time evolution of the spread magnetic field line above the sunspot. Therefore, it is need to observe specific horizontal magnetic field structures in the sunspot with high temporal and spatial resolution. So, we used the HAZEL (HAnle and ZEeman Light). HAZEL is a diagnostic tool of magnetic fields in the chromosphere and the prominence by Asensio Ramos & Trujillo Bueno et al. (2008). The full Stokes data used the diagnostic was taken the Vertical Spectropolarimeter onboard the Domeless Solar Telescope at the Hida Observatory. We selected to analyze the upper chromospheric He I 10830A multiplet because this line is very influenced by the Zeeman effect to be long wavelength and large Lande factor. As results before inversion, the wavelength-time diagram of Stokes V showed the sawtooth shape of propagating shock waves, and the space-time diagram of Stokes V showed propagating waves generated from near the umbral center. The power map of the latter clearly showed a 3 minute period in the umbra but a 5 minute period in the penumbra. In addition, we discuss inversion halfway results and future developments.

Hinode-7
Session 2: Atmospheric and Interior Couplings

Magnetic field of active region filaments observed with DST/Hida

Abstract Author(s): Shinpei Sawada, Tetsu Anan, Kiyoshi Ichimoto, Satoru Ueno, A Oi, Satoshi Nozawa, A Ohkawa

Institution(s): Ibaraki University, Kyoto University, Kyoto University, Kyoto University, Kyoto University, Ibaraki University, Ibaraki University

Presentation: S2-P-19

Abstract

Solar prominences are relatively cool and dense plasma located in the solar corona consisted of hotter and sparser plasma. Magnetic fields are interacting with prominences plasma is being supported against gravity. On the other hand, the eruption of a prominence often produces a coronal mass ejection, which may have a dramatic influence on near-Earth space weather. Therefore, it is very important to obtain good empirical knowledge of the three-dimensional structure of prominence magnetic fields. The most reliable strategy we have available for inferring the magnetic field vector is via the measurement and theoretical interpretation of Stokes profiles suitably chosen spectral lines. Our work is based on spectropolarimetry of the He 10830A multiplet.

We studied the vector magnetic field a filament observed over an active region NOAA 11476. The observation were carried out on 2012 May 13 with the Domeless Solar Telescope (DST) at Hida. Spectropolarimetric data got with DST of the 10830 spectral region provide full Stokes vectors that were analyzed using HAZEL(HAnle and Zeeman Light). The slit was fixed over the filament and we also studied temporal evolution of the vector magnetic field.

The inferred magnetic field strengths in the filament are around 600 $\sim$ 800 Gauss by HAZEL. Longitudinal fields are found in the range of 100 $\sim$ 200 G whereas the transverse components become dominant, with fields as high as 400 $\sim$ 700G. Also, the Stokes I intensity and magnetic field strength oscillated in a 3 minutes period. We will discuss oscillation source.

Hinode-7
Session 2: Atmospheric and Interior Couplings

Simultaneous multi-line observation of Ellerman bombs using the DST in Hida observatory

Abstract Author(s): Yuri Kato, Naoaki Mouri, Yumi Hibino, Kenichi Otsuji, Takashi Sakae, Masaoki Hagino, Akihito Oi, Satoru Ueno, Kiyoshi Ichimoto

Institution(s): Meisei University, Meisei University, Meisei University, National Astronomical Observatory of Japan, Saitama Prefectural Urawa Nishi High School, Kyoto University, Kyoto University, Kyoto University, Kyoto University

Presentation: S2-P-20

Abstract

When one observes the solar chromosphere with the wing part of H alpha line, small bright points are found around sunspots or inside the emerging flux region. These phenomena are called as “Ellerman bombs”, which was found by Ellerman in 1917. The formation mechanism and the characteristics of Ellerman bombs are not fully understood yet. The height-dependent physical information of Ellerman bombs is required for investigation of them. We performed simultaneous multi-line observation of Ellerman bombs using the horizontal spectrograph of the Domeless Solar Telescope (DST) in Hida observatory. The observation lines are H alpha and Ca II K. From the observation data using these lines, we derived the time evolution of the intensities at the line cores and the wing parts. As the result, the light curve of the line cores shows typical pattern of 3 minutes oscillation. On the other hand, we can identify several short-term intensity fluctuations at the wing parts. The average period of the fluctuations was about four and a half minutes. The brightening in the wing parts of H alpha and Ca II K appeared at the same time. All these results are consistent with the preceding studies, and indicate that the sporadic magnetic reconnections occur in the lower chromosphere.

Hinode-7
Session 2: Atmospheric and Interior Couplings

Numerical study on the generation of waves by asymmetrical magnetic reconnection

Abstract Author(s): Ryugo Sato, K Takahashi, Satoshi Nozawa

Institution(s): Ibaraki university, JAMSTEC, Ibaraki University

Presentation: S2-P-21

Abstract

The heating mechanism of the solar corona is one of the most mysterious issues in solar physics. X-ray observations from early space experiments have shown that the corona is not uniform. It is therefore suggested that the magnetic activity is related to heating of the solar corona. Related to magnetic activity, two theories currently dominate to solve the solar coronal heating problem. One is Alfvén wave heating model, and the other is nano-flare (caused by magnetic reconnection) heating model. Actually, Hinode observed transverse wave of magneto hydro dynamic wave such as Alfvén wave, so nano-flare was observed a survey of solar atmosphere, too. However, recent studies point out the possibility of unificational two theories (hybrid model), since the kinetic Alfvén wave propagates at reconnection point. In such situation, this study calculates energy fluxes of some waves which are occured by the magnetic reconnection using 2.5-dimensional MHD simulation. We discuss the simulation results of the uniform atmosphere condition (model A) and the solar atmospheric condition under magneto-hydrostatic equilibrium (model B). In both model A and B, the magnetic fields have a component perpendicular to the computational plane, that is, a guide field. As a result, it is found that the required energy for the heating of quiet corona can be generated in both model A and B. This suggest that the hybrid model plays a more important role of solar coronal heating.

On the Signature of Waves and Oscillations in IRIS Observations

Abstract Author(s): Bernhard Fleck, T. Straus, B. De Pontieu

Institution(s): ESA, INAF/OAC, LMSAL

Presentation: S2-P-22

Abstract

The Interface Region Imaging Spectrogragh (IRIS) was successfully launched on 27 June 2013 and had first light on 17 July 2013. Its UV spectrograph and slit jaw images provide information about the structure and dynamics of the upper solar atmosphere at unprecedented spatial and temporal resolution. We analyze a 1-hour long sit-and-stare spectral time series of C II 1335 & 1336, C I 1352, O I 1356, Si IV 1394 & 1403 and Mg h and k. The temporal resolution of the series is 8 sec. The accompanying slit jaw time series in the Mg h line, the 1330 (C II) filter and the 1440 (Si IV) filter have a temporal resolution of 24 s. The objective of this study is to explore the signatures of acoustic waves and oscillations in the IRIS data.

Hinode-7

Session 3

Coronal Heating and Solar Wind Acceleration

Hinode-7
Session 3: Coronal Heating and Solar Wind Acceleration

The Observation and Modeling of Active Region Emission: Constraints from Hinode

Abstract Author(s): Harry P Warren, Ignacio Ugarte-Urra

Institution(s): NRL

Presentation: S3-I-01

Abstract

Understanding how the solar corona is heated to high temperatures is one of the most important open questions in solar physics. The instruments on Hinode observe the atmosphere at high spatial resolution across a very broad range of temperatures, making them ideally suited for investigating this problem. Unfortunately, the complex nature of the solar corona, transition region, chromosphere, and photosphere make it difficult to relate the available observables directly to the properties of the heating. Our approach is to couple non-linear force-free magnetic field extrapolations to time-dependent hydrodynamic simulations to create fully three-dimensional, time-dependent models of solar active regions that cover a wide range of magnetic conditions. We use these models to test our ability to employ time series and differential emission measure analysis to make inferences about the properties of the coronal heating mechanism. In this talk we review previous observational work on the coronal heating problem with Hinode and present some initial simulation results. Our initial models are able to reproduce both the temporal evolution and temperature distributions observed in the largest active regions of the solar cycle.

Hinode-7
Session 3: Coronal Heating and Solar Wind Acceleration

Coronal loops above an active region – observation versus model

Abstract Author(s): Philippe Andre Bourdin, Sven Bingert, Hardi Peter

Institution(s): Max Planck Institute for Solar System Research, Max Planck Institute for Solar System Research , Max Planck Institute for Solar System Research

Presentation: S3-C-01

Abstract

We conducted a high-resolution numerical simulation of the solar corona above a stable active region. Our 3D-MHD model is driven from below by Hinode observations of the photosphere, in particular a high-cadence time series of line-of-sight magnetograms and horizontal velocities derived from the magnetograms. This driving applies stress to the magnetic field and thereby delivers magnetic energy into the corona, where currents are induced that heat the coronal plasma by Ohmic dissipation. We compute synthetic coronal emission that we directly compare to coronal observations of the same active region taken by Hinode.

In the model, coronal loops form at the same places as they are found in coronal observations. Even the trajectories of the synthetic loops in 3D space match those found from a stereoscopic reconstruction based on STEREO spacecraft data. Some loops turn out to be slightly overdense in the model, as expected from observations. The Doppler shifts of the synthesized emission lines match those observed by Hinode/EIS. The transition region lines are found to be redshifted, while the coronal lines show blue-shifts, just as in observations. This shows that the spatial and temporal distribution of the Ohmic heating produces the structure and dynamics of a coronal loops system close to what is found in observations.

Hinode-7
Session 3: Coronal Heating and Solar Wind Acceleration

High-Resolution Observations of Chromospheric Activity Associated with Small-Scale Emerging Flux in near Sunspot Regions

Abstract Author(s): Vasyl Yurchyshyn, Wenda Cao, Phil Goode

Institution(s): NJIT/Big Bear Solar Observatory

Presentation: S3-C-02

Abstract

We study the dynamics of magnetic fields emerging near sunspots and pores, as well as the associated chromospheric activity. We used photospheric intensity images and magnetic field measurements from the New Solar Telescope (NST) in Big Bear and Hinode to study the the effect that new small-scale emerging flux induces on solar granulation. Halpha-0.1 nm images and spectra from the NST's Visible Imaging Spectrometer (VIS) were utilized to understand associated chromospheric activity. We report that small-scale opposite polarity fields constantly appear inside the apparently unipolar fields surrounding a solar pore. The occurrence of chromospheric jets and small-scale energy release events is generally correlated with the appearance of these new fields. The chromospheric activity seems to be mainly limited to the interface between large-scale fields and small-scale dynamic magnetic loops and thus are likely to be associated with existence of the magnetic canopy. We further speculate that this interface is important in the production of even smaller events, such as type II spicules, as well as larger jet-like features surrounding sunspots.

Hinode-7
Session 3: Coronal Heating and Solar Wind Acceleration

Relation among low atmospheric reconnection, shock formation and chromospheric jets

Abstract Author(s): Shinsuke Takasao, Hiroaki Isobe, Kazunari Shibata

Institution(s): Kyoto University, Kyoto University, Kyoto University

Presentation: S3-C-03

Abstract

A large fraction of the energy carried from the photosphere should be dissipated in the upper atmosphere to heat the chromosphere and corona. A fundamental question is, how is the energy carried and dissipated? Observations have shown that chromosphere is filled with tiny collimated plasma flows (jets), which implies that those jets can be a result of the energy transport. Observations also have provided indirect evidence of magnetic reconnection, like the bi-directional apparent motions at the foot-points of jets. Thus it is worth investigating the relation between magnetic reconnection and the acceleration of chromospheric jets. We studied how chromospheric jets are created as a result of low atmospheric reconnection using a 2D MHD simulation. We found that after magnetic reconnection takes places, MHD slow shocks are naturally generated in the chromosphere and they accelerate chromospheric plasma. This means that the shocks play important role to carry and dissipate the magnetic energy. We will discuss how shocks generated by low atmospheric reconnection carry and dissipate the energy.

Hinode-7
Session 3: Coronal Heating and Solar Wind Acceleration

An IRIS look at spicules

Abstract Author(s): Tiago M. D. Pereira, Bart De Pontieu

Institution(s): Institute of Theoretical Astrophysics, University of Oslo, Lockheed Martin Solar & Astrophysics Laboratory

Presentation: S3-C-04

Abstract

Spicules are important chromospheric features that can be seen in the solar limb. While their formation is still unclear, it has been suggested that they may have an important part in the transfer of energy and mass to the outer atmosphere. Multi-wavelength observations of spicules are invaluable to trace their formation and histories. In this work we show some first observations of spicules as seen by the IRIS observatory. Taking advantage of its fast cadence and unique filtergrams, we analyse several time series and characterise the spicule properties as seen by IRIS.

Recent advances in theory and modelling of coronal wave heating

Abstract Author(s): Ineke De Moortel

Institution(s): University of St Andrews

Presentation: S3-I-02

Abstract

In this talk I will give an overview of current modelling of MHD waves and oscillations, emphasising in particular the process of mode coupling. Can models predict the observed damping rates and energy flux? How reliable are the comparisons between theory and observations? As observations of waves and oscillations become increasingly more detailed, it has become clear that the role of wave heating of the solar atmosphere has to be reassessed. I will highlight some of the recent modelling results as well as try to outline where future efforts are needed.

Hinode-7
Session 3: Coronal Heating and Solar Wind Acceleration

Quasi-periodic slow waves and intermittent high-speed outflows unified in a kinetic scenario

Abstract Author(s): Jiansen He, Liping Yang, Chuanyi Tu, Eckart Marsch, Hardi Peter

Institution(s): Peking University, Peking University, Peking University, Christian Albrechts University at Kiel, Max-Planck Institute for Solar System Research

Presentation: S3-C-05

Abstract

Since the spectral imaging observations of the solar corona by EIS, a debate on the nature of the propagation of intensity disturbance has been initiated and remains unsolved until now. Here, we propose a kinetic scenario to combine the phenomena related to these two viewpoints together. In our scenario, the intermittent high-speed outflow is due to kinetic acceleration by the slow waves through Landau resonance. The kinetic accelerated plasma is a small proportion travelling around the sound speed, and accounts for the asymmetry of the spectral profile at the blue wing. To illustrate our scenario, we make a simple test-particle-like simulation. In our simulation, the tracers behave somewhat different from the real particles. To imitate the macro-state of the coronal plasma, i.e., static equilibrium to the zero order approximation and slow-mode fluctuations to the first order approximation, we assume the particle-like tracers to evolve with their moments being governed by the momentum equation for the protons in the frame work of two-fluid MHD. The simulation shows that, as the slow waves propagate through the plasma tracers, a small fraction of tracers are accelerated to the order of sound speed thereby making the reduced velocity distribution asymmetric. Moreover, the moments of zero-order, first-order and second-order of the tracers' velocity distribution, which correspond to the number density, bulk velocity, and temperature, are oscillating in phase, which is a prominent signature of outward propagating slow waves. Therefore, this kinetic scenario, which unifies the waves and outflows together, might be the solution to the debate over the waves or outflows. However, the simple simulation for this scenario needs to be refined and extended to a more realistic Vlasov model, which is our objective in future work.

Hinode-7
Session 3: Coronal Heating and Solar Wind Acceleration

Observing coronal nanoflares in active region moss, with Hi-C and IRIS

Abstract Author(s): Paola Testa, Bart De Pontieu, Juan Martinez-Sykora, Viggo Hansteen, Connor Robinson, Ed DeLuca, Jonathan Cirtain, Amy Winebarger, Leon Golub, Ken Kobayashi, Kelly Korreck, Sergey Kuzin, Robert Walsh, Craig DeForest, Alan Title, Mark Weber

Institution(s): Harvard-Smithsonian Center for Astrophysics, LMSAL, LMSAL , Univ. of Oslo, Univ. of Montana, Missoula, Harvard-Smithsonian Center for Astrophysics, NASA, MSFC, NASA, MSFC, Harvard-Smithsonian Center for Astrophysics, NASA, MSFC, Harvard-Smithsonian Center for Astrophysics, NASA, MSFC, Harvard-Smithsonian Center for Astrophysics

Presentation: S3-C-06

Abstract

The variability of emission of the "moss", i.e., the upper transition region (TR) layer of high pressure loops in active regions provides stringent constraints on the characteristics of heating events. The High-resolution Coronal Imager (Hi-C) has provided Fe XII 193A images of the upper transition region moss at an unprecedented spatial (∼0.3 arcsec) and temporal (∼5.5 s) resolution. Hi-C moss observations have revealed in some moss regions variability on timescales down to ∼15 s, significantly shorter than the minute-scale variability typically found in previous observations of moss, therefore challenging the conclusion of moss being heated in a mostly steady manner. The Hi-C and SDO observations of these events show that these rapid variability moss regions are located at the footpoints of bright hot and highly dynamic coronal loops, and suggest that they are signatures of heating events associated with reconnection occurring in the overlying hot coronal loops, i.e., coronal nanoflares. We estimate the order of magnitude of the energy in these events to be of at least a few 10^{23} erg, also supporting the nanoflare scenario.

Here we will also present first results of analysis of moss variability observed with the Interface Region Imaging Spectrograph (IRIS). IRIS, launched in June 2013, provides imaging and spectral observations at high spatial (0.168 arcsec/pix), and temporal (down to ∼1s) resolution at FUV and NUV wavelengths. We will focus on IRIS time series of high cadence (<5s) slit-jaw images (SJI) in the 1400A band, centered around Si IV transition region emission. We compare the results with simultaneous analysis of AIA data, and with previous findings.

IRIS observations of transition region unresolved fine structure

Abstract Author(s): Viggo Haraldson Hansteen, Bart De Pontieu, Juan Martinez-Sykora, Paola Testa, Mats Carlsson

Institution(s): Instiute of Theoretical Astrophysics, University of Oslo, LMSAL, Palo Alto CA, LMSAL, Palo Alto CA, CfA, Cambridge MA, Instiute of Theoretical Astrophysics, University of Oslo

Presentation: S3-C-07

Abstract

The Interface Region Imaging Spectrograph was launched on 28-June-2013 and has been obtaining high resolution images and spectra in the far and near ultraviolet since 17-July-2013 covering temperatures from the photosphere into the corona. We analyze the presence of a multitude of short, relatively cool transition region loops as visible at the solar limb in slit jaw images dominated by C II 1335 Angstrom and Si IV 1402 Angstrom emission. We study the dynamical nature and temperature evolution of these loops and investigate how they relate to the so-called "unresolved fine structure" (UFS) that has been proposed as a dominant source of transition region emission, but that has not yet been directly observed to date.

Hinode-7
Session 3: Coronal Heating and Solar Wind Acceleration

Dark jets in coronal holes

Abstract Author(s): Peter R. Young, Karin Muglach

Institution(s): George Mason University

Presentation: S3-C-08

Abstract

A coronal hole was monitored continuously by Hinode for 44 hours in February 2011 as part of HOP 177 and the EIS data reveal a number of jet features in Fe XII 195.12 (logT=6.2) with a strong Doppler signature, but little or no intensity signature. We term these features "dark jets". Thirty-five blue-shifted features are found in the Fe XII Doppler maps within the coronal hole or at the boundary. Twenty-four of the features can be considered jets, and 14 of these are found not to have a jet signature in AIA 193 image sequences. Inspection of the line profiles shows that the jet plasma gives rise to an asymmetry to the emission line, consistent with the presence of plasma with speeds around 100 km/s. A Fe XII density diagnostic shows that the density of the jet plasma is around 10^9 cm^{-3}, thus not significantly enhanced above coronal hole or quiet Sun values. The temperature of the jet plasma is close to the formation temperature of Fe XII and is isothermal. The presence of dark jets in coronal holes suggests that there is significant mass flow from jets in coronal holes that can not be detected through imaging instruments alone.

In addition to the dark jets, an example of an expanding loop/blowout type jet event will be given. The event shows a clear signature in AIA 193 images, and the EIS Doppler image closely matches the AIA images. Line-of-sight jet velocities in Fe XII reach up to 250 km/s. Correlation tracking applied to HMI data reveals that the jet is triggered by converging flows in the photosphere.

Hinode-7
Session 3: Coronal Heating and Solar Wind Acceleration

Characteristic Length of Energy-containing Structures at the Base of a Coronal Hole

Abstract Author(s): Valentyna Abramenko, Gary Zank, Aleksander Dosch, Vasyl Yurchyshyn, Phil Goode, Kwangsu Ahn, Wenda Cao

Institution(s): NJIT/Big Bear Solar Observatory

Presentation: S3-C-09

Abstract

An essential parameter for models of coronal heating and fast solar wind acceleration that relay on the dissipation of MHD turbulence is the characteristic energy-containing length, $\lambda_\perp$, of the squared velocity and magnetic field fluctuations (u^2 and b^2) transverse to the mean magnetic field inside a coronal hole (CH) at the base of the corona. The characteristic length scale defines directly the heating rate. We use a time series analysis of solar granulation and magnetic field measurements inside two CHs obtained with the New Solar Telescope (NST). A data set for transverse magnetic fields obtained with the Solar Optical Telescope/Spectro-Polarimeter (SOT/SP) aboard *Hinode* spacecraft was utilized to analyze the squared transverse magnetic field fluctuations, b_t^2. Local correlation tracking (LCT) was applied to derive the squared transverse velocity fluctuations, u^2. We find that for u^2-structures, Batchelor integral scale, λ, varies in a range of 1800 - 2100 km, whereas the correlation length, ς, and the e-folding length, L, vary between 660 and 1460 km. Structures for b_t^2 yield $\lambda \approx 1600$ km, $\varsigma \approx 640$ km, and $L \approx 620$ km. An averaged (over λ, ς, and L) value of the characteristic length of u^2-fluctuations is 1260$\pm$500 km, and that of b_t^2 is 950$\pm$560 km. The characteristic length scale in the photosphere is approximately 1.5-50 times smaller than that adopted in previous models (3-30$\times 10^3$ km). Our results provide a critical input parameter for current models of coronal heating and should yield an improved understanding of fast solar wind acceleration.

Hinode-7
Session 3: Coronal Heating and Solar Wind Acceleration

Magnetic configurations responsible for the coronal heating and the solar wind

Abstract Author(s): Hwanhee Lee, Tetsuya Magara

Institution(s): Kyung Hee University, Kyung Hee University

Presentation: S3-C-10

Abstract

The heating of the solar corona is related to the solar-wind generation. Both physical processes are associated with magnetic structures formed on the Sun. We performed three-dimensional magnetohydrodynamic simulations to study magnetic-field configurations in emerging flux regions produced by a strongly and weakly twisted flux tube. We derive two key quantities: the force free parameter and the flux expansion rate which represent how much a magnetic field is twisted and expands, respectively. The twist of a magnetic field generates the electric current which is one of the possible sources of coronal heating while waves propagating along a magnetic field may dissipate to be another heating source when the field abruptly expands. On the basis of the simulation result, we derive the characteristics of those magnetic configurations and discuss the expansion profiles of coronal loops.

Hinode-7
Session 3: Coronal Heating and Solar Wind Acceleration

First IRIS observations of lower solar atmospheric activity

Abstract Author(s): Bart De Pontieu, Mats Carlsson, Viggo Hansteen, Ted Tarbell, Paola Testa, Scott McIntosh, Alan Title, Jim Lemen, Paul Boerner, Juan Martinez-Sykora, Tiago Pereira, IRIS Team

Institution(s): LMSAL

Presentation: S3-P-01

Abstract

The Interface Region Imaging Spectrograph (IRIS) was launched in June 2013 and has been obtaining spectra and images of the chromosphere and transition region in the near and far ultraviolet since end of July 2013. I will provide an overview of first IRIS observations of lower solar atmospheric activity, in coordination with Hinode and the Swedish Solar Telescope. I will focus in particular on the effects of small-scale flux emergence on the low solar atmosphere, the origin and impact of explosive events, and the presence of torsional motions.

The formation of the OI 135.56 nm and CI 135.58 nm lines in solar atmosphere

Abstract Author(s): Hsiao-Hsuan Lin, Jorrit Leenaarts, Mats Carlsson

Institution(s): Institute of Theoretical Astrophysics, University of Oslo

Presentation: S3-P-02

Abstract

The intersystem line from neutral oxygen at 135.56 nm and the allowed line from neutral carbon at 135.58 nm are both within the FUV range of the NASA/SMEX mission Interface Region Imaging Spectrograph (IRIS). The ratio between OI 135.56 nm and CI 135.58 nm has been reported showing drastic changes during solar flares (Skylab observations and others). The ratio has also been reported to be dependent on the electron density and could possibly provide a density diagnostic in the solar chromosphere. In this work we first determine the simplest possible model atoms for O I and C I to enable full radiative transfer calculations with the RH code even in big 3D model atmospheres. We use these atomic models to investigate the formation of these two lines in 3D snapshots produced with the Bifrost code. We find that the oxygen ionization degree is strongly coupled to the ionization degree of hydrogen. The intensity of the CI line is sensitive to the line profile of Lyman-alpha. For this reason, hydrogen has to be treated carefully in order to get realistic results. In principle PRD effects should be considered for both the Ly-alpha and Ly-beta lines. However, this is too computationally expensive if one is also to consider 3D effects. Our strategy is to run 1D simulations with full treatment of hydrogen and then seek for the best approximations based on these simulations. With these approximations we can possibly afford solving the full 3D problem.

Hinode-IRIS observations of prominences

Abstract Author(s): Joten Okamoto, Bart De Pontieu, Ted Tarbell, Alan Title

Institution(s): ISAS/JAXA

Presentation: S3-P-03

Abstract

A new solar physics satellite, Interface Region Imaging Spectrograph (IRIS), was launched on June 27, 2013. IRIS obtains UV spectra and images with high spatial resolution (0.33 arcsec) and high time cadence (1 sec / slit) of the chromosphere and transition region of the Sun.

The chromosphere is located between the photosphere and the corona. Recently, the Hinode satellite has revealed that the chromosphere is highly active and suggested that it is a very important region in terms of energy deposit and transfer for coronal heating and solar wind acceleration. However, we cannot have further chromospheric information by Hinode because the Hinode Solar Optical Telescope has only a filtergraph for chromospheric observations.

Now we have IRIS. IRIS performs spectroscopic observations to get the missing physical quantities of the dynamic chromosphere. Moreover, IRIS and Hinode is the most powerful collaboration to understand chromospheric activities. Hinode observes extremely high-cadence (1.6 sec) and high-spatial (0.2 arcsec) 2-D images, while IRIS measures line-of-sight velocity and Doppler width of fine structures with temperature dependence. This combination provides information about 3-D structures and dynamic phenomena of chromospheric features.

Here we focus on prominence observations performed by IRIS and Hinode, and introduce the initial results of prominence dynamics and magnetic structures such as helical configurations, propagating waves and their damping mechanisms, and formation processes.

Hinode-7
Session 3: Coronal Heating and Solar Wind Acceleration

Initial Calibration and Performance of the IRIS Instrument

Abstract Author(s): Jean-Pierre Wuelser, Theodore D Tarbell, Bart De Pontieu, C Jake Wolfson, Paul Boerner, James R Lemen, Neal E Hurlburt, Alan M Title, Carel J Schrijver, Rock I Bush, Lucia Kleint, Bruce W Lites, Sarah Jaeggli, Charles C Kankelborg, Ed E DeLuca, Leon Golub, Sean McKillop, Katharine K Reeves, Steve Saar, Paola Testa, Hui Tian, Mark Weber, Viggo H Hansteen, Mats Carlsson

Institution(s): Lockheed Martin Solar & Astrophysics Lab, Lockheed Martin Solar & Astrophysics Lab, Lockheed Martin Solar & Astrophysics Lab, Lockheed Martin Solar & Astrophysics Lab, Lockheed Martin Solar & Astrophysics Lab, Lockheed Martin Solar & Astrophysics Lab, Lockheed Martin Solar & Astrophysics Lab, Lockheed Martin Solar & Astrophysics Lab, Stanford University, Montana State University, Montana State University, SAO, SAO, SAO, SAO, SAO, SAO, SAO, SAO, University of Oslo, University of Oslo

Presentation: S3-P-04

Abstract

The Interface Region Imaging Spectrograph (IRIS) is a NASA Small Explorer mission with the primary objective to understand how the solar atmosphere is energized. IRIS was successfully launched on June 27 2013 and now observes high resolution spectra and images in the 133-141 nm and 278-283 nm wavelength bands focused on the chromosphere and transition region of the Sun.

The IRIS First-Light observations have been very promising and are meeting high expectations. We present preliminary calibration results and a first assessment of the on-orbit performance of the IRIS instrument.

Chromospheric and Coronal Wave Generation in the Network Magnetic Elements Through the Magnetic Pumping

Abstract Author(s): Yoshiaki Kato, Oskar Steiner, Viggo Hansteen, Mats Carlsson, Boris Gudiksen

Institution(s): NAOJ, KIS, ITA, University of Oslo, ITA, University of Oslo, ITA, University of Oslo

Presentation: S3-P-05

Abstract

Using radiation magnetohydrodynamic simulations of the solar atmosphere comprising the layers from the upper convection zone to the lower corona, we investigate the self-consistent process of the generation for the slow magnetoacoustic body waves (slow modes) in the magnetic flux concentrations (flux tubes/sheets). We find that the convective downdrafts in the close surroundings of the flux tube "pump" the atmosphere inside the tube in the downward direction. This action produces a downflow inside the flux tube which propagates at the tube speed as a rarefaction wave. The slow mode, excited by the adiabatic compression of the downflow near the optical surface, travels along the magnetic field lines in the upward direction, developing into a shock wave in chromospheric heights, and propagating further into the corona. In the wake of propagating downflows inside the flux tube, the atmosphere in the chromosphere and corona tends to oscillate near the chromospheric cutoff period. We conclude that this process, the so-called "magnetic pumping", is the most plausible mechanism for the generation of longitudinal chromospheric and coronal waves within the magnetic flux concentrations, which may explain certain types of dynamic fibrils.

Hinode-7
Session 3: Coronal Heating and Solar Wind Acceleration

Torsional motion of spicules

Abstract Author(s): Hakon Skogsrud, Luc Rouppe van der Voort, Bart De Pontieu

Institution(s): Institute of Theoretical Astrophysics, University of Oslo, Institute of Theoretical Astrophysics, University of Oslo, Lockheed Martin Solar & Astrophysics Lab

Presentation: S3-P-06

Abstract

Spicules are small, ubiquitous jets that permeate the low solar atmosphere. They are typically observed in spectral lines such as Halpha and Ca II 8542. Recent studies have shown that their dynamics is governed by an interplay of field-aligned flows along their axis, transverse swaying and torsional motion around their axis. We study the torsional motion in more detail by detecting and measuring upon spicules off-limb in high spectral and spatial resolution observations obtained with the CRISP instrument at the Swedish 1m Solar Telescope. We provide statistics of the torsional motion properties for a large number of spicules and compare with previous studies. We will also show some initial results of coordinated IRIS/Hinode measurements of torsional motions on spicules.

Hinode-7
Session 3: Coronal Heating and Solar Wind Acceleration

Spatial and temporal correspondence between enhanced blue wing observed with Hinode/EIS and propagating disturbances in fan loops seen in AIA images

Abstract Author(s): Naomasa Kitagawa

Institution(s): The Univ. of Tokyo

Presentation: S3-P-07

Abstract

We investigated a correspondence between enhanced blue wings (EBWs) in emission line profiles and propagating disturbances in fan loops seen in consecutive AIA images. The upflows from active region peripheries (also referred to as AR outflows) have been analyzed from the viewpoint of coronal heating. One idea is that these upflows are induced by impulsive heating. The property that AR outflows are seen at AR peripheries has been confirmed by many observations, however, their driving mechanism has not been revealed yet. One approach is to seek the counterpart of EBWs in imaging observations. Recently, McIntosh et al. interpreted these upflows in terms of propagating disturbances (PDs) in fan loops, based on the fact that EBWs were observed at their footpoints.

In this study, we analyzed emission line profiles in the wide temperature range from Si vii to Fe xiv (i.e., log T [K] = 5.8–6.3) observed with Hinode/EIS and investigate whether the PDs seen in AIA consecutive images coincide with the EBWs in those line profiles. Using the spectroscopic data of AR11106, we revealed that weak EBWs were indeed seen inside AIA fan loops, however, the strongest EBWs were located at a dark region outside those fan loops. It is also shown that the fluctuation caused by the PDs is up to 4% in AIA 193 Å passband images which is consistent with the relative intensity of EBWs, while the EBWs in the dark region exceed 20% in Fe xii. Our results imply that the EBWs do not always coincide with the PDs. Tiny transient brightenings were detected at the dark region clearly in AIA images, which might be related to the source of the upflows.

Hinode-7
Session 3: Coronal Heating and Solar Wind Acceleration

Report of Cooperative Observations between Hida Observatory & Hinode Satellite (HOP0012, 0075, 0128)

Abstract Author(s): Satoru UeNo, Kiyoshi Ichimoto, Reizaburo Kitai, Kazunari Shibata, Shin'ichi Nagata, Satoshi Morita, Ken'ichi Otsuji, Tetsu Anan, Akihito Oi, Kengo Yoshida, Ayumi Asai, Takuma Matsumoto, Hiroaki Isobe, Yuki Hashimoto, Takako Takeuchi Ishii, Masaoki Hagino, Hiroyuki Komori, Keisuke Nishida, Tahei Nakamura, Tomoko Kawate, Hiroko Watanabe, Andrew Hillier, Akihiro Ohkawa, Shinpei Sawada, Shun Miyawaki, Yuri Kato, Naoaki Mohri

Institution(s): Kwasan and Hida Observatories, Kyoto University

Presentation: S3-P-08

Abstract

Chromospheric active phenomena that are all related with the solar magnetic field have become clearer by recent MHD simulations and high-resolution observations with the HINODE satellite. In order to quantitatively verify the present models of such phenomena, we have continued simultaneous and high-cadence observations of diversified observation from the photosphere to the corona with the HINODE satellite and spectrum observation at the Hida Obs. For example, Hinode has found many and various chromospheric jets (Ca jets). We must verify whether the mechanisms of such jets are all magnetic reconnection (ubiquitous reconnection ?), and investigate the amount of contribution of such jets to the coronal heating process. Therefore, we measure the 3D distributions & evolutions of the velocity field (bidirectional flow, reconnection flow, shock wave), temperature, density and magnetic field configuration around various type of jets. Gas dynamics in flare kernels will differ between compact flares and two-ribbon flares. Especially the directions of initial gas flows will be different between the two due to the the difference of energy release heights in the atmosphere, which leads to the asymmetric emission profiles of the chromospheric lines. On the other hand, Hinode has also found wave-like phenomena in prominences. By adding chromospheric spectral informations, we intend to verify whether such phenomena in the prominences or dark filaments correspond to Alfven waves or fast-mode kink waves, from the point of view of the coronal heating, prominence-seismology and formation of magnetic field structures around prominences. Moreover, we have observed wave propagation from the photosphere to corona around sunspot region and investigate relationship between spatial distribution of coronal heating rate and spatial difference of characteristics of oscillation. In this poster, we introduce some typical results of such cooperative observations during these several years.

Hinode-7
Session 3: Coronal Heating and Solar Wind Acceleration

Non-equilibrium helium ionization and its effects on the He II 304 and He I 10830 lines

Abstract Author(s): Thomas Peter Golding, Jorrit Leenaarts, Mats Carlsson

Institution(s): Institute of Theoretical Astrophysics, University of Oslo, Institue of theoretical astrophysics, University of Oslo , Institue of theoretical astrophysics, University of Oslo

Presentation: S3-P-09

Abstract

Helium plays an important role in the energy balance of the upper chromosphere and transition region and its spectral lines are often used diagnostics. Its non-equilibrium ionization balance and radiative losses should therefore be treated in detail in numerical simulations of the solar atmosphere.

We perform 1D radiation-hydrodynamics simulations to show that the helium ionization balance is mostly set by photoionization (chromosphere) and collisional ionization (transition region), counteracted by radiative recombination. We derive a simplified 3-level helium model atom that reproduces this behavior and is suitable for use in 3D stellar atmosphere simulations.

We studied the formation of the He I 10830 and He II 304 spectral lines in the 1D simulation. The helium ionization relaxation timescale is up to 100 seconds in the line-forming regions. This leads to significant differences in the emergent intensity compared to statistical equilibrium computations. Inversions and interpretations of observations of these lines assuming statistical equilibrium should therefore be viewed with caution.

Hinode-7
Session 3: Coronal Heating and Solar Wind Acceleration

Spectroscopic properties of a dark lane and a cool loop in a limb active region observed by Hinode/EIS

Abstract Author(s): Kyoung-Sun Lee, Shinsuke Imada, Yong-Jae Moon, Jin-Yi Lee

Institution(s): ISAS/JAXA, Nagoya Univ., Kyung Hee Univ., Kyung Hee Univ.

Presentation: S3-P-10

Abstract

We determine spectral properties of a cool loop and a dark lane over a limb active region on 2007 March 14 by the Hinode/EUV Imaging Spectrometer. The cool loop is clearly seen in the spectral lines formed at the transition region temperature. The dark lane is characterized by an elongated faint structure in coronal spectral lines and rooted on a bright point. We examine their electron densities, Doppler velocities, and non-thermal velocities as a function of distance from the limb. We derived electron densities using the density sensitive line pairs of Mg VII, Si X, Fe XII, Fe XIII and Fe XIV spectra. Under the hydrostatic equilibrium and isothermal assumption, we determine their density scale heights and compare them to observed density scale height. For the non-thermal velocity, we have found that the non-thermal velocity in the cool loop slightly decreases along the loop while that in the dark lane sharply falls off with height. The variation of non-thermal velocity with height in the cool loop and the dark lane is contrast to that in off-limb polar coronal holes which are considered as source of the solar wind. Such a decrease in the non-thermal velocity may be explained by wave damping near the solar surface or turbulence due to magnetic reconnection near the bright point.

Off-limb hot thermal structure of AR 11459

Abstract Author(s): Susanna Parenti, Fabio Reale, Paola Testa, Helen Mason

Institution(s): Royal Observatory of Belgium

Presentation: S3-P-11

Abstract

The thermal structure of active regions and loops are one important element needed to characterize the way these structures are heated. In particular, in recent years much attention has been devoted to identify the properties of the high temperature component (> 3MK) of the plasma seen during non-flaring conditions. This, in fact, is the observational aspect predicted by impulsive heating models which is not expected to be seen when the steady heating is at work. We present results of an investigation aiming at characterizing the thermal structure of AR 11459 under non-flaring conditions. In particular, for the first time the spatial properties of the hottest component are highlighted. The AR was observed at the west limb using coordinated observations of Hinode/EIS and SOHO/SUMER spectrometers. The data cover the temperature range up to about 8 MK, and include the full Fe IX-XIX and Ca XIV-XVII series.

Hinode-7
Session 3: Coronal Heating and Solar Wind Acceleration

Observational signatures of Alfven Wave Turbulence

Abstract Author(s): Mahboubeh Asgari-Targhi, Shinsuke Imada, Adriaan van Ballegooijen

Institution(s): Nagoya University, Nagoya University

Presentation: S3-P-12

Abstract

The non-thermal width in coronal emission lines could be due to the Alfven wave turbulence. In order to find observational evidence of the Alfven waves that result in coronal heating, we examine and analyse the dynamics of an active region observed on 2012 September 7. We use spectral line profiles obtained by Extreme-ultraviolet Imaging Spectrometer (EIS) on Hinode spacecraft. Line profile observations from EIS were generated and compared with our computations of Alfven wave amplitude perpendicular to the line of sight. We show non-thermal velocities, Doppler outflows, and intensities for loops in this active region. And derive comparisons between our numerical results and observations from EIS. Also, we test the relationship between the width of the coronal emission lines and the orientation of the coronal loops with respect to the line-of-sight direction. The imaging spectra that we use are based on line profiles of Fe XII, Fe XIII, Fe XV and Fe XVI.

Hinode-7
Session 3: Coronal Heating and Solar Wind Acceleration

How to determine the physical parameters that govern wave dissipation time and spatial scales

Abstract Author(s): Inigo Arregui, Andres Asensio Ramos, David J Pascoe

Institution(s): Instituto de Astrofisica de Canarias, Instituto de Astrofisica de Canarias (IAC) , School of Mathematics and Statistics, University of St. Andrews

Presentation: S3-P-13

Abstract

To quantify the importance of magnetohydrodynamic wave dissipation in the solar atmosphere requires the determination of the cross-field density structuring of magnetic waveguides. We show how this can be accomplished using MHD wave seismology techniques.

Recent analyses of the damping of propagating transverse waves show the existence of two separate damping regimes for the wave amplitude decay. The observational identification of those regimes and the measurement of the associated damping length scales can be used to constrain the density contrast and its transverse inhomogeneity length scale across the field. Our parameter inference is performed in the Bayesian framework, to accomodate a proper propagation of uncertainty.

The obtained parameters determine the time/spatial scales for damping of transverse waves; how fast energy is transferred to small length scales; the timing for the onset of dissipative effects; and the fraction of the wave energy that can be converted into heat.

Hinode-7
Session 3: Coronal Heating and Solar Wind Acceleration

On the Signature of Alfven Wave Dissipation in the Localized Coronal Funnel as a Source of Nascent Solar Wind

Abstract Author(s): Bhola N. Dwivedi, Abhishek K. Srivastava, Anita Mohan

Institution(s): IIT (BHU) Varanasi

Presentation: S3-P-14

Abstract

We analyse Hinode/EIS 2?-spectroscopic scan data containing the spectral lines formed around typical coronal and transition region temperatures. They show the existence of a funnel-like expanding flux-tube which exhibits the signature of the out-flowing plasma in the off-limb equatorial corona as a possible source of the slow solar wind. This coronal funnel is expanding in the form of open magnetic field channel that may be a part of a large-scale and closed magnetic fields existing higher in the diffused equatorial corona. We also find the signature of decreasing line-widths with altitude in the observed coronal funnel which may be the signature of Alfven wave dissipation. We conclude that the Alfven wave dissipation along the expanding field lines of the coronal funnel may impart its energy to the out-flowing plasma and may contribute to the formation of the nascent solar wind in the inner corona.

Hi-C and AIA observations of transverse magnetohydrodynamic waves in active

Abstract Author(s): Richard Morton, James McLaughlin

Institution(s): Northumbria University, Northumbria University

Presentation: S3-P-15

Abstract

The recent launch of the High resolution Coronal imager (Hi-C) provided a unique opportunity of studying the EUV corona with unprecedented spatial resolution. We utilize these observations to investigate the properties of low-frequency (50-200 s) active region transverse waves, whose omnipresence had been suggested previously. The five-fold improvement in spatial resolution over SDO/AIA reveals coronal loops with widths 150-310 km and that these loops support transverse waves with displacement amplitudes <50 km. However, the results suggest that wave activity in the coronal loops is of low energy, with typical velocity amplitudes <43 km s^{-1}. An extended time-series of SDO data suggests that low-energy wave behaviour is typical of the coronal structures both before and after the Hi-C observations.

Hinode-7
Session 3: Coronal Heating and Solar Wind Acceleration

Fine-scale Fluctuations in the Corona observed with Hi-C

Abstract Author(s): Amy R Winebarger, Timothy Schuler

Institution(s): NASA MSFC

Presentation: S3-P-16

Abstract

The High-Resolution Coronal Imager (Hi-C) flew aboard a NASA sounding rocket on 2012 July 11 and captured roughly 345 s of high spatial and temporal resolution images of the solar corona in a narrowband 193 Angstrom channel. We have analyzed the fluctuations in intensity of Active Region 11520. We selected events based on a lifetime greater than 11 s (two Hi-C frames) and intensities greater than a threshold determined from the average background intensity in a pixel and the photon and electronic noise. We find fluctuations occurring down to the smallest time scale ($\sim$ 11 s). Typical intensity fluctuations are 20% background intensity, while some events peak at 100% the background intensity. Generally the fluctuations are clustered in solar structures, particularly the moss. We interpret the fluctuations in the moss as indicative of heating events. We use the observed events to model the active region core.

Hinode-7
Session 3: Coronal Heating and Solar Wind Acceleration

Structure of solar coronal loops: from miniature to large-scale

Abstract Author(s): H. Peter, S. Bingert, J. A. Klimchuk, C. de Forest, J. W. Cirtain, L. Golub, A. R. Winebarger, K Kobayashi, K. E. Korreck

Institution(s): Max Planck Institute for Solar System Research, Katlenburg-Lindau, Germany

Presentation: S3-P-17

Abstract

We will use new data from the High-resolution Coronal Imager (Hi-C) with unprecedented spatial resolution of the solar corona to investigate the structure of coronal loops down to 0.2". During a rocket flight Hi-C provided images of the solar corona in a wavelength band around 193 A that is dominated by emission from Fe X showing plasma at temperatures around 1.5 MK. We analyze part of the Hi-C field-of-view to study the smallest coronal loops observed so far and search for the a possible sub-structuring of larger loops. We find tiny 1.5 MK loop-like structures that we interpret as miniature coronal loops. These have length of the coronal segment above the chromosphere of only about 1 Mm and a thickness of less than 200 km. They could be interpreted as the coronal signature of small flux tubes breaking through the photosphere with a footpoint distance corresponding to the diameter of a cell of granulation. We find loops that are longer than 50 Mm to have a diameter of about 2" or 1.5 Mm, consistent with previous observations. However, Hi-C really resolves these loops with some 20 pixels across the loop. Even at this greatly improved spatial resolution the large loops seem to have no visible sub-structure. Instead they show a smooth variation in cross-section. The fact that the large coronal loops do not show a sub-structure at the spatial scale of 0.1"/pixel implies that either the densities and temperatures are smoothly varying across these loops or poses an upper limit on the diameter of strands the loops might be composed of. We estimate that strands that compose the 2" thick loop would have to be thinner than 15 km. The miniature loops we find for the first time pose a challenge to be properly understood in terms of modeling.

Constant cross section of loops in the solar corona

Abstract Author(s): H. Peter, S. Bingert

Institution(s): Max Planck Institute for Solar System Research, Katlenburg-Lindau, Germany

Presentation: S3-P-18

Abstract

The corona of the Sun is dominated by emission from loop-like structures. When observed in X-ray or extreme ultraviolet emission, these million K hot coronal loops show a more or less constant cross section. In this study we show how the interplay of heating, radiative cooling, and heat conduction in an expanding magnetic structure can explain the observed constant cross section. We employ a three-dimensional magnetohydrodynamics (3D MHD) model of the corona. The heating of the coronal plasma is the result of braiding of the magnetic field lines through footpoint motions and subsequent dissipation of the induced currents. From the model we synthesize the coronal emission, which is directly comparable to observations from, e.g., the Atmospheric Imaging Assembly on the Solar Dynamics Observatory (AIA/SDO). We find that the synthesized observation of a coronal loop seen in the 3D data cube does match actually observed loops in count rate and that the cross section is roughly constant, as observed. The magnetic field in the loop is expanding and the plasma density is concentrated in this expanding loop; however, the temperature is not constant perpendicular to the plasma loop. The higher temperature in the upper outer parts of the loop is so high that this part of the loop is outside the contribution function of the respective emission line(s). In effect, the upper part of the plasma loop is not bright and thus the loop actually seen in coronal emission appears to have a constant width. From this we can conclude that the underlying field-line-braiding heating mechanism provides the proper spatial and temporal distribution of the energy input into the corona — at least on the observable scales.

Hinode-7
Session 3: Coronal Heating and Solar Wind Acceleration

Distributions of energy of EUV bright points in the solar corona

Abstract Author(s): Vincent Joulin

Institution(s): IAS

Presentation: S3-P-19

Abstract

To explain the high temperature of the corona, much attention has been paid to the distribution of energy in dissipation events. Indeed, if the power-law slope of the dissipated energy distribution is less than -2, the smallest, unobservable events could be the largest contributors to the total energy dissipation in the corona. Observations in EUV and X-rays have actually shown a distribution of event energies extending over 8 decades, with a slope close to -2, but they remain inconclusive about the precise slope. Furthermore, these results rely on a very crude estimate of the (thermal) energy. On the other hand, more detailed spectroscopic studies of events such as coronal bright points do not provide enough statistical information to derive their total contribution to heating.

In this work we aim at getting a better estimate of the distributions of the energy dissipated in coronal heating events, by detecting EUV brightenings at small spatial and temporal scales in high-cadence (one image every five minute during three days) multi-channel SDO/AIA data (94Å, 131Å, 171Å, 193Å, 211Å, 335Å), and then by using temperature and emission measure maps derived from the same data to compute the thermal and radiative energies associated to these events. We compare the distributions of event energies obtained by this method with previous results.Moreover, we match the SDO/AIA-detected brightenings with Hinode/EIS observations when they are available; this will allow us to use spectroscopic temperature and density diagnostics to check the thermal energy deduced from the SDO/AIA temperature and emission measure, and to estimate also the kinetic energy in events.

Hinode-7
Session 3: Coronal Heating and Solar Wind Acceleration

Synthezided spectra of optically thin emission lines produced by the Bifrost stellar atmosphere code

Abstract Author(s): Kosovare Olluri, Boris V. Gudiksen, Viggo H. Hansteen, Bart De Pontieu

Institution(s): Institute of Theoretical Astrophysics, UiO

Presentation: S3-P-20

Abstract

3D numerical models try to recreate and mimic the solar atmosphere as seen from the observer in the best way, making it possible to do an in depth study of the physical quantities such as the temperatures, densities, magnetic fields etc. causing the phenomenons we observe on the sun. It has therefore become more and more common to use simulations in parallel with observations when analyzing spectra of the solar atmosphere. But the simulations have to be able to produce synthesized spectra that resembles previously reported results from observations. We will therefore here do a spectroscopic study of synthetic spectra created using the Bifrost code, and investigate how well the results hold when compared to reported results from observations. We present a study of the synthetic intensity, non–thermal linewidths, Doppler shifts, and correlations between any two of these three components of the spectra first assuming statistical equilibrium. The small dynamical timescales in the transition region and corona, makes us question the validity of this assumption. We therefore test the effect including non-equilibrium ionization, by solving the full 3D time-dependent rate equations, will have on the synthesized spectra.

Magnetothermal Instability in the Solar Atmosphere

Abstract Author(s): Takaaki Yokoyama

Institution(s): The University of Tokyo

Presentation: S3-P-21

Abstract

We discussed an application of the magnetothermal instability (MTI) to the solar atmosphere. This instability proposed by Balbus (2000) occurs in weakly collisionless plasmas where non-isotropic thermal conduction plays a role in a magnetized atmosphere. Suppose a stratified atmosphere under the gravity with horizontal magnetic fields. When the outward temperature gradient is negative even though it is sub-adiabatic, this instability is triggered. By the given perturbation to the magnetic field lines, the outer gas is heated by the conduction, becomes lighter, and obtains the buoyancy. As it moves outward, this cycle is repeated and suffers from the positive feed-back leading to the instability. The time scale of the maximum growth is given as approximately sqrt(H/g) where H is the scale height, and g is the gravity. The magnetic field must be weak enough since its tension force contributes as a restoring force. The solar corona is a dilute hot atmosphere where the thermal conduction is non-isotropic. The MTI is possible to work in the upper corona around a few solar radii above the photosphere where the temperature is decreasing outward and the scale height is about one solar radius. The condition for weak horizontal magnetic field might be satisfied above a closed loop in the lower corona. If the MTI is effective in such regions, it might contribute to generate the waves or perturbations in the solar wind.

Hinode-7
Session 3: Coronal Heating and Solar Wind Acceleration

The response of the corona to different heating mechanisms.

Abstract Author(s): Tijmen van Wettum, Sven Bingert, Hardi Peter

Institution(s): Max Planck Institute for Solar System Research, Max-Planck-Institut fur Sonnensystemforschung

Presentation: S3-P-22

Abstract

We explore the observational consequences of different heating mechanisms using 3D MHD numerical experiments. This provides some insight on which of these mechanisms is dominant. For this we replace the Ohmic heating term in the energy equation with a parametrized form of the heating derived from reduced MHD for heating through.

We find that the different heating parametrizations give similar coronae in terms of synthesized emission as it would be observed e.g. by EUV imaging. Thus EUV imaging alone will not be sufficient to distinguish between these parametrizations. However, Doppler shift observations acquired by e.g. Hinode/EIS can provide the pivotal information. In our numerical experiments the different parametrizations of the heating lead to significantly different distributions of the Doppler shifts of the synthesized emission lines in the transition region and corona. In particular, this applies to the average redshifts seen in the transition region and the average blueshifts in the coronal lines. Based on this, our results favor the turbulent cascade over the Alfven wave heating, at least when considering an active region. Future observational and numerical studies will have to show to what extend this will hold in general.

Hinode-7
Session 3: Coronal Heating and Solar Wind Acceleration

Synthetic spectra for the kappa-distributions using modified CHIANTI

Abstract Author(s): Elena Dzifcakova, Jaroslav Dudik, Frantisek Farnik, Pavel Kotrc

Institution(s): Astronomical Institute Odrejov

Presentation: S3-P-23

Abstract

An idea of the presence of non-Maxwellian distributions in the solar corona is supported by many theoretical calculations and few attempts to diagnose them from UV and EUV lines. The kappa-distributions or distributions exhibiting high-energy tails can also be expected as a result of particle acceleration processes by " nanoflare " heating in the solar corona.

Non-Maxwellian distributions generally lead to modification of line intensities compared to Maxwellian ones. This is because rates of individual ionization, recombination and collisional excitation are an integral product of the cross-section multiplied by the distribution. This in principle enables diagnostics of non-Maxwellian distributions from observed spectra.

The exitation rates for coronal lines are usualy known only for the commonly accepted a widely used assumption of the Maxwellian distribution of particles. The widely used software and atomic database CHIANTI allows us to calculate synthetic spectra only for the Maxwellian distribution. Therefore, we modified CHIANTI 7.1 software and extended its database. This modified version of CHIANTI for the kappa-distributions contains data for calculation of the excitation rates together with the newest calculations of the ionization equilibrium. It allows for fast calculation of synthetic spectra, search for diagnostic opportunities for kappa-distributions, and the study the influence of the kappa-distribution on the observed temperature distribution in emitting plasma represented by DEM.

Hinode-7
Session 3: Coronal Heating and Solar Wind Acceleration

Forward modelling of MHD kink oscillations in the solar corona

Abstract Author(s): Patrick Antolin, Takaaki Yokoyama, Tom Van Doorsselaere

Institution(s): Centre for mathematical Plasma Astrophysics, Department of Mathematics, KU Leuven, Department of Earth and Planetary Sciences, Graduate School of Science, University of Tokyo, Japan , Centre for mathematical Plasma Astrophysics, Department of Mathematics, KU Leuven, Belgium

Presentation: S3-P-24

Abstract

The aim of this work is to characterise the EUV observational signatures of the MHD kink mode in the solar corona. This transverse MHD mode has been frequently observed in the solar corona and is therefore especially relevant in the context of coronal heating and coronal seismology. Reported damping times of kink modes are often much shorter than expected from linear MHD theory. Understanding such characteristics of MHD waves is crucial to the correct derivation of the physical properties of the plasma through application of coronal seismology. The main physical mechanism responsible for these short damping times is resonant absorption. Despite being predicted to be fairly common in the solar corona, no direct observational evidence of this mechanism exists so far. Here, we perform forward modelling of 3D MHD simulations of the MHD kink mode. The resonant absorption mechanism and the Kelvin-Helmholtz instability are two main processes obtained in the simulations. We consider line-of-sight geometric effects and instrumental effects (spatial, temporal and wavelength resolution), and determine the observational characteristics of these processes. The K-H instability can severely deform the cross-sectional shape of the tube resulting in irregular emissivity cross-sections and a highly inhomogeneous and turbulent internal density structure. After a few damping times the global transverse mode can barely be distinguished, agreeing with observational results. However, internal Alfvenic motions exist for longer times, leaving a distinct spectral broadening imprint. We determine the instrumental requisites necessary for the detection of these processes in coronal flux tubes.

Can the Differential Emission Measure diagnostic be used to constrain the timescale of energy deposition in the corona?

Abstract Author(s): Chloe Guennou, Frederic Auchere, James A. Klimchuk, Karine Bocchialini, Susanna Parenti

Institution(s): Institut d'Astrophysique Spatiale

Presentation: S3-P-25

Abstract

Differential emission measure (DEM) analysis is a widespread tool used to diagnose the thermal properties of coronal plasmas. The slope of the DEM distribution coolward of the coronal peak (near 3-4MK in active regions) can be used to diagnose the timescale for the energy deposition repeating on a given magnetic strand. Recent AR studies suggest that some active region cores are consistent with low frequency heating mechanisms, where the plasma cools completely before being reheated, while other show consistency with high frequency energy deposition, where rapid reheating causes the temperature to fluctuate about a particular value. Distinguishing between these possibilities is important for identifying the physical mechanism of the heating. It is therefore crucial to understand the uncertainties in measurements of observed DEM slopes.

In this work, based on a probabilistic approach and Monte Carlo simulations, we carefully assess the errors in the slopes determined from EIS data. We consider both the random errors due to photon counting statistics, and the systematic errors associated with uncertainties in atomic physics and instrument calibration. The technique developed provides all the solutions consistent with the data and their associated probabilities. We demonstrate how the quality and the accuracy of the inversion are affected by the presence of noises and systematic errors, and we characterize the quality of the DEM inversion and its statistical properties. From these results, estimation of the uncertainties in the reconstructed slopes can be derived, thereby allowing a proper interpretation of the degree of agreement between observations and heating model predictions.

Hinode-7
Session 3: Coronal Heating and Solar Wind Acceleration

What DEM Analysis Can and Cannot Tell Us

Abstract Author(s): Mark Weber

Institution(s): Smithsonian Astrophysical Observatory

Presentation: S3-P-26

Abstract

Deducing the temperature and density of coronal structures is an important step towards understanding their physical processes, such as heating mechanisms, and the structures' subsequent responses. Differential emission measure analysis is a technique that uses multiple passbands to solve for the temperature and emission measure of multithermal, optically thin coronal plasma along a line of sight. However, the inversion is ill-posed, and several difficulties in interpreting the results can give one the impression that DEM analysis might be hopeless. This talk will explore the mathematical basis of the DEM inversion, and explain how far the solution can be constrained by data, and how much can only be constrained by physical, a priori constraints. It is crucial to understand this distinction of parts, and how to calculate them, in order to confidently interpret the data. Applications to coronal data illustrate these points.

Hinode-7
Session 3: Coronal Heating and Solar Wind Acceleration

Quantification of the Energy Dissipated by Alfven Waves in a Polar Coronal Hole

Abstract Author(s): Michael Hahn, Daniel Wolf Savin

Institution(s): Columbia University, Columbia University

Presentation: S3-P-27

Abstract

Recently, line width measurements using EUV Imaging Spectrometer data have verified previous suggestions that line widths decrease with height over polar coronal holes. This implies that Alfven waves are damped at lower heights than predicted by simple models. However, in order to quantify the amount of energy dissipated, it is necessary to separate the thermal and non-thermal contributions to the line width. We present an analysis which determines the ion temperature and non-thermal velocity at the lowest heights (< 1.1 R_{sun}) by using the observation that at those heights the waves are not damped and by assuming that in that region the ion temperature is constant. We then extrapolate these results to larger heights (> 1.1 R_{sun}), where damping is observed, and estimate the energy dissipated from the waves and length and time scales for the damping. The analysis implies that the dissipated energy matches that required to heat the coronal hole and accelerate the fast solar wind and that the waves are dissipated over a length of about 0.2 R_{sun} or a time of about 70 s.

Hinode-7
Session 3: Coronal Heating and Solar Wind Acceleration

Anisotropic Ion Temperatures, Non-Thermal Velocities, and Doppler Shifts in a Coronal Hole

Abstract Author(s): Michael Hahn, Daniel Wolf Savin

Institution(s): Columbia University, Columbia University

Presentation: S3-P-28

Abstract

Various models for ion heating in the corona predict ion temperatures that are anisotropic with respect to the magnetic field. Such anisotropy is observed in-situ in the solar wind, but has not been measured in the solar corona. Here, we present a method for performing such measurements and apply the technique to an observation of an equatorial coronal hole. For the analysis we combined spectroscopic line width measurements with a magnetic potential field source surface model. We then studied how the line width varied as a function of the inclination angle between the line of sight and the magnetic field direction. Perpendicular to the magnetic field, the ion temperatures and non-thermal velocities agree with those inferred from off-limb measurements, as expected. For the parallel component, we find that the temperature is uniform for all the ion species. The parallel temperature is expected to reflect the proton temperature, which we inferred to be about 1.8 +/- 0.2 MK. Using a similar technique, but applied to Doppler shifts, we found the outflow velocity to be about 5 km/s in the coronal hole.

Hinode-7
Session 3: Coronal Heating and Solar Wind Acceleration

On the Coronal Reconnection Height and Hot Jet Formation in the North Polar Coronal Hole (NPCH) as Observed by Hinode/EIS

Abstract Author(s): Pradeep Kayshap, Abhishek K. Srivastava

Institution(s): Aryabhatta Research Institute of Observational Sciences (ARIES)

Presentation: S3-P-29

Abstract

We analyze a coronal jet from Hinode/EIS 2" slit observations, which was triggered on 22nd April 2009 in the north polar coronal hole (NPCH). Many bright points and an elongated jet-like structure above a distinct bright point were present in the observed NPCH. For this study, we have chosen this jet and associated bright point in the NPCH. Spectroscopic analysis (Fe XII 195.12 A,Log T∼6.1) revels the red-shifted base and blue-shifted jet plasma column above it, which suggests that the jet is formed by magnetic reconnection. The straight elongation of the jet provides a great opportunity to measure the reconnection height in the polar atmosphere. Reconnection occurs at a height of $\sim$ 20 Mm from the footpoint of the jet lying at the limb as visible in Fe XII 195.12 A, where the red-shift is inverted into the blue-shift in the Doppler velocity component along the jet plasma column. Intensity analysis of Si VII 275.35 A (Log T $\sim$ 5.8) shows that transition region (TR) is located $\sim$ 5 Mm above the limb. Therefor, the reconnection point is well above the TR and resides in the corona. From the reconnection point, plasma flows in upward as well downward direction with a maximum speed of 9 ± 3 km s^{-1} and $\sim$ 15 km s^{-1} respectively. Cool TR line Si VII (VII 275.35 A; Log Te $\sim$ 5.8) emission does not show the jet that infer the absence of cool plasma components inside it. This clearly indicates that the reconnection at higher coronal heights above TR only forms the hot plasma component in the polar jets, which is in agreement with the standard numerical models of reconnection driven coronal jets.

Hinode-7
Session 3: Coronal Heating and Solar Wind Acceleration

Double-thread structure of spicules generated by magnetic reconnection

Abstract Author(s): Takenori Suda

Institution(s): Kyoto University

Presentation: S3-P-30

Abstract

Spicules are high-speed (∼25km/s), cool (∼10000K) jets propelled upwards from the lower chromosphere into the corona and observed ubiquitously on the solar surface. Spicules are an intrinsic component of the upper chromosphere which works as the interface between the cool photosphere and the hot corona, and are hypothesized to play an important role in corona heating and acceleration of the solar wind. However, the origin of spicules is still not clear. Recently, spicule observations using the Solar Optical Telescope on the Hinode satellite revealed that more than 50% of spicules show double-thread structure (Suematsu et al 2008) highlighting that we still do not fully understand the spicule formation mechanism. One explanation for the formation of double-thread spicules is that three-dimensional component reconnection is occurring in current sheets formed by convective motions creating shear in a unipolar magnetic field. However, there is still no theoretical study that investigates formation of double-thread spicules through component reconnection. In order to understand the 3D effects of component reconnection on the spicule acceleration, we performed 1.5D MHD simulations to follow the evolution of shocks created by component reconnection in a model solar atmosphere.

In the simulations, we observed that slow shocks and intermediate shocks are generated in the lower chromosphere and both types of shock launch chromospheric plasma into the corona, i.e. they form spicules. As our simulations follow the shock evolution along one of the pair of reconnected field lines, it can be expected that spicules would form along both field lines creating the observed double-thread structure.

Hinode-7

Session 4

Flares and Coronal Mass Ejections

Hinode-7
Session 4: Flares and Coronal Mass Ejections

The Evolution of Small Solar Flares Observed with Hinode and SDO (AIA and EVE)

Abstract Author(s): Helen E Mason, Giulio Del Zanna, Giota Petkaki, Stephen J Bradshaw

Institution(s): University of Cambridge, University of Cambridge, University of Cambridge , Rice University

Presentation: S4-I-01

Abstract

Compact flares have been observed and studied since the early days of Skylab in the 1970s. Hinode/EIS together with SDO/AIA and EVE now provide an excellent opportunity to study these small flares in great detail, in particular to match the evolution of plasma parameters derived from observations (spectroscopy and imaging) against theoretical models. Recent studies of compact flares will be discussed.

Hinode-7
Session 4: Flares and Coronal Mass Ejections

Coordinated observations of X-ray and high-resolution EUV active region dynamics

Abstract Author(s): Sabrina L Savage

Institution(s): NASA / MSFC

Presentation: S4-C-01

Abstract

The recently-launched High-resolution Coronal imager (Hi-C) sounding rocket provided the highest resolution images of coronal loops and other small-scale structures in the 193 Angstrom passband to date. With just 5 minutes of observations, the instrument recorded a variety of dynamic coronal events – including even a small B-class flare. We will present our results comparing these extreme-ultraviolet (EUV) observations with X-ray imaging from Hinode/XRT as well as EUV AIA data to identify sources of hot plasma rooted in the photosphere and track their affect on the overall topology and dynamics of the active region.

Hinode-7
Session 4: Flares and Coronal Mass Ejections

The location of non-thermal velocity in the early phases of large flares - revealing pre-eruption flux ropes

Abstract Author(s): Louise Harra, Sarah Matthews, Len Culhane, Mark Cheung, Eduard Kontar, Hirohisa Hara

Institution(s): UCL-MSSL, UCL-MSSL, UCL-MSSL, LMSAL, University of Glasgow, NAOJ

Presentation: S4-C-02

Abstract

Non-thermal velocity measurements of the solar atmosphere, particularly from UV and X-ray emission lines have demonstrated over the decades that this parameter is important in understanding the triggering of solar flares. Enhancements have often been observed before intensity enhancements are seen. However, until the launch of Hinode, it has been difficult to determine the spatial location of the enhancements to better understand the source region. The Hinode EUV Imaging Spectrometer (EIS) has the spectral and spatial resolution to allow us to probe the early stages of flares in detail. We analyse four events, all of which are GOES M or X-classification flares, and all are located towards the limb for ease of flare geometry interpretation. Three of the flares were eruptive and one was confined. In all events, pre-flare enhancement in non-thermal velocity at the base of the active region and its surroundings has been found. These enhancements seem to be consistent with the footpoints of the dimming regions, and hence may be highlighting the activation of a coronal flux rope for the three eruptive events. In addition pre-flare enhancements in non-thermal velocity were found above the looptops for the three eruptive events.

Hinode-7
Session 4: Flares and Coronal Mass Ejections

An MHD Model of a Solar Eruption Starting from NLFFF Initial Conditions

Abstract Author(s): Edward E. DeLuca, Yingna Su, Bernhard Kliem

Institution(s): Harvard-Smithsonian Center for Astrophysics, Harvard-Smithsonian Center for Astrophysics , University of Potsdamn

Presentation: S4-C-03

Abstract

The structure of the coronal magnetic field prior to eruptive processes and the conditions for the onset of eruption are important issues that can be addressed through studying the magnetohydrodynamic stability and evolution of nonlinear force-free field (NLFFF) models. This talk uses data-constrained NLFFF models of a solar active region that erupted on 2010 April 8 as initial conditions in three-dimensional MHD simulations. These models, constructed by the techniques of flux rope insertion and magnetofrictional relaxation, include a stable, an approximately marginally stable, and an unstable conguration. The simulations first confirm the results of previous related studies that solely used-magnetofrictional relaxation, in particular that stable equilibria containing a flux rope represent key features of the observed coronal structures prior to the considered eruption very well and that there is a limiting value of the axial flux in the rope for the existence of stable NLFFF equilibria.

Hinode-7
Session 4: Flares and Coronal Mass Ejections

Evolution of electric currents and their connection with the 2011 February 15 X-class flare ribbons

Abstract Author(s): Miho Janvier, Guillaume Aulanier, Veronique Bommier, Brigitte Schmieder

Institution(s): Lesia - Observatoire de Paris

Presentation: S4-C-04

Abstract

We propose a coupled analysis of an eruptive flare and its associated flare ribbons in the light of optical observations and MHD simulations. In particular, we investigate the relation between the time evolutions of flare ribbons and photospheric electric currents.

As such, we use SDO observations of the two-ribbon, X-class eruptive flare that occurred on 2011, February 15 combined with a 3D MHD numerical simulation reproducing the dynamics of an eruptive flare. Observational maps of the current density are derived from the UNNOFIT inversion code from SDO/HMI from which the source magnetic field is obtained. Maps of current density before and after the flare show the thickening and the radial expansion of negative current after the peak of the flare, as well as an intensification of the positive current density. This evolution is then compared with that of the vertical current density obtained in the 3D MHD simulation. In particular, we find similar structures for the current density such as the straight and hooked parts J-shape structure. The evolution of the current density is then directly linked with the dynamics of the reconnection happening at higher heights in the solar corona. Finally, the SDO/HMI observations of the vertical current density evolution for the X-class flare are directly correlated with observations of flare ribbons monitored by the SDO/AIA instrument. SDO/HMI provides observations of the magnetic field evolution with a high time cadence. However, its spatial resolution limits the study of thin structures such as flare ribbons. Therefore, the present analysis would benefit from the coupling of observational data such as HINODE/SOT that has a better spatial resolution for the measure of the vector magnetic field and therefore of photospheric currents.

High speed photospheric flows observed around polarity inversion lines of a delta-type sunspot

Abstract Author(s): Toshifumi Shimizu

Institution(s): ISAS/JAXA

Presentation: S4-C-05

Abstract

Most of large flares are produced in delta-type sunspots, which show complex around the polarity inversion lines (PILs) formed inside the sunspot. Observations of behaviors around the PILs may give hints on understanding the magnetic configuration and conditions responsible for producing large flares. Flow fields at the photosphere are one of important parameters because flare energy is stored in non-potential coronal structures and their formation and destabilization may be caused with footpoint motions of coronal fields at the photosphere, such as shearing flows along the PIL and converging flows toward the PIL. This presentation will discuss on SOT(Stokes Polarimeter) observations of remarkable high speed photospheric flows along a PIL. The PIL was formed in the delta-type sunspot (NOAA 11429), which produced an X5.4 flare on 7 March 2012. This flare was well observed with XRT and SDO/AIA imaging observations. The high speed flows are distributed along the polarity inversion line (PIL) between the footpoint position of flare ribbons. Their Doppler speed is up to 3-5 km/s and they are observed in magnetic flux almost in parallel to the solar surface. They seem to be persistent gas flows, which can be seen in some maps acquired both before and after the flare. Similar photospheric flows may be commonly observed in the PILs of other delta-type sunspots produced X-class flares.

Hinode-7
Session 4: Flares and Coronal Mass Ejections

A solar flare observed by Fast Imaging Solar Spectrograph

Abstract Author(s): Hyungmin Park, Jongchul Chae

Institution(s): Seoul National University, Seoul National University

Presentation: S4-C-06

Abstract

We observed an M-class flare using the Fast Imaging Solar Spectrograph (FISS) on August 17, 2013. In the FOV of FISS, sudden brightening, horizontal mass flow, flare ribbon, and strong downflow were observed. Combining these results with SDO and HINODE data, we aim to understand the dynamics of flare. Here we introduce the preliminary results we obtained.

Nonlinear Fragmentation of Flare Current Sheets

Abstract Author(s): Naoto Nishizuka, Keisuke Nishida, Kazunari Shibata

Institution(s): National Astronomical Observatory of Japan, Kwasan and Hida observatories, Kyoto University, Kwasan and Hida observatories, Kyoto University

Presentation: S4-I-02

Abstract

Recent space solar observations, such as Hinode, SDO, STEREO and RHESSI, revealed that magnetic reconnection is ubiquitous in the corona and chromosphere, ranging from small scale (nanoflares) to global scale (CME related flares). These reconnection events are often associated with mass ejections with various sizes. This implies that the magnetized solar atmosphere consist of self-similar structure, i.e., fractal structure and dynamics. Bursty radio and hard X-ray emissions in solar flares also suggest fractal-like time variability of reconnection and associated particle acceleration. Recent theoretical studies have revealed that multiple plasmoids make a current sheet turbulent in 3D and enable intermittent ejections and their interactions. In such a process, particles are accelerated at multi X-lines with locally enhanced electric field and at multiple shocks collided by plasmoids. High resolution observations have also discovered small scale structures of a current sheet, i.e. multiple plasmoids. They show the slow rising motion in pre-flare phase and strong acceleration during impulsive phase associated with hard X-ray bursts, indicating particle acceleration occurring at the same time. Plasmoid ejections are observed to increase reconnection inflow and reconnection rate. The similar phenomena have been discovered in laboratory experiments, in which a plasmoid ejection increases reconnection electric field in a current sheet. Furthermore, a larger plasmoid ejection induces stronger electric field. These are evidence of plasmoid-induced-reconnection, and in a fractal current sheet this process can repeat several times. We will discuss recent observations and theories related to fractal reconnection and plasmoids, and discuss possible implication to reconnection physics and particle acceleration in solar flares.

Hinode-7
Session 4: Flares and Coronal Mass Ejections

Spatially Resolved Measurements of Turbulence in the Flare Reconnection Region

Abstract Author(s): David E. McKenzie, George Doschek, Harry Warren, Michael Freed

Institution(s): Montana State University

Presentation: S4-C-07

Abstract

The physical conditions such as temperature, density, and dynamical properties in the flare reconnection region are poorly known, although there have been measurements of non-thermal hard X-ray emission properties by RHESSI and earlier by HXT on Yohkoh. The spatially resolved observations provided by Hinode and the Solar Dynamics Observatory (SDO) have improved this situation, and it is now possible to measure in sharper detail some of the properties of the reconnection region. Imaging in extreme ultraviolet (using AIA on SDO) and soft X-rays (with Hinode/XRT), and EUV spectroscopy (with Hinode/EIS), allow non-thermal motions in the reconnection region to be measured with unprecedented clarity. Turbulence is predicted by theoretical models of magnetic reconnection in flares, and has long been inferred spectroscopically from non-thermal broadening of flare emission lines. Studies with Hinode/XRT and SDO/AIA demonstrate that two-dimensional investigations of flare velocity fields can be made by imaging the plasma sheets in the reconnection region. These velocity measurements are made possible through the use of local correlation tracking (LCT) and reveal signatures of turbulence, including temporally and spatially varying vorticity. For some flares the AIA and XRT results can be combined with Doppler measurements of turbulence obtained with EIS. We will present coordinated analyses of EIS and AIA observations of plasma sheets in post-CME flares, including spectroscopic measures of the plasma temperatures in the reconnection region, and demonstrate that the turbulent speeds found by LCT closely resemble those derived from EIS spectral line profiles obtained in the same or nearby locations.

Hinode-7
Session 4: Flares and Coronal Mass Ejections

Spectroscopy at the Site of Magnetic Reconnection in the X-class Solar Flare on 2013 May 15

Abstract Author(s): Hirohisa Hara

Institution(s): National Astronomical Observatory of Japan

Presentation: S4-C-08

Abstract

We report loop-top structures and dynamical phenomena in the X-class eruptive solar flare that occurred on 2013 May 15, based on the EIS spectroscopic observations with other imaging observations. Dark fast outflow structures have been identified above the loop-top region of the flare. Especially, the incoming flows to the flare loop have also been observed. The hot structures in the outflow region and hot ridge located outside flare loops are investigated by the sufficient number of photons from the bright X-class flare. Positional relationships of structures that EIS observed to the hard X-ray imaging from RHESSI may be discussed.

Thermal Structure of Supra-arcade Downflows and Flare Plasma Sheets

Abstract Author(s): Kathy Reeves, Will Hanneman, David McKenzie, Michael Freed

Institution(s): Smithsonian Astrophysical Observatory, Smithsonian Astrophysical Observatory

Presentation: S4-C-09

Abstract

We use Hinode/XRT and SDO/AIA data to determine the thermal structure of supra arcade downflows as well as the surrounding plasma sheet. Using the multiple filters and broad temperature coverage provided by the combination of these two telescopes, we construct DEMs in the fan plasma and the supra-arcade downflows. Several models have indicated that the plasma inside the supra-arcade downflows should be significantly hotter than the surrounding plasma, but about an order of magnitude less dense. However, we find that the temperatures of the plasma within the downflows are either roughly the same as or lower than the surrounding fan plasma, with only one exception. We also compare the thermal structure of the supra-arcade plasma with calculations of the divergence of the velocity of the plasma in the sheet in order to locate evidence for adiabatic cooling and heating, and with the velocity shear in order to find evidence for viscous heating. The velocity fields are calculated using local correlation tracking applied to high-resolution sequences of AIA images.

Review on Current Sheets in CME development

Abstract Author(s): Jun Lin

Institution(s): Yunnan Astronomical Observatory, CAS

Presentation: S4-I-03

Abstract

Most of the universe fills with magnetized plasma. When twisted or sheared, the magnetic field may reconnect rapidly, converting magnetic energy into heat and kinetic energy. Because these phenomena often occur in environments of large electric conductivity, the energy conversion is usually confined to a small local region [an X-type neutral point, a current sheet (CS), or a quasi-separatix layer]. The catastrophe theory of the solar eruption suggests the formation of a CS following the onset of the eruption due to the catastrophic loss of equilibrium in the system. The CS is suggested to be long because the time-scale of diffusion is long compared to that of the catastrophe. On the other hand, the CS is traditionally expected too thin to be observable since its thickness is believed to be roughly the proton Larmor radius, which is about tens of meters in the coronal environment. However, the first direct observation of the CME/flare CS showed that it could be as thick as a few times 10^4 km! A set of follow-ups by different instruments, and in different wavelengths consistently brought its thickness to the range from about 10^4 km to about 10^5 km!

This talk will weave through the prediction of the catastrophe model for the long CS in the major eruptive process, the first identification of such structures, direct measurements of its thickness, discussions of the huge difference in the thickness between observations and theoretical expectations, possible impacts that may affect measurements, physical causes leading to a thick CS in which reconnection can still undergo at a reasonably fast rate, the numerical results displaying complex structures inside the sheet, as well as the results of the most recent laboratory experiments of reconnection driven by the energetic laser beams. Finally, conclusions based on the facts that could be collected so far are drawn.

Hinode-7
Session 4: Flares and Coronal Mass Ejections

The topology of supersonic outflows in a filament eruption

Abstract Author(s): David R. Williams, Lucie M Green, Deborah Baker, Lidia van Driel-Gestelyi, David M Long

Institution(s): MSSL, University College London, MSSL, University College London, MSSL, University College London, MSSL, University College London

Presentation: S4-C-10

Abstract

The standard model of flux rope eruptions includes topological locations where reconnection is expected, and critical evidence for or against this model can be provided by spectroscopic observations of temperature and flow speed at these sites. We report on unique observations of a filament eruption by Hinode/EIS, SDO/AIA and STEREO, in which extended regions of supersonic flow are spectroscopically detected along the flank of filament material ejected in a CME. Analysis of the pre-eruption topology indicates a modified view of tether-cutting reconnection in which large amounts of CME material are suddenly heated and accelerated in a quasi-continuous way, during the eruption itself, producing a non-standard but potentially common feature alongside the standard model.

Hinode-7
Session 4: Flares and Coronal Mass Ejections

Measuring the Magnetic Field Strength of the Quiet Solar Corona Using "EIT Waves"

Abstract Author(s): David Long, David Williams, Stephane Regnier, Louise Harra

Institution(s): UCL/MSSL, UCL/MSSL, UCLAN, UCL/MSSL

Presentation: S4-C-11

Abstract

Variations in the propagation of globally-propagating disturbances (commonly called "EIT waves") through the low solar corona offer a unique opportunity to probe the plasma parameters of the solar atmosphere. Here, high-cadence observations of two "EIT wave" events taken using the Atmospheric Imaging Assembly (AIA) instrument onboard the Solar Dynamics Observatory (SDO) are combined with spectroscopic measurements from the Extreme ultraviolet Imaging Spectrometer (EIS) onboard the Hinode spacecraft and used to examine the variability of the quiet coronal magnetic-field strength. The combination of pulse kinematics from SDO/AIA and plasma density from Hinode/EIS is used to show that the magnetic-field strength is in the range $\sim$2-6G in the quiet corona. The magnetic-field estimates are then used to determine the height of the pulse, allowing a direct comparison with theoretical values obtained from magnetic-field measurements from the Helioseismic and Magnetic Imager (HMI) onboard SDO using PFSS and local-domain extrapolations. While local-scale extrapolations predict heights inconsistent with prior measurements, the agreement between observations and the PFSS model indicates that "EIT waves" are a global phenomenon influenced by global-scale magnetic field.

Hinode-7
Session 4: Flares and Coronal Mass Ejections

High-sensitivity hard X-ray solar observation with the FOXSI rocket

Abstract Author(s): Shin-nosuke Ishikawa, Sam Krucker, Steven Christe, Lindsay Glesener, Brian Ramsey, Shinya Saito, Tadayuki Takahashi, Shin Watanabe, Hiroyasu Tajima, Takaaki Tanaka

Institution(s): NAOJ, University of California, Berkeley, University of California, Berkeley, University of California, Berkeley, NASA/MSFC, ISAS/JAXA, ISAS/JAXA, ISAS/JAXA

Presentation: S4-C-12

Abstract

We performed the first hard X-ray (HXR) observation of the Sun using HXR focusing optics with the Focusing Optics X-ray Solar Imager (FOXSI) sounding rocket. Accelerated electrons in solar flares emit HXRs by the bremsstrahlung process as they travel and lose their energy in the solar corona. Therefore, HXR observations of the Sun provide important information about the energy release process in solar flares. Although observing HXRs is important to investigate particle acceleration, the sensitivity and dynamic range are limited with the past and current non-focusing HXR instruments such as Yohkoh/Hard X-ray Telescope and RHESSI. Especially, HXR emissions from the quiet Sun are not well detected, and the energy release is still not well understood. Combining high-resolution focusing X-ray optics and fine-pitch imaging sensors, FOXSI achieves superior sensitivity in the target energy range of 5-15 keV; more than 1 order of magnitude better than that of the RHESSI spacecraft at 10 keV. The angular resolution of the optics is $\sim$6 arcseconds with the focal length of 2 m. FOXSI was successfully launched on November 2, 2012, from the White Sands Missile Range in New Mexico, USA. HXR emissions from a microflare were observed, and higher dynamic range is successfully demonstrated. The energy spectrum of the flare was successfully obtained, and the high capability of imaging and spectroscopy is clearly shown. In addition to the flare observation, HXR emissions from non-flaring region were detected. In this presentation, we will show an instrument description and results of the FOXSI mission. We will also show the comparison of the FOXSI HXR data at a non-flaring active region to the differential emission measure estimated by the Hinode/XRT multifilter observation.

'Realistic' 3D simulations of a small flare resulting from flux emergence

Abstract Author(s): Viggo Haraldson Hansteen, Vasilis Archontis

Institution(s): Institute of Theoretical Astrophysics, University of Oslo, School of Mathematics and Statistics, St. Andrews University

Presentation: S4-P-01

Abstract

We have performed three-dimensional (3d) magnetohydrodynamic simulations of magnetic flux emergence in a model that spans the convection zone and into the outer solar atmosphere with the Bifrost code. This is a "realistic" model, in the sense that the parameters and physical effects that control the atmosphere can be used to produce diagnostics that can be directly compared with observations. The emerging flux leads to the formation of several current sheets as it rises into the modeled corona. Multiple plasmoids are ejected from the current sheets. Reconnection occurs impulsively, producing heating and fast outflows near or in the current sheet, arranged in a manner reminiscent of the CSHKP flare model. This includes a cusp like arcade and a flux rope in the lower atmospere underneath the current sheet. We discuss the evolution of the model and several synthetic observables.

Hinode-7
Session 4: Flares and Coronal Mass Ejections

MHD Simulation of Filament Formation by Thermal Instability

Abstract Author(s): Takafumi Kaneko, Takaaki Yokoyama

Institution(s): Department of Earth and Planetary Science, The University of Tokyo, Department of Earth and Planetary Science, The University of Tokyo

Presentation: S4-P-02

Abstract

We propose a new theoretical model of formation of a filament and demonstrate by 2.5-dimensional MHD simulation with anisotropic thermal conduction, radiative cooling and gravity. Filaments appear along PILs (polarity inversion lines) of coronal arcade fields and it is thought that the cool dense plasmas are sustained by magnetic forces. One candidate to explain the formation of the cool dense plasma is the thermal instability model. In this formation model, localized heating is added to the footpoints of the long low-lying loop, leading to trigger thermal instability and generate cool dense plasma blobs in the loops (e.g. Xia et al.,2012). However, the current model does not consider the flux rope structure suggested by observation. We propose a new model to understand both the formation of flux rope and that of cool dense plasma, and verified it by simulation. We use the model in which the emerging flux is injected to the PIL of the arcade field as a method to form flux rope. As a result, it is found that the formation of a flux rope plays a significant role to trigger the thermal instability as follows: the effect of thermal conduction is limited in the newly formed flux rope because the magnetic filed lines are closed and the effect of radiative cooling is enhanced because the dense plasma at the lower corona is trapped in the flux rope and transported to the upper corona where the heating effect is relatively small. Consequently, the time scale of cooling is smaller than that of conduction in the flux rope, leading to trigger the thermal instability and generate cool dense plasma.

Hinode-7
Session 4: Flares and Coronal Mass Ejections

MHD Simulation of Plasma Eruption by Interaction between Emerging Flux and Coronal Arcade Field

Abstract Author(s): Takafumi Kaneko, Takaaki Yokoyama

Institution(s): Department of Earth and Planetary Science, The University of Tokyo, Department of Earth and Planetary Science, The University of Tokyo

Presentation: S4-P-03

Abstract

Many kinds of eruptive phenomena such as filament eruptions and CMEs are seen in the solar atmosphere. One candidate of their triggering mechanisms is an interaction between the newly emerging flux and the coronal arcade field (e.g. Feynman & Martin,1995). However, its physical role for eruptions is still unclear. In order to investigate the triggering mechanism associated with newly emerging flux and conditions required to trigger eruptions, we performed 2.5-dimensional magnetohydrodynamic simulations and carried out parameter survey about the magnetic field strength, the location of the emerging flux and the shear angle of the arcade field. As a result, two distinct mechanisms are seen and occurrence of these two depends on the location of the emerging flux. One is dominant in the region where the location of the emerging flux is around the edges of the arcade fields and the other is dominant in the region where the location of the emerging flux is around the PIL (polarity inversion line) of the arcade fields which has an opposite polarity to the emerging flux. Eruptions by former mechanism are due to the compression of the arcade field by the emerging flux and likely to occur when the magnetic field strength is larger or the location of the emerging flux is closer to the PIL. Eruptions by latter mechanism are due to the coupling of several reconnections and likely to occur when the magnetic field strength of the emerging flux is smaller and the location of emerging flux is closer to the PIL. For both mechanisms, the strongly sheared arcade field is preferable for eruptions.

Hinode-7
Session 4: Flares and Coronal Mass Ejections

Simulation study of magnetic reconnection in high magnetic Reynolds number plasmas

Abstract Author(s): Takashi Nakabo, Kanya Kusano, Takahiro Miyoshi, Grigory Vekstein

Institution(s): STEL, Nagoya University, Hiroshima University, Higashi-Hiroshima, Japan , Manchester University, Manchester, United Kingdom

Presentation: S4-P-04

Abstract

Magnetic reconnection is the major mechanism for explosive energy liberation in various plasmas. However, the mechanism of fast reconnection in high magnetic Reynolds number (S) plasmas like the solar corona, in which $S > 10^{10}$, is still unclear. The observations suggested that the reconnection rate in solar flares is as large as 10^{-2}, although the classical theory by Sweet (1958) and Parker (1963) predicted that the reconnection rate is given by $S^{-1/2}$.

In this paper, we developed the high-resolution magnetohydrodynamics (MHD) simulation of magnetic reconnection for the high-S (S$\sim 10^4$-10^6) regime aiming at revealing the acceleration mechanism of magnetic reconnection. We applied the HLLD Riemann solver developed by Miyoshi and Kusano (2005) to the high resolution two-dimensional MHD simulation of current sheet dynamics. The initial state is given by the Harris sheet equilibrium plus perturbation, and the uniform and constant resistivity model is adopted.

As a result, we found a new type of fast reconnection. For S=10^5, multiple X-line reconnection appears as a result of the secondary tearing instability and magnetic reconnection is accelerated through the formation of multiple magnetic islands. Furthermore, we found that the electric current sheets between some particular magnetic islands bifurcate to V-shape current layers and that the reconnection at the apex of bifurcated current layers is preferentially accelerated. For S = 10^6, it is shown that the bifurcated current layers create slow mode shocks which more increase the reconnection rate up to about 0.05. The slow mode shocks are repeatedly created and dissolved corresponding to the formation and transportation of magnetic islands. These results indicate that, even though resistivity is uniform, when the magnetic Reynolds number is as high as 10^6, the multiple X-line reconnection of Sweet-Parker current sheets is switched to a new regime called “ dynamical Petschek's type reconnection ” .

Thermal x-ray emission in flaring coronal loops

Abstract Author(s): Rui F. Pinto, Nicole Vilmer, Sacha Brun

Institution(s): LESIA, Observatoire de Paris & AIM/SAp, CEA Saclay, LESIA, Observatoire de Paris, AIM/SAp, CEA Saclay

Presentation: S4-P-05

Abstract

We study the temporal evolution of the thermal x-ray emission on kink-unstable coronal loops during a solar flare through a series of MHD numerical simulations. The numerical setup used consists of twisted coronal loops embedded in a region of uniform and untwisted background coronal magnetic field. Magnetic reconnexion occurs continuously near the flux-rope's boundaries, heating up the plasma to high temperatures (> 20 MK) there. The total thermal X-ray emission peaks very quickly during the impulsive phase and slowly fades away as the flare proceeds and the loops relax to a lower energy state. We show the evolution of the fine-structure of the X-ray emission during the whole flaring episode.

Hinode-7
Session 4: Flares and Coronal Mass Ejections

The Role of a Flux Rope Ejection in Three-dimensional Magnetohydrodynamic Simulation of a Solar Flare

Abstract Author(s): Keisuke Nishida, Naoto Nishizuka, Kazunari Shibata

Institution(s): Kyoto University

Presentation: S4-P-06

Abstract

We investigated the dynamic evolution of a three-dimensional (3D) flux rope eruption and magnetic reconnection process in a solar flare, by simply extending two-dimensional (2D) resistive magnetohydrodynamic simulation model of solar flares with low beta plasma to 3D model. We succeeded in reproducing a current sheet and bi-directional reconnection outflows just below the flux rope during the eruption in our 3D simulations. We found that there is a positive feedback between the ejection speed of a flux rope and the reconnection rate both in the 2D and 3D simulations, and we conclude that the plasmoid-induced reconnection model can be applied to 3D. We also found that small scale plasmoids are formed inside a current sheet and make it turbulent. These small scale plasmoid ejections have a role in locally increasing the reconnection rate intermittently as observed in solar flares, coupled with a global eruption of a flux rope.

Hinode-7
Session 4: Flares and Coronal Mass Ejections

Reconnection in partially ionized plasma with radiation cooling – Fast magnetic reconnection with multiple plasmoids applied in the partially ionized plasma

Abstract Author(s): Lei Ni

Institution(s): Yunnan Astronomical Observatory

Presentation: S4-P-07

Abstract

Through 2.5-dimensional MHD numerical simulations, the magnetic reconnection in partially ionized plasmas with radiation cooling is studied, using the Spitzer resistivity in the low solar atmosphere. Though the magnetic Reynolds number is high (10^5 $\sim 10^6$), fast magnetic reconnection still can happen because of multiple levels of the plasmoid instability occurring inside the current sheet. As secondary instabilities start to appear, slow-mode shocks are detected between secondary plasmoids and secondary fragments of the current sheet. Our numerical simulations also indicate that the radiation cooling is important. The radiation cooling can make the secondary plasmoids appear earlier and the maximum current density reach a value more than two times higher than in the case without radiation cooling; the maximum reconnection rate during the secondary instability is also five times higher in the case with radiation cooling. The upward out-flow velocity in our simulations approaches the velocity of chromospheric jets, with the maximum velocity reaching 24 km/s. The temperature enhancement in the case with radiation cooling is about 1000 K, which is close to the temperature enhancement of Ellerman bombs and micro-flares in the chromosphere. We conclude that the plasmoid instability with radiation cooling can be a very important mechanism to study various dynamic phenomena in the low solar atmosphere.

Analysis on Mechanisms of Reconnection Rate Enhancement in 3D MHD simulation of a Current Sheet

Abstract Author(s): Shuoyang Wang, Takaaki Yokoyama, Hiroaki Isobe

Institution(s): University of Tokyo, University of Tokyo , Kyoto University

Presentation: S4-P-08

Abstract

The main purpose of this study is to investigate three-dimensional current sheet evolution under a guide field, initially with stochastically located diffusivity. Many solar activities, especially the impulsive eruptions, demand rapid energy conversion. Recent studies could achieve a fast magnetic reconnection if localized resistivity is applied, with assumption of uniformity on the direction perpendicular to the reconnection plane. When a time-dependent third component is added to the environment, 2-D parallel reconnection is generalized into “component reconnection”. In our simulation results, due to the periodic boundary condition, we found a quickly developing resonance netlike pattern. Small current sheets mainly reside in a thin sheet between safety factors q = 1 and q = -1 and form a zigzag chain. Outflow from one current sheet is fed into a nearby current sheet and accelerate the engine. In the nonlinear growing phase, the reconnection rate increases by a few times compared with linear phase and gradually becomes saturated. Slow-mode compression waves develop eventually on both sides of the upstream and downstream extend from individual current sheet. Thus we have achieved quicker reconnection without permanent localized resistivity in a more universal idea.

Three-dimensional instability of spontaneous fast magnetic reconnection in solar flares

Abstract Author(s): Tohru Shimizu

Institution(s): ISAS/JAXA

Presentation: S4-P-09

Abstract

Some three-dimensional instability models observed in the spontaneous fast magnetic reconnection process are discussed with MHD simulations, where the classical two-dimensional model of the spontaneous fast magnetic reconnection can be destabilized in three-dimension, resulting in intermittent and random three-dimensional reconnection process. We focus on solar flares considered to be caused in almost one-dimensional current sheet, which is finally developed to three-dimensional field structure. In that case, three-dimensional resistive-MHD instability of the fast reconnection process and ideal-MHD instabilty of mangetic loops may be often competitive but it is shown that the former should be important to be resolved.

Ellerman bombs - physical parameters derived from high-resolution multiline spectroscopic observations

Abstract Author(s): Arkadiusz Berlicki, Petr Heinzel

Institution(s): Astronomical Institute, Academy of Sciences, Czech Republic

Presentation: S4-P-10

Abstract

Observations of Ellerman bombs (EBs) show them as small brightenings, which are well observed in the wings of hydrogen H-alpha line. H-alpha line profiles of EBs exhibit enhanced emission at a distance of 0.8 ang. on the both sides of the line core. These increases of emission can be extended even up to a few angstroms from the line core and were reported in the past as a " moustaches " phenomenon (Bruzek 1968). EBs can be also observed in other chromospheric lines (e.g. Ca II 8542 ang.) and in UV as a bright points often located close to sunspots within active regions. EBs are probably a manifestation of small reconnection processes occurred in the solar lower atmosphere. In this work we will use high-resolution spectroscopic observations of EBs to derive the model of the active solar atmosphere in Ellerman bombs. In 2011 some Ellerman bombs were observed with high-resolution Dunn Solar Telescope located in National Solar Observatory (Sacramento Peak, USA). We used Interferometric BIdimensional Spectrometer (IBIS) instrument to obtain spectroscopic observations of EBs in H-alpha, Ca II and Na I lines.

The observed spectral lines were compared with the grid of the theoretical line profiles computed with NLTE radiative transfer code for different atmospheric models. By modifying the solar atmospheric model we found the best fit between observations and theoretical spectrum. In this way we obtained the most probable semiempirical model of the active atmosphere in Ellerman bombs. Some global physical parameters of Ellerman bombs will be also discussed.

Hinode-7
Session 4: Flares and Coronal Mass Ejections

Modeling Active Region Transient Brightenings observed with XRT to Constrain the Heating Function of Active Regions

Abstract Author(s): Adam Robert Kobelski, David E McKenzie

Institution(s): Montana State University, Montana State University

Presentation: S4-P-11

Abstract

In this study we model Active Region Transient Brightenings (ARTBs) as multi-stranded structures, to better understand the spatial and temporal heating of coronal loops. Using a simple 0D model (EBTEL) for the individual strands, we use a genetic minimization algorithm (pikaia) to determine the heating parameters of observed ARTBs. By using multiple heating functions to model a large number of ARTBs observed with XRT, we can better constrain the spatial and temporal heating of active region structures. We will demonstrate a tool for automatically detecting ARTBs, some of which are at the limit of XRT's sensitivity, and also present our results constraining the energy budget of these coronal transients.

Hinode-7
Session 4: Flares and Coronal Mass Ejections

Comparison between Hinode/SOT and SDO/HMI, AIA data for the study of solar flare trigger processes

Abstract Author(s): Yumi Bamba, Kanya Kusano, Shinsuke Imada, Yusuke Iida

Institution(s): STEL, Nagoya Univ.

Presentation: S4-P-12

Abstract

There are numerous observational and simulation studies, which attempted to reveal the onset mechanism of solar flares. However, the underlying mechanism of flare onset remains elusive. To elucidate flare trigger mechanism, we have analyzed several flare events which were observed by Hinode/SOT (Bamba et al. 2013, submitted). The observed signatures strongly support the idea of flare trigger mechanism presented by Kusano et al. (2012), which proposed that solar flares can be triggered by the interaction between the sheared arcade and one of the two types of small magnetic disturbances.

However, because of the SOT's limited field of view (FOV) (328"×164" for NFI, 218"×109" for BFI), only four data sets were able to be utilized. In this study, in order to increase the number of event analysis, we applied the analysis method of our previous study with SOT to the SDO/HMI and AIA data, which has a full-disk FOV (2000"×2000"). We evaluated the reliability of method by comparing the results of our previous study.

Here, we use the data of photospheric line-of-sight magnetic field by HMI and chromospheric emissions by AIA (1600 Å). We compare them with the previous study with the SOT data of filter magnetograms in Fe I (6302 Åor Na D1 (5896 Å) lines and filtergrams in Ca II H line (3968 Å). As a result, we confirm that SDO data deduces the same results as those from Hinode data in the analyzed events. It is also shown that if the size of flare-trigger-regions is as large as ∼10", they are detectable even with HMI. In this presentation, we will make further discussions the prospect of event analyses for flare trigger study using HMI and AIA data.

Hinode-7
Session 4: Flares and Coronal Mass Ejections

Coronal Behaviors before the Large Flare Onset

Abstract Author(s): Shinsuke Imada, Yumi Bamba, Kanya Kusano

Institution(s): Solar-Terretrial Environment Laboratory, Nagoya University

Presentation: S4-P-13

Abstract

A solar flare is a sudden brightening observed in almost all wavelengths. Flares are powered by the sudden (timescales of minutes to tens of minutes) release of magnetic energy stored in the corona. They are mainly followed by a colossal coronal mass ejection also known as a CME. CMEs typically reach Earth a day or two after the event. Solar flares strongly influence the local space weather in the vicinity of the Earth. So far, various studies aiming to predict when and where the flare will occur. Most of studies are mainly discussed through the photospheric/chromospheric activity before the flare, although there are some studies about the coronal features before the flare onset. We will discuss the coronal features before the famous large flare occurring on December 13th, 2006. We used HINODE/EIS, XRT, and SOHO/EIT data to discuss the coronal features in the large scale ($\sim$ a few 100 arcsec) before the flare onset. What we found is as follows: 1) the upflows in and around active region were growing from a few to a few ten km/s a few 10 hours before the flare onset, 2) the expanding coronal loops were clearly observed a few hour before the onset, 3) X-ray intensity was gradually getting weaker toward the onset. From those observed signatures, we interpret that the outer part (low density loops) of active region is expanding a few 10 hours before, and inner part (high density loops) is expanding a few hour before the onset. From this viewpoint, we will discuss what is happening in the corona before the flare onset. We also discuss the flare predictability by using these coronal features.

Hinode-7
Session 4: Flares and Coronal Mass Ejections

An energetics study of X-ray jets

Abstract Author(s): Nobuharu Sako, Masumi Shimojo, Tetsuya Watanabe, Takashi Sekii

Institution(s): The Graduate University for Advanced Studies (SOKENDAI)

Presentation: S4-P-14

Abstract

For plasma acceleration mechanism in X-ray jets, three forces have been considered, based on the reconnection model of X-ray jets; pressure gradient, magnetic tension, and magnetic pressure. ' Chromospheric evaporation ' refers to acceleration of plasma by the pressure gradient that is generated by heating of the chromosphere. A speed of the evaporation flow is similar to the sound speed of the heated plasma. It is believed that the hot plasma flows in the X-ray jets are produced by the evaporation because the typical apparent speed of X-ray jets is around 200 km/s, nearly equal to the coronal sound speed. On the other hands, there is a threshold of energy flux (10^{10} erg/cm^2/s) below which the plasma flow with the coronal temperature cannot be ' explosive ' (Fisher et al. 1985). A previous study based on Yohkoh/SXT data predicts that the energy flux of AR jets in the energy deposition region is above the threshold. Is the energy flux in the energy deposition region of an X-ray jet is above the threshold? In order to study the acceleration of the X-ray jet, we compare the characteristics of X-ray jets in ARs with those in CHs, and examine the energetics of X-ray jets. We studied X-ray jets greater than of 3×10^4 km, and found no large difference in the life time, the width of the jet, and the area of the footpoint flare. On the other hand the ratios of X-ray intensity in the footpoint flare to that of the jet differed in CHs and in ARs, and assuming the filling factor to be unity, they can roughly classified into two groups. In this paper, we present more detailed analysis and discuss the physical description of X-ray jets and footpoint flares.

A New Catalog of Sigmoidal Active Regions: Statistical Properties and Evolutionary Histories

Abstract Author(s): Antonia Savcheva, Sean McKillop, Elizabeth Hanson, Patrick McCauley, Duncan MacKay, Karen Mayer, Edward DeLuca

Institution(s): Smithsonian Astrophysical Observatory, Smithsonian Astrophysical Observatory, Smithsonian Astrophysical Observatory, University of St.Andrews , University of St.Andrews, Smithsonian Astrophysical Observatory

Presentation: S4-P-15

Abstract

Sigmoids are sinuous structures located in active regions that have characteristic " s-shaped " or inverted " s-shaped " loops. Active regions containing sigmoids are observed to have higher rates of flaring and CMEs. Previous work detailing the properties of sigmoids has generally focused on creating static 3D magnetic field models of a handful of regions. Although these models are representative of the magnetic evolution of these regions, significant insight can be gained by an observational overview approach with systematic and statistical analysis of a large sample of sigmoids. This sample of 72 regions is spanning a wide wavelength range and in different parts of the solar atmosphere by various instruments such as the Hinode/XRT, SDO/AIA, STEREO, LASCO, SOHO/MDI and SDO/HMI. From this data we compiled a comprehensive list of many different parameters including: size and aspect ratio, presence of H alpha or EUV filaments, flare and CME association, number of sunspots, and active region and sigmoid lifetimes, etc. Among our results are that sigmoids have a higher eruption rate than other active regions. We also find that the ratio of the long axis to short axis of the sigmoids has a strong peak at 2.5 and average lifetime of 2 days, which can provide constraints for flux rope models. We also study the evolutionary histories of all sigmoids in the sample in terms of their photospheric flux evolution and coronal features.

Prominence visibility in soft X-rays using Hinode XRT observations

Abstract Author(s): Petr Heinzel, Sonja Jejcic, Pavol Schwartz, Ulrich Anzer

Institution(s): Astronomical Institute

Presentation: S4-P-16

Abstract

Prominences observed in EUV appear as dark structures against the background corona and this is explained as the combined effect of absorption and emissivity blocking. The latter is supposed to work also in the range of soft X-rays and was used to disentangle between the two mechanisms. On the other hand, the absorption of coronal X-rays by the cool prominence body has been shown to be rather inefficient, at least when only hydrogen and helium resonance continua are considered. In this study we extend our modeling of the X-ray absorption also to other elements and investigate the conditions under which such absorption could be significant. Our motivation is the XRT imaging of a very dense and extended prominence which exhibits a clear darkening at position of the spine. To explain this feature, we discuss the relative importance of the X-ray absorption and emissivity blocking. The absorption is computed using our previous analysis of EUV images which resulted in determination of the hydrogen column density on which the absorption by other elements considered in this work directly depends.

Hinode-7
Session 4: Flares and Coronal Mass Ejections

Are Jets CMEs? The Jet Response Mass Loading of Solar Wind Plasma

Abstract Author(s): Hsiu-Shan Yu, Bernard V. Jackson, Andrew Buffington, P. Paul Hick, Masumi Shimojo, Nobuharu Sako

Institution(s): Center for Astrophysis and Space Sciences, University of California, San Diego

Presentation: S4-P-17

Abstract

The brightest jets observed by the Hinode XRT produce high-speed responses and enhanced brightness that can be traced through coronagraph fields of view and into the heliosphere. Specifically, LASCO C2 and STEREO COR2 coronagraph images measure the coronal responses to some of the largest jets, and analyses using velocities from interplanetary scintillation (IPS) observations and from the Solar Mass Ejection Imager (SMEI) 3D reconstructions measure these jet responses in the heliosphere. We determine approximate masses and energies for these large jet responses over polar coronal hole regions, and relate them to the jet peak brightness spectrum observed by Hinode during a three-week survey period in September 2007. The analyses show that jets contribute about 2.5% of the total solar wind mass during this period. Assuming that this material outflow associated with jets continues globally throughout the solar cycle, we find that their total mass is nearly comparable to that of the globally combined CMEs.

Hinode-7
Session 4: Flares and Coronal Mass Ejections

Solar Flare Observations with EIS

Abstract Author(s): George A. Doschek, Harry P. Warren, Peter R. Young

Institution(s): Naval Research Laboratory, Naval Research Laboratory

Presentation: S4-P-18

Abstract

Hinode has obtained many observations of flares observed from a range of viewing angles. This has allowed detailed comparisons with predictions of the Standard Flare Model. We present observations of flare footpoint regions in disk flare arcades over a temperature range from about 1-2 MK (e.g., Fe X, Fe XII, Fe XV) up to about 17 MK (Fe XXIII, Fe XXIV). From Gaussian fits to spectral lines, we have determined evaporation speeds as a function of temperature in these regions along with electron densities and non-thermal motions (turbulence). Evaporation speeds range from about 20 km/s (e.g., Fe XII) up to about 150 km/s (e.g., Fe XXIII). Downflows are also observed in some flare regions. The results are complex spatially and show variations over 2 arcsec spatial scales. This scale is limited by the raster step size and variations on smaller scales are possible. Where feasible, we relate the results to predictions based on 1D multi-temperature flare models. We also present temperatures, flow speeds, and non-thermal motions for flares for which RHESSI data are available. We attempt to identify hard X-ray footpoint emission with EIS footpoint regions and relate the results to temperature and non-thermal motions at the loop tops. XRT and SDO data are used for context. We connect the EIS observations to measurements of temperature and non-thermal motions in X-ray flare lines of Fe XXV and Ca XIX recorded years earlier by Bragg crystal spectrometers (BCS) on Yohkoh. There are no flare EUV lines as hot as the strong Fe XXV line at 1.85 Angstroms. This work is sponsored by a NASA Hinode grant.

Hinode-7
Session 4: Flares and Coronal Mass Ejections

Calibration on EIS Instrumental Width from Observations and Its Application

Abstract Author(s): Megumi Kasuga, Hirohisa Hara

Institution(s): Department of Astronomy, School of Science, The University of Tokyo

Presentation: S4-P-19

Abstract

We report a new method that enables us to improve the knowledge of the EIS instrumental width that is added to the intrinsic emission-line width. The instrumental width provided in the current EIS analysis software was derived from the observed solar spectra by using Fe XII 193 line, and it is a function of the position along the slit. Since the non-thermal velocity cannot be known by the EIS observations alone, the values in the analysis software may be overestimated and they may not be applicable to other wavelengths. The following has been investigated in our study:
(1) To estimate the instrumental widths from simultaneous observations with the ground-based coronagraph, which has little instrumental width, by using Fe X and Fe XIV emission lines in the visible and EUV wavelengths.
(2) To derive the instrumental widths at different wavelengths by interpolating the known widths of Fe X and Fe XIV in the EIS wavelength bands.
(3) To estimate the instrumental widths over the slit direction from the data obtained at different spacecraft pointing coordinates in the slit direction to widen the applicable range from a small field of view to the whole EIS field of view.
Methods (1) and (2) were partially used in Hara et al. (2008) and Hara et al. (2011). We show some examples to apply the instrumental width obtained in the present work to EIS data that were analyzed in the previous works.

Hinode-7
Session 4: Flares and Coronal Mass Ejections

Simultaneous observation of high temperature cusp loops and bi-directional inflow in the limb flare with Hinode/EIS and SDO/AIA

Abstract Author(s): Yuki Matsui, Takaaki Yokoyama

Institution(s): University of Tokyo, University of Tokyo

Presentation: S4-P-20

Abstract

We succeeded in the simultaneous observation of high temperature cusp loops and bi-directional inflow of a limb flare. The standard model of solar flares based on the magnetic reconnection includes bi-directional inflow toward the reconnection point. Corresponding to the bi-directional inflow, high temperature loops like a cusp shape are formed due to the the magnetic reconnection. Recent imaging data from SDO/AIA have revealed the detail around the reconnection. On the other hand, it is difficult to know the temperature from the imaging data only because it includes emission from different lines. Therefore simultaneous spectroscopic observation with Hinode/EIS is important.

We analyzed imaging data with SDO/AIA and spectroscopic data with Hinode/EIS of a C-class flare that occurred beyond the limb. As a result, bi-directional inflow are observed with the images of 171A filter (around 1MK). At the same time, cusp loops are observed with the raster scans of FeXXIV emission line (over 10 MK) at the region surrounded by the bi-directional inflow. Cusp loops are also observed with high temperature filter 131A (over 10MK). 131A filter also includes cool temperature emissions (logT $\sim$ 5.6), however the results of the simultaneous spectroscopic observation of FeXXIV supports that these cusp loops have high temperature over 10MK. This is clear evidence that coronal temperature loops are heated over 10MK by the magnetic reconnection. Additionally, a strong blueshift over 300km/s is observed with FeXXIV at the region of the current sheet. This speed might reach Alfv'en speed considering the angle of the loop, which also supports the magnetic reconnection. These results indeed support the standard model and this is the first simultaneous observation of bi-directional inflow with imaging and cusp loops with spectroscopy as long as we know.

Hinode-7
Session 4: Flares and Coronal Mass Ejections

Hot Reconnection Outflows Associated to an X-class Flare

Abstract Author(s): Tetsuya Watanabe, Hirohisa Hara, Kyoko Watanabe

Institution(s): National Astronomical Observatory, Japan, NAOJ , ISAS

Presentation: S4-P-21

Abstract

The EUV Imaging Spectrometer (EIS) on board the Hinode Mission found hot and fast outflows associated to an X1.4 flare. This flare occurred near the disk center (S13W04) at 2012 July 12 15:37UT. The maximum line of sight velocity reached more than 600 km s^{-1} in FeXXIII and FeXXIV lines formed at Te $> 10^7$. One of the neutral lines ran along the boundary of a transient coronal hole created on the north side of AR11520, and the north flare ribbons showed rapid expanding motion in AIA 1600A images. Successive magnetic reconnection is considered to take place along the archade of coronal loops over the neutral line. Hard X-ray sources seen in the RHESSI images of 25 - 50 keV energy band were so elongated at this time that the east-end of the sources reached the region of the above activity. Coronal iron lines ($6 <$ log T < 6.3) show downflows ($<$ + 30 km s^{-1}) at the south legs of arcade, while modest upflows of -30 $\sim$ -150 km s^{-1}at the north legs. The density sensitive FeXIV line intensity ratio (FeXIV 264.8/274.2) is almost to its high density limit, indicating ne $> 10^{11}$ cm^{-3}. The FeXXIII and FeXIV lines formed at log T $\sim$ 7.1 on the other hand, show two distinctly separated components in their line profiles: One is almost stationary and the other is blue-shifted. The latter increases its velocity linearly toward the direction of the north, and reaches $>$ 600 km s^{-1} 20 arcsec off north of the apices of the archade loops. The east-west width of this "outflow arcade" is about 20,000 km.

The EUV Late Phase of Solar Flares: Additional Heating or Cooling Signature?

Abstract Author(s): Ying Li

Institution(s): Nanjing University

Presentation: S4-P-22

Abstract

The EUV late phase of solar flares is a second enhancement (mainly in Fe XVI 33.5 nm) separated from the primary flare event by tens of minutes to hours. It has been clear that the late EUV emission comes from the higher and related flare loops, rather than the flare core region. So far there are two major explanations for the EUV late phase: one is additional lower heating (Hock et al. 2012; Dai et al. 2013), and the other is long-lasting cooling signature (Liu et al. 2013). Our work focuses on distinguishing these two phenomena combining experiments via the EBTEL model and observations from AIA and EVE. Our preliminary results show that the loop length is a key parameter in the time delay of the EUV emission. We also discuss the effect of different heating histories in the EUV late phase.

Hinode-7
Session 4: Flares and Coronal Mass Ejections

On M2.2 Solar Flare and CMEs Observed on 26 November, 2000 from NOAA AR 9236

Abstract Author(s): V. K. Verma, R CHandra, Abhishek Shrivastava

Institution(s): Uttarakhand Space Application Center, Physics Department, Kumaun University, Nainital, India , ARIES, Nainital, India

Presentation: S4-P-23

Abstract

The solar active region NOAA AR 9236 was one of the most flare productive active region of solar cycle 23 and it has a large positive polarity spots surrounded by small positive and negative emerging polarities which might make this active region more flare productive. Here, we present a study based on the high cadence ($\sim$ 1 sec) CCD data of flare (M2.2) in H α emission on 26 November, 2000 from NOAA AR 9236. The flare was observed by various ground and space borne instruments (SOHO, HXRS, GOES) on 26 November 2000 in time 02:30 UT to 04:00 UT. The flare started with long arc-shape outer ribbons. Afterwards, the main flare starts with two ribbons. Initially the outer ribbons start to expand and later it also shows contraction. An appearance of flare ribbons initiated by the magnetic breakout mechanism (Antiochos, DeVore and Klimchuk: 1999, ApJ, 510, 486). The H α emissions Kernels from the different ribbons of the flare exhibit intensity oscillations of the period of $\sim$126 s. The solar flare was accompanied by CMEs having maximum speed of 494 km/sec and also accompanied by SEPs. This small flare occurs in an area closed to a coronal hole (within 10?) which guides the triggered CMEs implying the scenario of the reconnection/ interaction between closed magnetic field lines related to the flaring active region and open field lines of the coronal hole as earlier reported by Verma (1998, Journal of Geophysical Indian Union, 2, 65.1998). In conclusion, we have presented a detail analysis in the light of mufti-wavelength observations of solar flares and discussed the observations in view of latest scenario of solar flares and CMEs triggering mechanisms.

Hinode-7
Session 4: Flares and Coronal Mass Ejections

On Classification of Solar Coronal Mass Ejections Observed by LASCO/SOHO during period 1996-2011

Abstract Author(s): V K VERMA

Institution(s): Uttarakhand State Application Center

Presentation: S4-P-24

Abstract

We present a classification of solar coronal mass ejection (CME) events based on 4785 CME events observed during January 11, 1996 to December 31, 2011. A detailed study is performed to address the question of whether two classes of CME events exist or not. It is usually observed that some CMEs are accelerated or decelerated depending upon their mechanism of origin. Keeping this fact in mind, we have investigated and classified the solar CME events using acceleration or deceleration of each CME events observed during the period of 1996-2011. From the study of LASCO CMEs observed between 1996- 2011, we find that about 49.4% of CME events are decelerated while 50.6% of CMEs are accelerated during their journey from solar surface to corona and beyond. The present study suggests that CMEs may be classified as two types of CMEs: accelerated CMEs and decelerated CMEs. Further, we are of the view that the accelerated type of CMEs may be originating through mass ejection by small flares or activation/ eruptive prominences and early reconnection to open magnetic field of coronal holes at lower height in corona and moves as CMEs to higher coronal height including earth and beyond while the decelerated types of CMEs may be originating through mass ejection by huge energy solar flares or large eruptive prominence and late reconnection to open magnetic field of coronal holes at higher height and moves as CMEs to higher coronal height including earth and beyond. We are also of view that for the formation CMEs, the occurrence of flare or active prominence or filament activation is necessary condition while presence of CHs in nearby area is sufficient and without fulfilling these two conditions CMEs formation is not possible.

SDO/AIA Observations of a Spotless Two-ribbon Flare and associated Sympathetic Flare

Abstract Author(s): Ram Ajor Maurya, Sanjay Gosain, Jongchul Chae

Institution(s): Seoul National University

Presentation: S4-P-25

Abstract

Erupting solar filaments are observed to be closely associated with Coronal Mass Ejections (CMEs). Further, they are observed to form the core of three part structure of CMEs. Although, it is common to observe a two ribbon flare in association with eruptive filaments associated with solar active regions, however, one can also observe the flare emission in association with the quiescent filament eruptions. One such event was observed in great detail by the Atmospheric Imaging Assembly (AIA) instrument on-board Solar Dynamics Observatory (SDO) during the eruption of a large ($\sim$600 - 700 Mm) quiescent filament on 22 October 2011. We evaluate the ribbon separation speed (1.5 - 2 km/s) and photospheric magnetic field strength, and computed the reconnection rate and energy release during the event under the standard flare reconnection model assumption. We noticed that flare-ribbons expansion is observable to extremely large distance from the filament location and continues for several (>10) hours. Furthermore, it appears that one of the expanding ribbons, on reaching a nearby active region, triggers a flare in that active region, presenting evidence for sympathetic connection between the two events. While the flares and related coronal disturbances (EUV waves) interact with distant quiescent filaments causing them to oscillate and sometimes erupt, in the present event the reverse is true, i.e., a quiescent filament eruption leads to a sympathetic flare in nearby active region.

Slipping flare loops observed by SDO/AIA and the slipping magnetic reconnection

Abstract Author(s): Jaroslav Dudik, Miho Janvier, Guillaume Aulanier, Giulio Del Zanna, Marian Karlicky, Helen E. Mason, Brigitte Schmieder

Institution(s): RS Newton International Fellow, LESIA, Observatoire de Paris, LESIA, Observatoire de Paris, DAMTP-CMS, University of Cambridge, Astronomical Institute of the Academy of Sciences of the Czech Republic, DAMTP-CMS, University of Cambridge, LESIA, Observatoire de Paris

Presentation: S4-P-26

Abstract

We report on SDO/AIA observations of an X-class eruptive flare exhibiting sigmoid-to-arcade evolution. The flare is triggered by a brightening occurring elsewhere in the active region complex. During the rising phase, flare loops are observed to slip with velocities of several tens of km s^{-1} along the developing flare ribbons. Localized brightenings in AIA 171, 304 and 1600A in the flare ribbons correspond to transition-region emission from the footpoints of flare loops. Both ribbons are hook-shaped and undergo rapid evolution connected to slipping of flare loops. A long loop connecting both hooks is observed and participates in the eruption. We compare the obsevations to the prediction of the "standard solar flare model in 3D" of Aulanier et al. (2012) that involves torus-unstable flux rope. In the absence of null-points and separatrices, the reconnection in the model is of slipping nature. We find good agreement between the model and observations in terms of direction of flare loop slipping, ribbon evolution including their hooks, and flux rope expansion. Radio data obtained at 200-500 MHz frequencies show presence of noise-storm, which can be a signature of slipping magnetic reconnection.

A 3-Dimensional View of the Filament Eruption and Coronal Mass Ejection Associated with the 2011 March 8 Solar Flare

Abstract Author(s): Maria V. Gutierrez, Raul Terrazas, Mutsumi Ishitsuka, Jose Ishitsuka, Yusuke Yoshinaga, Naoki Nakamura, Andrew Hillier, Satoshi Morita, Ayumi Asai, Takako T. Ishii, Satoru Ueno, Reizaburo Kitai, Kazunari Shibata

Institution(s): Geophysical Institute of Peru

Presentation: S4-P-27

Abstract

We present a detailed 3-dimensional features of the filament ejection and coronal mass ejections associated with the M4.4 flare that occurred on 2011 March 8 flare at the active region NOAA 11165. The Ha full disk images of the flare and filament ejection were successfully obtained by the Flare Monitoring Telescope (FMT) relocated from Hida Observatory of Kyoto University to Ica University in Peru under the international collaboration of the CHAIN (Continuous H Alpha Imaging Network) - project. The observation in multi wavelenghs around the Ha line enabled us to derive the 3-dimensional velocity field of the Ha filament ejection. The features in extreme ultraviolet were also obtained by the Atmospheric Imager Assembly (AIA) on board the Solar Dynamic Observatory (SDO) and the Extreme Ultraviolet Imager (EUVI) of the Sun Earth Connection Corona and Heliospheric Investigation (SECCHI) on board the Solar Terrestrial Relations Observatory (STEREO) - A head satellite. In this presenation we report in the detail the evolution of the ejection followed by a coronal mass ejection. We also discuss the evolution of the active region in the context of the coronal magnetic field of the flare region.

Hinode-7
Session 4: Flares and Coronal Mass Ejections

Magnetic reconnection rate in eruptive and non-eruptive events as calculated with flare ribbons

Abstract Author(s): Nariaki V. Nitta, Brian T. Welsch, Theodore D Tarbell, Zoe A. Frank

Institution(s): Lockheed Martin Advanced Technology Center, Space Sciences Laboratory, University of California, Berkeley, Lockheed Martin Advanced Technology Center, Lockheed Martin Advanced Technology Center

Presentation: S4-P-28

Abstract

Magnetic reconnection is believed to play a fundamental role in solar flares, but its importance in coronal mass ejections (CMEs) is not well understood. We know that many flares, including X-class events, are essentially non-eruptive. It is suggested that the way magnetic reconnection initiates and proceeds may be different in eruptive and non eruptive flares. One of the immediate consequences of magnetic reconnection is the flare ribbon. Based on their close relation, a method was developed during last solar cycle to calculate the magnetic reconnection rate from the photospheric magnetic flux swept over by flare ribbons. With uninterrupted high quality data from HMI and AIA on board SDO, we can do this routinely. Furthermore, in some selected events, we can greatly refine the calculation of the reconnection rate by using Hinode SOT/SP data. Studying a handful of flares observed by Hinode, we discuss the magnetic reconnection rate in terms of whether the flare is eruptive. For eruptive flares, we also compare the reconnection rate with the kinematic parameters of the associated CME, and possibly with the magnetic flux within the subsequent ICME as observed at 1 AU. One interesting aspect of this study is whether the magnetic reconnection rate is correlated with CME acceleration. Such a correlation might be expected if the CME gets accelerated by reconnected flux that wraps around the ejection and produces an increased outward "hoop force."

CME Observations with TESIS EUV Telescopes and LASCO C2 Coronograph

Abstract Author(s): Anton Reva, Artem Ulyanov, Sergey Bogachev, Sergey Kuzin

Institution(s): Lebedev Physical Institute, Lebedev Physical Institute, Lebedev Physical Institute, Lebedev Physical Institute

Presentation: S4-P-29

Abstract

We present observations of CME, which occurred in 2009 May 13, with TESIS/CORONAS-Photon EUV telescopes and LASCO C2 images. This observations are unique:
1) we see entire CME evolution from the solar surface till the boundaries of LASCO field of view;
2) we observe it in two channels (171 and 304 A), so we can see how prominence plasma interacts with more hot coronal plasma;
3) we see it from the convenient angle (it occurred on the limb).

CORONAS-Photon is a Russian satellite developed for solar investigations. It was launched in 2009 January 30. TESIS EUV telescopes built solar images in 171 and 304 A wavelength range, with angular resolution 1.7 arc seconds, cadence 10 minutes, and field of view 1 degree.

TESIS EUV telescopes had a special regime for observations of the far corona. Images with long exposure have visible far corona and overexposed solar disk, while images with short exposure have unsaturated solar disk and faint far corona. If we consequently take images with exposures 0.3, 3, and 30 seconds, and then merge them together, we will get an image with the visible far corona and the unsaturated solar disk. The resulting image has enough dynamic range to distinguish structures of the far corona even at the boundaries of TESIS field of view. These images are especially useful for observation of CME evolution.

The movement of the observed CME is not radial – it is released at high latitudes, then it follows bended trajectory, and in LASCO images it moves in equatorial latitudes. It takes 14 hours for CME to reach LASCO field of view, its average speed is approximately 20 km/s, and the acceleration of an order 1 m/s^2.

The maximum energy particles accelerated by the CME-driven shock

Abstract Author(s): Xin Wang

Institution(s): Xinjiang Astronomical Observatory, CAS

Presentation: S4-P-30

Abstract

The previous simulation show that the energy spectrum with a consistent with the observed fitting results in the low energy spectrum of 14-Dec-2006 CME-driven shock event. There was a “ break ” in the further energy range of the spectrum of fitting results, but the simulated results have not show that energy spectrum by the restrict of the computation. In order to verify this “break” of the energy spectrum, we do simulation for the CME-driven shock for the further size of the free escaped boundary (FEB) to achieve more maximum energy particles. The FEB is an important factor which is connected with the maximum energy particle in the diffusive shock. In present simulations, the maximum momentum is calculated by allowing us to use a larger size of FEB in the simulation system. We obtain the shape of the energy spectrum with cutoff at some maximum momentum. Maybe we can verify the “break” characteristic of the energy spectrum observed from the spacecrafts.

The energetics of microflares observed with Hinode, RHESSI and SDO

Abstract Author(s): Iain G Hannah, Gillian Young

Institution(s): University of Glasgow, University of Glasgow

Presentation: S4-P-31

Abstract

Microflares are small active region flares (GOES A and B-class) that demonstrate similar signatures of electron acceleration and plasma heating as larger flares. This, combined with their high occurrence rate, simpler configurations and weaker emission that does not substantially saturated observations, makes them ideal candidates for studying flare energetics. RHESSI spectral data allows the non-thermal flare energy to be estimated and the thermal response to this is seen not only in RHESSI but also SDO/AIA and Hinode/XRT. Using a regularized inversion method to determine the Differential Emission Measure (DEM) we can quantify the thermal properties of the microflares (i.e. density, radiative loss, energy). This coupling of RHESSI, SDO/AIA and Hinode/XRT data analysis allows us to present comprehensive non-thermal and thermal energetics in a selection of microflares.

EM maps of hot ribbons during the rise phase of a flare

Abstract Author(s): Iain G Hannah, Lyndsay Fletcher

Institution(s): University of Glasgow, University of Glasgow

Presentation: S4-P-32

Abstract

Strong heating of the chromosphere and transition region during flares results in ribbons containing plasma at temperatures ranging from a few thousand K to 10 million K. We have used SDO to construct emission measure maps in the extended rise phase of the M1.0 event SOL2010-08-07T17:55 using the method of Hannah & Kontar (2012), allowing a pixel-by-pixel examination of the development of thermal plasma in the ribbons, and detailed comparison with the ribbons' magnetic environment. Using RHESSI hard X-ray observations we set limits on the non-thermal emission from the ribbons, and examine the contribution of energy loss by non-thermal electrons to the ribbon heating in this phase.

Hinode-7
Session 4: Flares and Coronal Mass Ejections

Combining simulations of radiative hydrodynamics and particle acceleration to model solar flares

Abstract Author(s): Fatima Rubio da Costa, Vahe' Petrosian, Wei Liu, Mats Carlsson

Institution(s): Stanford University, Department of Physics. Stanford University , Department of Physics. Stanford University , Institute of Theoretical Astrophysics. University of Oslo

Presentation: S4-P-33

Abstract

It has been recently recognized that modelling the coupling between the particle acceleration and transport processes in solar flares and the dynamical response of the atmosphere to particle collisional heating is critical to our understanding of flare dynamics. We present here a numerical study combining the RADYN radiative hydrodynamic code (Carlsson & Stein, 1992) in a modified version describing the atmospheric response to a beam of non-thermal electrons (Allred et al., 2005) and the " flare " code from Stanford University (Petrosian & Liu, 2004) modeling the acceleration and transport of particles and the radiation of a solar flare in non-local thermodynamical equilibrium (non-LTE). In this way we can achieve several advancements over the results from Liu et al. (2009) who combined the " flare " particle acceleration code with a 1D hydrodynamic code without radiative transfer.

The model solves the dynamics of the flaring atmosphere which allows us to compare numerical estimates of parameters such as density, velocity or temperature with estimates derived from observations. Since H, He, Ca and Mg atoms are treated in non-LTE, the transitions between the different energy levels can be studied in detail, allowing us to compare the numerically calculated emission from the bound-bound transitions of the mentioned atoms with observational intensities and spectra. Some of the chromospheric lines such as Ly- α or H- α are influenced by non-thermal processes; understanding their formation is crucial for the correct interpretation of the line observations. Upcoming chromospheric observations of flares to be conducted with the high resolution IRIS imaging spectrograph will provide an excellent basis for this study as they will allow us to compare numerically modelled and observed emissions of solar flares in several lines.

Hinode-7
Session 4: Flares and Coronal Mass Ejections

White-Light Emission and related Particle Acceleration Phenomena in an X1.8-class Flare on 2012 October 23

Abstract Author(s): Kyoko Watanabe, Toshifumi Shimizu, Shinsuke Imada

Institution(s): ISAS/JAXA, ISAS/JAXA , STE Lab., Nagoya Univ.

Presentation: S4-P-34

Abstract

In association with solar flares, we sometimes observe enhancements of visible continuum radiation, which is known as a ”white-light flare”. These flares are mainly associated with energetic events, such as X-class flares, and they are still only rarely observed. Because many observed events show a close correlation between the time profiles and locations of white-light emission, and the hard X-rays and/or radio emission, there is some consensus that the origin of white-light emission is due to accelerated particles, especially non-thermal electrons.On October 23, 2012, white-light emission was observed by Hinode/SOT in association with the X1.8 class flare. Although the main phenomena of this solar flare occurred in a very compact region and the two Ca II H ribbons are separated only by less than 5 arcseconds, the white-light kernels are clearly observed along the Ca ribbons. Moreover, hard X-ray, and gamma-ray emission is up to about 1 MeV, is also observed by the RHESSI satellite, and most of this emission is associated with the white-light kernels. However, there are some white-light kernels without hard X-ray emission.Furthwemore, the Hinode/EIS also performed a coarse raster scan (2 arcseconds slit and 5 arcseconds step) with about 6 minutes cadence over this flaring active region before the flare, and the flare occurred during the scan. Because the main flare was very compact, the main EUV emission was caught only by a part of two scans. However, strong red shifts were observed in FeXXIV etc. over the white-light kernel without any hard X-ray radiation. In this paper, we will report the observed white-light emission, its temperature distribution, and a comparison of the white-light emission with the hard X-ray emission (energy of non-thermal electrons). We also discuss the relationship between the downflows over a white-light kernel and the strength of the white-light emission.

Hinode-7
Session 4: Flares and Coronal Mass Ejections

Properties of the optical sources in the 15th February 2011 solar flare

Abstract Author(s): Graham Stewart Kerr, Lyndsay Fletcher

Institution(s): University of Glasgow, University of Glasgow

Presentation: S4-P-35

Abstract

White light flares (WLFs) are observational rarities, making them understudied events. However, optical emission is a significant contribution to flare energy budgets and the emission mechanisms responsible could have important implications for flare models. Using Hinode/SOT optical continuum data taken in broadband red, green and blue filters, we investigate impulsive white-light emission from the X2.2 flare SOL2011-02-15T01:56:00. We develop a technique to robustly identify enhanced flare pixels and, using a knowledge of the RGB filter transmissions, determined the source color temperature and effective temperature. We investigated two idealized models of WL emission - an optically thick photospheric source, and an optically thin chromospheric slab. Under the optically thick assumption, the color temperature and effective temperature of flare sources in sunspot umbra and penumbra were determined as a function of time and position. Values in the range of 5000-6000K were found, corresponding to a blackbody temperature increase of a few hundred kelvin. The power emitted in the optical was estimated at $\sim 10^{26}$ ergs/s. In some of the white-light sources the color and blackbody temperatures are the same within uncertainties, consistent with a blackbody emitter. In other regions this is not the case, suggesting that some other continuum emission process is contributing. An optically thin slab model producing hydrogen recombination radiation is also discussed as a potential source of WL emission; it requires temperatures in the range 5,500 - 15,000K, and total energies of $\sim 10^{27}$ergs/s-

Sequential Filament Oscillations Caused by An Invisible Moreton Wave

Abstract Author(s): Yuandeng Shen

Institution(s): Kwasan Observatory

Presentation: S4-P-36

Abstract

On 06 September 2011, several filaments (prominence) can be observed on the solar disk. Just after a GOES X2.1 flare occurred in NOAA AR 11283 locating close to the disk center. Some of these filaments started to oscillate sequentially according to their distance to the flare center. It is strange that no observable Moreton wave can be identified on the H-alpha images taken by The Solar Magnetic Activity Research Telescope (SMART). On the EUV images taken by SDO/AIA, we can observe an EUV wave that can be related to the flare. With the SMART dopplergram images and the cloud model assumption, we measure the line-of-sight velocity of each filaments. The relationship between the flare, EUV wave, and the filament oscillations are analyzed, and the observational results are used to estimate the magnetic field strength of the filaments. We conclude that the filament oscillations are caused by an Invisible Moreton wave associated with the flare.

Hinode-7
Session 4: Flares and Coronal Mass Ejections

Statistical Study of Filament Eruptions and Moreton Waves Observed by the Flare Monitoring Telescope at Hida Observatory, Kyoto University

Abstract Author(s): Masashi Yamaguchi, Abdelrazak Shaltout, Ayumi Asai, Kiyoshi Ichimoto, Satoshi Morita, Kazunari Shibata, Reizaburo Kitai, Takako Ishii, Satoshi Ueno, Naoki Nakamura, Shinsuke Takasao, Yusuke Yoshinaga, Andrew Hillier, Kenichi Otsuji, Noriyuki Narukage, Denis P Cabezas, Lurdes M Martinez, Yovanny J Buleje, Maria V Gutierrez, Raul A Terrazas

Institution(s): Kyoto University

Presentation: S4-P-37

Abstract

Moreton waves are flare-associated phenomena observed in Hα as a propagating feature across the solar surface with a velocity of about 1000 km/s. They often show arc-like front with a relatively narrow opening angle. In almost all cases Moreton waves are associated with (or followed by) filament eruptions, and the propagating direction is the same as that of the filament eruptions. Based on various observed features, Moreton waves are thought as the intersection of a fast-mode MHD shock propagating in the corona with the chromosphere, while the shocks are piston-driven caused by filament eruptions. These indicate that the elevation angle of filament eruptions is an important factor to generate Moreton wave, since the shocks excited in front of ejected filament must intersect with the chromosphere. We investigated elevation angles of filament eruptions of 14 Moreton waves, by using the Hα images taken by the Flare Monitoring Telescope (FMT) at Hida Observatory, Kyoto University during the Solar Cycle 23. We also investigated the difference between the elevation angles of filament eruptions with Moreton waves and those without Moreton waves. As a result, we found that the direction of filament eruptions that produce the Moreton waves tend to be almost horizontal, which supports the piston driven model of the Moreton wave. In this paper we report the results of our analyses.

Hinode-7
Session 4: Flares and Coronal Mass Ejections

Microwave and X-ray observations of an X-class flare on 13 May 2013

Abstract Author(s): Satoshi Masuda

Institution(s): Solar-Terrestrial Environment Laboratory, Nagoya University

Presentation: S4-P-38

Abstract

Four X-class flares took place in May 2013. Fortunately three of four were observed with Nobeyama Radioheliograph (NoRH). One of them occurred behind the east limb on 13 May 2013. It is a good chance to investigate the height distribution of nonthermal electrons in the corona. In the framework of the standard flare model based on magnetic reconnection, Minoshima et al. (2011) showed that height distribution of accelerated/heated electrons depends on the energy of the electrons. NoRH has a capability to observe a solar flare in 17 and 34 GHz with a high time resolution (100 ms). The mean-energy of electrons emitting 34 GHz is higher than that for 17 GHz. Hard X-rays are emitted by electrons in the lower energy range compared with the case of microwaves. These dataset can cover a wide energy range of accelerated electrons. In order to understand the electron acceleration/transport/loss processes, multi-wavelength observation is crucially important. The 13 May 2013 flare was simultaneously observed with NoRH, RHESSI, and Hinode/XRT. Investigating the distribution of these emission sources in the corona, we discuss the electron acceleration/transport/loss processes.

Hinode-7
Session 4: Flares and Coronal Mass Ejections

The origin of nonthermal electrons in solar flares

Abstract Author(s): Tomoko Kawate, Kiyoshi Ichimoto

Institution(s): Kwasan and Hida Observatory, Kyoto University, Kwasan and Hida Observatory, Kyoto University

Presentation: S4-P-39

Abstract

There are many unsolved problems in solar flares. One of them is so-called "number problem;" the number of nonthermal electrons estimated from hard X-ray emissions is much larger than the number of electrons estimated from coronal density. To explain this problem, there are some discussions that the nonthermal electrons observed by hard X-ray are accelerated in the dense chromosphere. We study the electron density evolution in corona on solar flares with EUV imaging spectroscopy by using Hinode/EIS data to investigate the position of the electrons which are to be accelerated. From these analyses, we find the decreasing of electron density at the beginning of several flares. In this presentation, we show the results of the time-dependent density distribution of the electrons in the coronal flare region. Moreover, we discuss the electron acceleration site on the solar flares by comparing the amount of the decreased electrons in the corona to the amount of the nonthermal electrons estimated from hard X-ray observation using RHESSI data.

Hinode-7
Session 4: Flares and Coronal Mass Ejections

Three kinds of MHD waves excited around flare due to impact of reconnection-induced plasmoids into ambient plasma

Abstract Author(s): Jiansen He, Liping Yang, Lei Zhang, Hardi Peter, Chuanyi Tu, Linghua Wang, Shaohua Zhang, Xueshang Feng

Institution(s): Peking University, Peking University, Peking University, Max-Planck Institute for Solar System Research, Peking University, Peking University, IGG, CAS, CSSAR, CAS

Presentation: S4-P-40

Abstract

Quasi-periodic fast-propagating (QFP) magnetosonic waves have been discovered from AIA observations to successively emanate from the solar flare kernel. In this study, we perform a numerical investigation of the excitation of QFP waves in the interchange-reconnection-induced flare scenario. The shearing flow at the footpoint is used to drive the reconnection. The modeling results show that plasmoids are generated in the reconnection current sheet as a result of tearing instability. The plasma around the magnetic null point is heated up by Joule dissipation to X-ray temperature ($\sim$ 10 MK), and is ejected both upwards and downwards. Due to the collision between the impacting plasmoids and the ambient open magnetic field, QFP waves are consecutively launched, and propagate divergently outward with a phase speed of $\sim$ 1000 km/s. In the ω - κ diagram of the wave power spectral density, we find a broad frequency distribution with a straight ridge that represents the dispersion relation of the fast waves. Aside from the fast waves, Alfven waves and slow waves are generated simultaneously as the plasmoids collide with the ambient open magnetic field. Different from the quasi-circularly divergent propagation of fast waves, both Alfven waves and slow waves are confined to propagate in the column of jet outflow. As an output of the energy conversion due to reconnection, the energy partition among these three waves is also estimated.

Long-period oscillations of solar flare emissions

Abstract Author(s): Elena Gennadievna Kupriyanova, V F Melnikov, K Shibasaki

Institution(s): Central Astronomical Observatory at Pulkovo of the RAS

Presentation: S4-P-41

Abstract

Spatial structure of the intensity and polarization of the microwave emission from five long-lasting solar flares are studied. Data with high angular and temporal resolution from Nobeyama Radioheliograph and Radiopolarimeters in frequency range from 1 GHz to 35 GHz are used. The duration of flares selected exceeds 40 minutes. This allows us to find reliably quasi-periodic pulsations (QPPs) with periods of up to 10 minutes. The temporal profile of each flare consists of a short impulsive burst and a following long-lasting smooth component. QPPs with stable in time periods from 1 minute to 9 minutes are found in the smooth component. Amplitudes and phases of the QPPs from different parts of flaring areas are compared. Spectral properties of the QPPs are studied using methods of correlation, Fourier and wavelet analyses. Physical origin of the QPPs features detected as well as possible mechanisms of the QPPs are discussed.

Hinode-7
Session 4: Flares and Coronal Mass Ejections

The Spectrometer Telescope for Imaging X-rays (STIX) onboard Solar Orbiter

Abstract Author(s): Frantisek Farnik

Institution(s): Astronomical Institute AV CR

Presentation: S4-P-42

Abstract

The Spectrometer Telescope for Imaging X-rays (STIX) is one of 10 instruments on board Solar Orbiter, a confirmed M-class mission of the European Space Agency (ESA) within the Cosmic Vision program scheduled to be launched in 2017. STIX applies a Fourier-imaging technique using a set of tungsten grids (at pitches from 0.038 to 1 mm) in front of 32 pixelized CdTe detectors to provide imaging spectroscopy of solar thermal and non-thermal hard X-ray emissions from 4 to 150 keV. The poster presents the status of the instrument development as prepared for the Critical Design Review.

Hinode-7
Session 4: Flares and Coronal Mass Ejections

Investigation of shock nature of an EUV wave using a prominence activation

Abstract Author(s): Takuya Takahashi, Ayumi Asai, Kazunari Shibata

Institution(s): Kyoto University, Kyoto-U. , Kyoto-U.

Presentation: S4-P-43

Abstract

Associated with a large solar flare occurred on Mar 7, 2012, a wave-like coronal disturbance (known as EUV waves) was observed. The EUV wave 'hit' a polar prominence leading to its oscillation. We also found that the prominence strongly brightened when EUV wave 'pushed' it. Based on observational features, we interpreted the EUV wave as fast mode MHD shock. By using the physical features of a fast mode MHD shock, we successfully explained prominence acceleration and compression, and got a potential tool to diagnose physical quantities in the corona that are very difficult to directly observe.

Hinode-7

Session 5

Space Weather and Space Climate

Upper limit for solar flare energies

Abstract Author(s): Carolus J Schrijver

Institution(s): Lockheed Martin Advanced Technology Center

Presentation: S5-I-01

Abstract

The most extreme solar events drive the most extreme space weather throughout the solar system. Direct measurements of the most energetic events, limited to the past half century, reveal a continuing distribution of ever lower frequency with increasing total energy. Information on the rarest, most energetic events can only be obtained indirectly by the analysis of radionuclides on Earth and on the Moon, comparison with observations of Sun-like stars, and inferences from four centuries of sunspot observations. Do these records yield a coherent picture, or are we left with substantial uncertainty on the most extreme space weather that the Sun can generate?

Hinode-7
Session 5: Space Weather and Space Climate

Active Region Upflow Plasma: Does it Reach the near-Earth Environment?

Abstract Author(s): J. L. Culhane, D. H. Brooks, L. van Driel-Gesztelyi, P. Demoulin, D. Baker, M. L. DeRosa, C. H. Mandrini, L. Zhao, T. H. Zurbuchen

Institution(s): UCL Mullard Space Science Laboratory

Presentation: S5-C-01

Abstract

In a recent study of persistent active region upflow from AR 10978 in the period 10 - 15, December, 2007, Brooks and Warren (2011), using the Hinode EUV Imaging Spectrometer (EIS) instrument showed the presence of a strong low-FIP element enhancement in the upflowing plasma that appeared to be replicated three days later in the in-situ solar wind measurements made by the ACE/SWICS instrument. In the present work, we examine the upflowing plasma properties (Te, ne, v, abundances) as a function of time in greater detail as AR 10978 passes the Earth-Sun line. The structure of the magnetic field above the two upflow regions – E and W of the AR, was determined by Demoulin et al., 2013 who also established the upflow inclinations to the line-of-sight. The Eastern upflow is steadier than that from the West and has higher density and FIP-bias values. However AR 10978 is bisected by the Heliospheric Current Sheet (HCS) as a magnetic inversion line and a PFSS magnetic field model indicates that the region is completely covered by a helmet streamer. Thus while it is not clear how any of this upflowing plasma could reach the Earth, plasma of active region composition e.g. large FIP-bias, is detected by ACE approximately three days later. From back-mapping to the source surface at 2.5 RS, the plasma appears to originate from West of the AR. It will be briefly indicated how the complex magnetic topology in the neighbourhood of AR 10978 could allow this to happen. An account of this latter work has been submitted by Mandrini and co-workers for poster presentation at the meeting.

Hinode-7
Session 5: Space Weather and Space Climate

Extreme Interplanetary Shocks/Coronal Mass Ejections and Consequences for the Magnetosphere and Earth

Abstract Author(s): Bruce T. Tsurutani, Gurbax S. Lakhina

Institution(s): Space Plasma Research Institute, Indian Institute of Geomagnetism

Presentation: S5-C-02

Abstract

A "perfect" ICME (Interplanetary Coronal Mass Ejection)-generated shock is considered to estimate the consequences for the Sun-Earth environment. The maximum shock speed and magnetosonic Mach number are calculated. The transit time to Earth will be ∼12 hrs, faster than either the August 1972 event or the Carrington 1859 event. The interplanetary sheath ram pressure and its impact on the magnetosphere will push the subsolar magnetopause in to an equilibrium distance of ∼4.0 Earth-radii (R_e) from the Earth's surface. Low-altitude Earth-orbiting satellites like the GPS transmitters will be exposed to the ICME shock-accelerated particle radiation. The magnetospheric electric field associated with the dB/dt can be as large as ∼1.9 V/m and will form a new relativistic electron radiation belt. This electric field is ∼6 times larger than a previously reported event in 1991. The estimated dB/dt rate can be used to design transformers to protect power grids for an event of this magnitude. For the perfect storm, the interplanetary drivers are intense enough to lead to a Dst/SYM-H almost double that of the Carrington event. However there are predictions that the magnetosphere might saturate at a lesser storm intensity.

Hinode-7
Session 5: Space Weather and Space Climate

Rapid events in the carbon-14 content of tree-rings

Abstract Author(s): Fusa Miyake, Kimiaki Masuda, Toshio Nakamura, Fuyuki Tokanai, Kazuhiro Kato, Katsuhiko Kimura, Takumi Mitsutani

Institution(s): Nagoya University

Presentation: S5-C-03

Abstract

Measurement of cosmogenic nuclides can provide us important information to search for past extraterrestrial high-energy events such as supernova, solar proton event (SPE), and so on. Until now, the contents of 14C in tree rings and 10Be in ice cores have been used for this purpose. Although no clear evidence has been found by 14C and 10Be, it is possible that these high energy cosmic ray events are hidden in unmeasured period. We show the results of 14C content measurement in Japanese cedar and Japanese cypress annual tree rings from AD 600 to AD 1100 with 1- to 2-year resolution, and report two findings of rapid increases of 14C content from AD 774 to AD 775 and from AD 993 to AD 994. These are clear increases against its measurement errors. The shapes of the two series are very similar, i.e., a rapid increase within one year followed by a decay due to the global carbon cycle. The scale of the AD 994 event is 0.6 times as large as the AD 775 event. The decadal 10Be flux in the Antarctic ice core also shows the peaks corresponding to these two 14C events. The proportions of flux increase (14C/10Be) of the two events are consistent with each other. Therefore, it is highly possible that these events have the same origin. Although the cause of the AD 775 event can be explained by a large solar proton event (SPE) or a short gamma-ray burst, we conclude that the solar activity is a more plausible cause because the occurrence rate of 14C increase events is inconsistent with the observed rate of short gamma-ray bursts and consistent with higher solar activity during the 8-10th centuries. This indicates the possibility that such large SPEs will occur in the future.

Hinode-7
Session 5: Space Weather and Space Climate

Mercury observed by Hinode SOT

Abstract Author(s): Shingo Kameda, Yukio Katsukawa, Ayaka Fusegawa

Institution(s): Rikkyo University , Rikkyo University

Presentation: S5-P-02

Abstract

Mercury has a thin atmosphere. It is often called a “surface-bounded exosphere” because its scale height near the surface is smaller than the mean-free path of atmospheric particles. Sodium density is relatively high in the detected neutral species of H, He, O, Na, Mg, K, and Ca. In these species, the alkali atoms are thought to be released from the surface by photon-stimulated desorption, thermal desorption, chemical sputtering, solar wind ion sputtering, and micrometeoroid vaporization. In the detected species, sodium has been most investigated because its emission is brightest. Though many observations have been done since its discovery in 1985, the source process of exospheric sodium atoms is still unclear. We conducted the observation of Mercury's sodium emission using Hinode SOT just before and after Mercury's superior conjunction on May 12, 2013. It is a prime opportunity to observe exospheric sodium on Mercury's full dayside. In this presentation, we report the preliminary result.

Hinode-7
Session 5: Space Weather and Space Climate

FIP bias in a sigmoidal active region-coronal hole complex

Abstract Author(s): Deborah Baker, David H. Brooks, Pascal Demoulin, Lidia van Driel-Gesztelyi, Lucie M. Green, Kimberley Steed, Jack Carlyle

Institution(s): UCL - MSSL

Presentation: S5-P-03

Abstract

Using spectra obtained by the EIS instrument onboard Hinode, we present a detailed spatially resolved abundance map of an active region (AR) - coronal hole (CH) complex that covers an area of $360'' \times 485''$. The abundance map provides first ionization potential (FIP) bias levels in various coronal structures within the large EIS field of view. Overall, FIP bias in the small, relatively young AR is 2-3. This modest FIP bias is a consequence of the AR age, its weak heating, and its partial reconnection with the surrounding CH. Plasma with a coronal composition is concentrated at AR loop footpoints, close to where fractionation is believed to take place in the chromosphere. Pathways of slightly enhanced FIP bias are traced along some of the loops connecting opposite polarities within the AR. We interpret the traces of enhanced FIP bias along these loops to be the beginning of fractionated plasma mixing in the loops. Low FIP bias in a sigmoidal channel above the AR's main polarity inversion line where ongoing flux cancellation is taking place, provides new evidence of a bald patch magnetic topology of a sigmoid/flux rope configuration.

Hinode-7
Session 5: Space Weather and Space Climate

What can we deduce from the 3D geometry of AR upflows?

Abstract Author(s): Deborah Baker, Pascal Demoulin, Lidia van Driel-Gesztelyi, Cristina H. Mandrini

Institution(s): UCL - MSSL

Presentation: S5-P-04

Abstract

One of the most intriguing Hinode/EIS results is the detection of high-speed upflows in coronal plasma at the edges of ARs (Doschek et al., 2007; Doscheck et al., 2008; Del Zanna, 2008; Harra et al., 2008; Hara et al., 2008). These persistent upflows are located in regions of low electron density and low radiance over strong magnetic flux concentrations of a single polarity. Though the general characteristics of AR upflows are now well-known, key questions remain open – How are these flows oriented? How broad is the angular extent of the flows? Are upflows observed in different spectral lines related? How are they linked? In Demoulin et al., 2013, we attempt to address these questions by analyzing the limb-to-limb evolution of AR 10978 in order to constrain the geometry, nature, and physics of large-scale upflows present on both sides of ARs.

Hinode-7
Session 5: Space Weather and Space Climate

Active Region Upflow Plasma: How can it escape from below a closed helmet streamer?

Abstract Author(s): D. Baker, C. H. Mandrini, F. A. Nuevo, A. M. Vasquez, P. Demoulin, L. van Driel-Gesztelyi, J. L. Culhane, G. D. Cristiani, M. Pick

Institution(s): UCL - MSSL

Presentation: S5-P-05

Abstract

Recent studies show that active region (AR) upflowing plasma, observed by the Hinode EUV Imaging Spectrometer (EIS), can gain access to open field lines and be released into the solar wind via magnetic interchange reconnection occurring below the source surface at magnetic null-points in pseudo-streamer configurations. When only one simple bipolar AR is present on the Sun and it is fully covered by the separatrix of a streamer, like AR 10978 on December 2007, it seems unlikely that the upflowing AR plasma could find its way into the slow unsteady solar wind. However, Culhane and co-workers (presentation at this meeting), find signatures of plasma with AR composition at 1 AU that appears to originate from the West of AR 10978. We present a detailed topology analysis of AR 10978 based on a PFSS model in which we show that via magnetic reconnection, occurring in at least two main steps, it is possible for the AR plasma to get around the topological obstacle of the streamer separatrix and be released into the solar wind. In a first step the AR expansion forces reconnection at quasi-separatrix layers (QSLs) between the AR closed loops anchored at its borders, where EIS upflows are prominent, and large scale network fields to the West of the AR. In a second step, the further diffusion of the photospheric AR field induces reconnection with the open field lines in the neighbourhood of the northern coronal hole at a high altitude magnetic null-point and associated separatrices. The reconnected open field lines bend towards the ecliptic so that plasma of AR origin can be detected at 1 AU.

Hinode-7
Session 5: Space Weather and Space Climate

Diagnosing flare productive active regions using EUV images for space

Abstract Author(s): Yuko Hada, Hiroaki Isobe, Ayumi Asai, Takako T Ishii, Daikou Shiota

Institution(s): Kyoto University, Kyoto University, Kyoto University, Nagoya University

Presentation: S5-P-06

Abstract

Solar flares and coronal mass ejections (CMEs) are the most significant phenomena for space weather. Therefore, establishing a method of flare prediction is the most essential task for space weather researches. However, current space weather researches are mainly for circumterrestrial space not for the deep space probes that are located far from the earth. Radiation hazard from solar flares and coronal mass ejections may cause significant damage not only to the satellites on geocentric orbits but also to the deep space probes. Although there are many researches on the space weather forecast and nowcast for the circumterrestrial space, those for deep space probes remain difficult because of there are few observational information on the invisible side of the Sun from the Earth.

Now, we can obtain the backside EUV images of the sun, by the Solar Terrestrial RElations Observatory (STEREO). In order to develop a flare prediction algorithm for deep space probes by using STEREO EUV images, we analyzed 13 active regions with different flare productivity observed by Extreme ultraviolet Imaging Telescope (EIT) of Solar and Heliospheric Observatory (SOHO).

We examined the differences between the time profiles of EUV intensity of flare productive active regions and those of non-flare productive Active regions. We found that, although total intensity of the EIT images are similar in flare productive and non-productive active regions, there are bright pixels (>1200 DN/s) in flare productive ARs even when flares were not occurring. On the other hand, in the non-flare productive ARs, the possibility of the appearance of bright pixels is much less than that in the flare productive ARs. This difference possibly may be used for an indicator of flare productivity of each AR. In this research, we will show comparison between flare productive active region (NOAA09415) and those of non-flare productive Active region (NOAA10923).

Hinode-7
Session 5: Space Weather and Space Climate

Dayside ionospheric equivalent current system of Pi 2 pulsations

Abstract Author(s): Shun Imajo, Akimasa Yoshikawa , Teiji Uozumi, Shinich Ohtani, Kiyohumi Yumoto, MAGDAS/CPMN group

Institution(s): Dept. Earth Planet. Sci., Kyushu Univ., ICSWSE, Kyushu Univ., APL, Johns Hopkins Univ., ICSWSE, Kyushu Univ.

Presentation: S5-P-07

Abstract

The conductivity in the dayside ionosphere is considarably high compared with the nightside ionosphere because the solar ultraviolet and X-ray contribute to ionize the upper atmosphere's neutral gas. The ionospheric current contributes greatly to ground geomagnetic variations in the sunlit hemisphere. Although Pi 2 pulsations typically are observed at nightime accompanied with onsets of substorm expansion phase, at low latitudes, they are also observed in daytime Amplitude of Pi 2s is enhanced in the dayside equatorial region where the conductivity peaks. This can be interpreted that ionospheric current oscillations induce the Pi 2 magnetic oscillations on the ground in this region. Considering the current continuity, these current should connect high latitude ionosphere where the source current from the magnetosphere impinges. In this study, we estimate the dayside ionospheric equivalent current associated with Pi 2 pulsations using magnetic data from the ground-based stations of the MAGDAS/CPMN and INTERMAGNET. The results show the existence of the dayside ionospheric current system for Pi 2 pulsations, which consists of the meridional currents along the terminator and zonal current around the noon.

Space weather research using MAGDAS/CPMN data

Abstract Author(s): Hiroki Matsushita, A Yoshikawa, T Umezu

Institution(s): Kyushu University, Kyushu University, Kyushu University

Presentation: S5-P-08

Abstract

The magnetic dip equator is a final destination of global solar wind-solar radiation-magnetosphere-ionosphere and atmosphere coupling system. Since it's very high conductivity nature produced by the Cowling effect enables it to pick up various electromagnetic coupling phenomena, the dip-equator can be used as a good sensor for space weather phenomena. To use this nature for space weather study, we developed EE index [T. Uozumi et al., 2008] by use of MAGDAS/CPMN network data. We will discuss how this data can be used for space weather study by taking advantage of the dip equator region as a good indicator for many phenomenon.

Hinode-7

Session 6

Solar-Stellar Connection

Hinode-7
Session 6: Solar-Stellar Connection

Superflares on solar-type stars

Abstract Author(s): Hiroyuki Maehara, Takuya Shibayama, Yuta Notsu, Shota Notsu, Satoshi Honda, Daisaku Nogami, Kazunari Shibata

Institution(s): University of Tokyo, Kyoto University, Kyoto University, Kyoto University, University of Hyogo, Kyoto University, Kyoto University

Presentation: S6-I-01

Abstract

Large stellar flares called "superflares" release $>10^{33}$ erg of energy, which are more than 10 times more energetic than the largest solar flares observed so far. Recent high-precision photometry from space enables us to investigate the nature of superflares on solar-type stars (G-type main sequence stars). We present the results of a search for superflares on solar-type stars using the data obtained by the Kepler space telescope. We found more than 1500 flares on G-type main sequence stars from the long time cadence data and about 150 flares from the short time cadence data. The energy of detected flares ranges from 10^{33} to 10^{36} erg. The occurrence frequency distribution of superflares can be fitted by a power-law function with the index of about -2 which is similar to that of solar flares. Moreover, the frequency distribution of superflares on Sun-like stars (G-type stars with rotation period >10 days and with effective temperature of 5600-6000K) and that of solar flares are roughly on the same power-law line. The frequency of superflares depends on the rotation period of the star. The frequency of flares decreases as P_{rot}^{-2} for a period range above a few days. On the other hand, the maximum energy of superflares observed in a given period bin does not depend the rotation period. The energy of superflares correlates with the amplitude of quasi-periodic light variations which corresponds to the total area of starspots. The correlation between the energy of superflares and the total area of starspots is similar to that between the GOES class of solar flares and the area of the sunspot group. These results suggest that slowly rotating stars like our Sun can produce superflares and the presence of large starspot groups is one of the necessary condition for the generation of superflares.

Convection and Dynamo Action in Solar-like stars

Abstract Author(s): Allan Sacha BRUN

Institution(s): AIM/CEA-Saclay

Presentation: S6-C-01

Abstract

We present a study of convection and dynamo action in solar-like stars at various rotation rates. Rotation is found to modify greatly the large scale flows such as differential rotation and meridional circulation yielding solar-like profiles and amplitude only in a limited range of Rossby number. Dynamo action modifies further the mean large scale flows due to the feed back effect of the Lorentz force. Magnetic fields take the shape of large magnetic wreaths for high rotation rate, thus becoming predominantly toroidal. Based on these results, simple mean field dynamo model of the Sun can't be easily extended to other solar-like stars in order to explain the general trend of a shorter activity cycle for higher rotation rate. We propose alternative solutions.

Hinode helps us to understand the nature of stellar flares

Abstract Author(s): Petr Heinzel, Arkadiusz Berlicki, Adam Kowalski

Institution(s): Astronomical Institute

Presentation: S6-C-02

Abstract

Using the multiwavelength observations of solar and stellar flares, we have detected principal differences between the light curves of CaII lines. While solar flares show the CaII time variation similar to that of the hydrogen H alpha line and soft X-rays, flares on dMe stars exhibit a significant time delay of CaII light curves behind those of H alpha and other lines . However, when using very high spatial resolution movies of flares provided by the Hinode/SOT instrument, one can identify a behavior similar to that discovered on dMe stars. We will demonstrate examples of relevant light curves in various spectral lines and discuss possible physical scenarios consistent with solar and stellar observations.

Hinode-7
Session 6: Solar-Stellar Connection

Saturation of Stellar Winds from Young Suns

Abstract Author(s): Takeru Ken Suzuki, Shinsuke Imada, Ryuho Kataoka, Yoshiaki Kato, Takuma Matsumoto, Hiroko Miyahara, Saku Tsuneta

Institution(s): Department of Physics, Nagoya University, Solar-Terrestrial Environment Lab., Nagoya University, National Institute of Polar Research, Japan, National Astronomical Observatory of Japan, Department of Physics, Nagoya University

Presentation: S6-C-03

Abstract

We investigate mass losses via stellar winds from sun-like main sequence stars with a wide range of activity levels. We perform forward-type magnetohydrodynamical numerical experiments for Alfven wave-driven stellar winds with a wide range of the input Poynting flux from the photosphere. Increasing the magnetic field strength and the turbulent velocity at the stellar photosphere from the current solar level, the mass loss rate rapidly increases at first owing to the suppression of the reflection of the Alfven waves. The surface materials are lifted up by the magnetic pressure associated with the Alfven waves, and the cool dense chromosphere is intermittently extended to 10 – 20 % of the stellar radius. The dense atmospheres enhance the radiative losses and eventually most of the input Poynting energy from the stellar surface escapes by the radiation. As a result, there is no more sufficient energy remained for the kinetic energy of the wind; the stellar wind saturates in very active stars, as observed in Wood et al. The saturation level is positively correlated with $B_{r,0}f_0$, where $B_{r,0}$ and f_0 are the magnetic field strength and the filling factor of open flux tubes at the photosphere. If $B_{r,0}f_0$ is relatively large $>\sim 5$ G, the mass loss rate could be as high as 1000 times. If such a strong mass loss lasts for ~ 1 billion years, the stellar mass itself is affected, which could be a solution to the faint young sun paradox. We derive a Reimers-type scaling relation that estimates the mass loss rate from the energetics consideration of our simulations. Finally, we derive the evolution of the mass loss rates, $\dot{M}t^{-1.23}$, of our simulations of our simulations,combining with an observed time evolution of X-ray flux from sun-like stars, which is shallower than $\dot{M}t^{-2.33+/-0.55}$ in Wood et al.(2005).

Hinode-7
Session 6: Solar-Stellar Connection

The thermal structure of the quiet Sun coronal emission

Abstract Author(s): Paola Testa, Steven Saar, Enrico Landi

Institution(s): Harvard-Smithsonian Center for Astrophysics , Harvard-Smithsonian Center for Astrophysics , University of Michigan, Ann Arbor

Presentation: S6-P-01

Abstract

We use spectral (SOHO/SUMER and Hinode/EIS) and imaging (Hinode/XRT and SDO/AIA) solar coronal data to systematically measure the thermal structure of different types of solar features (coronal hole, quiet Sun, X-ray bright points, active regions...). For the quiet Sun, we studied the coronal emission across the solar activity cycle, finding remarkably constant thermal structure. We use the results of our investigation of the thermal and spatial structure of the solar corona also to interpret stellar observations. We use a combination of solar coronal features to construct a model for the quiet corona of the inactive G8V star tau Ceti, which is a candidate stellar analog of a solar magnetic minimum. Since tau Ceti is significantly metal-poor relative to the Sun, we reconstruct the solar results with corresponding lower metallicities to generate more appropriate coronal structures.

Hinode-7
Session 6: Solar-Stellar Connection

SOT BFI plate scale re-calibration on June 2012 Venus transit event

Abstract Author(s): Miho Kanao, Toshifumi Shimizu, Takeshi Imamura, Yasumasa Kasaba, Takeshi Sakanoi, Atsushi Yamazaki, Masato Nakamura

Institution(s): ISAS / JAXA

Presentation: S6-P-02

Abstract

We re-calibrated pixel scale of SOT using the data on Venus transit event on June 5 and 6, 2012. The solar radiance refracted by Venus atmosphere, " aureole " , was detected clearly. The luminosity distribution would provide us the physical parameters in Venus atmosphere, such as the atmosphere altitude and the spatial distribution of the extinction function by the aerosol scatter. The absolute pixel scale with high accuracy enables us to measure the absolute altitude of the refracted solar radiance in Venus atmosphere with the precision < 10 km.The radius of dark Venus silhouette limb was fitted by least square method using the G band (430.5 nm) 1024 x 2048 images (2 x 2 summing) from 5th 22:54:02 to 6th 04:16:41 during transit. The limb was defined as the point where the solar luminosity decreases to 1/e, $\tau = 1$. The averaged limb radius was longer in the equator region than that in the polar region, and varies with the angle around Venus center. It indicates that the optical depth 1 altitude has the latitudinal variation.The plate scale of the optical instrument was calculated, comparing the limb radius with the semidiameter at $\tau = 1$ level. The $\tau = 1$ altitude was determined referring to SPICAV data, the most secure observation. The pixel scales were calculated using polar and equatorial Venus limb radius respectively. We considered the error by the latitudinal variation of Venus atmospheric altitude, the bias due to the diffraction limit, and the fitting errors. As a result, the pixel scale was defined as 0.05372 ± 0.0004 arc sec / pixel.

Hinode-7
Session 6: Solar-Stellar Connection

From high-resolution observations and models of the Sun towards cool stars

Abstract Author(s): Sven Wedemeyer

Institution(s): University of Oslo

Presentation: S6-P-03

Abstract

Recent advances in high-resolution ground-based and space-borne observations of the Sun enriched our physical understanding of our host star. Detailed comparisons of these observations with numerical models provide important tests, which nourish the development of numerical simulations with unprecedented levels of complexity and realism. Spatially resolved observations are unfortunately not possible for other dwarf stars. However, the numerical simulation codes, which are developed for the solar case, can also be applied to other stars because much of the modelled physics is valid there, too.

Dwarf stars of spectral type M (" M-dwarfs ") constitute about 75% of all stars in our galaxy, which makes them highly relevant for stars in general, incl. stellar magnetism and stellar activity, incl. flares, and for a multitude of fundamental questions in modern astrophysics like, e.g., the chemical evolution of the universe. Observations of these stars provide statistically significant samples that span large parameter ranges, which are not accessible from solar observations alone. The combination of solar and stellar studies yields therefore large potential for a better understanding of our Sun and stars in general.

Here I demonstrate the potential of comparative studies for M-dwarfs with the Sun as fundamental reference case. I will present results from 3D radiative magnetohydrodynamic (MHD) simulations of the Sun and M-type dwarf stars, which extend from the upper convection zone into the chromosphere. Selected examples concern the granulation pattern and flows in the low photosphere, the small-scale magnetic field structure of the atmosphere, and dynamic processes (e.g., so-called " magnetic tornadoes "), which exist both on the Sun and M-dwarfs. Synthetic spectra and intensity images, which are calculated based on the 3D models, are compared to solar and stellar observations.

Flare Rates for Solar-like Stars in the One Gigayear Year Old Kepler Cluster NGC 6811, With Implications for the Sun

Abstract Author(s): Steven H. Saar, Soeren Meibom, Paul J. Wright, Vinay Kashyap, Jeremy J Drake

Institution(s): Harvard-Smithsonian Center for Astrophysics, SAO, SAO, SAO

Presentation: S6-P-04

Abstract

We aim to better estimate the rate of very strong (Carrington event-type and larger) flares on the Sun by studying flares of stars in several open clusters with well determined ages. Here we derive white light flare distributions for a sample of near-solar-mass (G0-G5) dwarfs in NGC 6811 (age $\sim$ 1 Gyr) using Kepler data. We compare these with solar white light flare rates and, using a solar-based relationship, estimate the X-ray emission from the same flares. The X-ray estimates can then be used to compare the Kepler results to other solar and stellar X-ray flare data. We explore implications of our results for the rates of large solar flares.

More Evidence HD 3651 May be in a Maunder-like Magnetic Minimum

Abstract Author(s): Steven H. Saar, Hiroko Miyahara

Institution(s): Harvard-Smithsonian Center for Astrophysics, Musashino Art Univ.

Presentation: S6-P-05

Abstract

It has often been suggested that the K dwarf HD 3651 is entering a Maunder-like magnetic minimum based on its Ca II HK emission, which has declined significantly to a very low level. We note several other characteristics of the star's activity which support this idea: (1) the star's cycle amplitude decreased in two successive cycles prior to reaching the base level, similar to the sunspot record pre-Maunder minimum; (2) the cycle length increased steadily into minimum, also consistent with the solar record; (3) a low level cycle continues in the minimum, again, analogous to the sunspot record. We further explore the properties of HD 3651, searching for insight into characteristics of solar magnetic minima and the parameters which control such states.

Differential Rotation at One Gigayear: Rotational Period Changes in Kepler Cluster NGC 6811

Abstract Author(s): Steven H. Saar, Soeren Meibom

Institution(s): Harvard-Smithsonian Center for Astrophysics, SAO

Presentation: S6-P-06

Abstract

Differential rotation (DR) is thought to be a key component of cycling solar-like dynamos. Lower limits on the surface DR rate can be made by following the rotation of spot groups on stars, and how the rotation period (P_{rot}) changes as new groups appear at different latitudes. We study over 100 cool dwarf stars in the one gigayear old open cluster NGC 6811 using Kepler data. A moving window period analysis is applied to over four years of low cadence (30 min), nearly continuous data for each star. Some spectral types show fewer more distinct P_{rot} values than others, suggesting they either have narrow activity belts, low DR, long cycles with slow latitude migration, or some combination of these. Stars with at least five distinct P_{rot} measurements are flagged for further study and used to estimate a DR rate. We find that these rates agree well with measurements of field stars with similar P_{rot}. Hotter F dwarfs show different behavior with mass than cooler stars. We discuss implications for the evolution of solar DR and its dynamo.

Superflares on Solar Type Stars Observed with Kepler

Abstract Author(s): Takuya Shibayama, Hirouki Maehara, Yuta Notsu, Shota Notsu, Satoshi Honda, Daisaku Nogami, Kazunari Shibata, Takako T. Ishii

Institution(s): Kyoto University, University of Tokyo, Kyoto University, Kyoto University, University of Hyogo, Kyoto University, Kyoto University, Kyoto University

Presentation: S6-P-07

Abstract

High precision photometry of Kepler spacecraft enables us to detect superflares on G-type dwarfs. In Maehara et al. (Nature, 2012, 485, 478), we reported 365 superflares on 148 G-type dwarfs detected from light curves of 120 days. The occurrence frequency (dN/dE) of superflares vs. flare energy (E) shows power-law distribution with $dN/dE \propto E^{\alpha}$, where $\alpha \sim -2$. It is interesting that this distribution is roughly on the same line as that for solar flares. In the case of the Sun-like stars (with surface temperature 5600-6000K and slowly rotating with a period longer than 10 days), the occurrence frequency of superflares with energy of 10^{34} - 10^{35} erg is once in 800-5000 years. No hot Jupiters were found in these superflare stars. These superflare stars often show quasi periodic brightness variation, which might be evidence of the large starspot. We can estimate the rotational period from the brightness variation period. It is interesting that superflares are detected on slowly rotating stars ($P > 10$ days) like the Sun. By extending this previous study, we searched for superflares on G-type dwarfs using Kepler data of 500 days. We found 1547 superflares on 279 G-type dwarfs, including 44 superflares on 19 Sun-like stars (Shibayama et al. 2013arXiv1308.1480S). Using these new data, we studied the statistical properties of occurrence frequency of superflares, and basically confirmed the previous results. We compare the flare frequency distribution of the superflare and solar flare, and study the similarity of them. We also found that some G-type dwarfs show very high activity and exhibit superflares once in ~ 10 days. In the case of Sun-like stars, the most active stars show one superflare in ~ 100 days.

High Dispersion Spectroscopy of Solar-Type Stars showing Superflares

Abstract Author(s): Yuta Notsu, Satoshi Honda, Hiroyuki Maehara, Shota Notsu, Takuya Shibayama, Daisaku Nogami, Kazunari Shibata

Institution(s): Kyoto University, University of Hyogo, University of Tokyo, Kyoto University, Kyoto University, Kyoto University, Kyoto University

Presentation: S6-P-08

Abstract

Superflares are very large flares that release total energy of 10^{33}-10^{38} erg. Recent Kepler spacecraft observations found many superflares on solar-type stars and such superflare stars show quasi-periodic brightness modulations with the typical period of one to a few tens of days (Maehara et al., 2012, Nature, 485, 478). Such modulations are thought to be caused by the rotation of the star with large starspots (Notsu et al. 2013, ApJ, 771, 127), but we need to investingate whether the modulation is really due to the rotation. It is also important to investigate whether superflares really occur on single Sun-like stars.

We carried out spectroscopic observations of 25 solar-type superflare stars with brightness varitation period of 1-10 days, using the Subaru telescope. The wavelength range is 6100-8820A, including important lines CaII IR triplet (8498/8542/8662) and Ha. About half of the targets are judged to be single stars. In this research, we carried out detailed analyses for the targets which are not confirmed to be binary stars. All the targets which are expected to have large starspots show high chromospheric activity compared to the Sun. Assuming that the brightness variation period correspond to the rotational period is consistent with the value of v sin(i) (projected rotational velosity) measured from spectroscopic results.

We have already reported the results of the spectroscopic observation or one superflare star KIC6934317 in Notsu et al. (2013 PASJ in press, arXiv:1307.4929)

Hinode-7
Session 6: Solar-Stellar Connection

High-Dispersion Spectroscopy of the Superflare Star KIC6934317

Abstract Author(s): Shota Notsu, Satoshi Honda, Yuta Notsu, Takuya Shibayama, HIroyuki Maehara, Daisaku Nogami, Kazunari Shibata

Institution(s): Dept. of Astronomy, Kyoto-U., University of Hyogo, Dept. of Astronomy, Kyoto-U., Dept. of Astronomy, Kyoto-U., Kiso Obs., Univ. of Tokyo, Kwasan and Hida Obs., Kyoto-U., Kwasan and Hida Obs., Kyoto-U.

Presentation: S6-P-09

Abstract

We conducted high-resolution spectroscopic observation with Subaru/HDS for a G-type star (KIC6934317). We selected this star from the data of the Kepler spacecraft. This star produces many superflares (e.g., Maehara et al., 2012, Nature, 485, 478, Shibayama et al., 2013, ApJS, in press), and the total energy of the largest recorded superflare on this star was $\sim 10^3$ times larger ($\sim 2.2\times10^{35}$ erg) than that of the most energetic flare on the Sun ($\sim10^{32}$ erg). The core depth and emission flux of Ca II infrared triplet lines and Ha line show high chromospheric activity in this star, in spite of its low lithium abundance and the small amplitude of the rotational modulation. Using empirical relations between the emission flux of chromospheric lines and X-ray flux, this star is considered to show much higher coronal activity than that of the Sun. It probably has large starspots that can store a large amount of magnetic energy, enough to give rise to superflares. We also estimated the stellar parameters, such as the effective temperature, surface gravity, metallicity, projected rotational velocity (v sin(i)), and radial velocity. KIC6934317 is then confirmed to be an early G-type main sequence star. The value of v sin(i) is estimated to be ~ 1.91 km s^{-1}. In contrast, the rotational velocity is calculated to be ~ 20 km s^{-1} by using the period of the brightness variation as the rotation period. This difference can be explained by its small inclination angle (nearly pole-on). The small inclination angle is also supported by the contrast between the large superflare amplitude and the small stellar brightness variation amplitude.

This poster is based on the results reported in Notsu et al. (2013, PASJ in press, arXiv:1307.4929)

Hinode-7
Session 6: Solar-Stellar Connection

3D test particle simulation of ISM Oxygen interacting with Heliosphere for IBEX observations

Abstract Author(s): Akito D. Kawamura, Jacob Heerikhuisen, Nikolai V Pogorelov, Gary P Zank

Institution(s): Kwasan Observatory, Kyoto Univ., CSPAR / Department of Space Sciences, University of Alabama in Huntsville , CSPAR / Department of Space Sciences, University of Alabama in Huntsville , CSPAR / Department of Space Sciences, University of Alabama in Huntsville

Presentation: S6-P-10

Abstract

Recently, the structure of our Heliosphere has retained interests with several milestones on observations; one is Interstellar Boundary EXploerer (IBEX) which observes neutral atoms of interstellar origin. IBEX measures flux of Hydrogen, Helium, Oxygen, and Neon to construct the all-sky view of our neighborhood plasma. With IBEX observations, many theoretical works indicate the influence of Heliospheric structure onto the neutral particle flux of IBEX observed. In this poster, we present the method we developed to simulate IBEX observation of ISM oxygen with statistical Heliospheric model.

When plasma of solar wind (SW) and interstellar medium (ISM) met and create the tangential discontinuity Heliopause, shockwaves propagate to both upstream and construct several boundaries of plasma. However, a neutral atom does not interact with local collisionless plasma environment and travels through the Heliospheric boundaries. On the way to the Earth, a neutral atom can be ionized by exchanging its charge with an ion in a close range, and the new ion would be trapped onto the local plasma. This is a scenario of a creation of pick-up ion (PUI) by charge exchange collision. A PUI can also exchange its charge with neighboring neutral atom to become a neutral again, then this new neutral atom is able to move freely. IBEX has detected neutral particles experienced couple of charge exchange collisions, but characteristics of neutral flux is direction dependent. To reveal the information about the Heliospheric boundaries from IBEX observations, numerical and analytic studies are required for every particle species.

This poster presents a work completed as MS thesis research of Akito Davis Kawamura, MS graduate from UAHuntsville, USA, and new PhD student in Kwasan Observatory, Kyoto university.

Hinode-7

Session 7

Future Problems and Observations

A New Analysis of Photospheric Fields and Flows

Abstract Author(s): Br T Welsch

Institution(s): Space Sciences Laboratory, University of California, Berkeley

Presentation: S7-I-01

Abstract

Magnetic evolution observed in high-cadence sequences of high-resolution, seeing-free magnetograms of the photosphere by Hinode (and of the chromosphere by Solar-C) can constrain the dynamics of near-surface magnetic and velocity fields. Such observations can address open questions about several key topics in solar physics, including coronal heating, flux emergence and submergence, and impulsive magnetic dynamics in flares. I will discuss research ideas in these and other subject areas.

On the need for high-res/small-FOV vs. large-FOV magnetograms

Abstract Author(s): Valentin Martinez-Pillet

Institution(s): National Solar Observatory

Presentation: S7-I-02

Abstract

The answer to the dichotomy posed by the title is exactly the one you are thinking: we need them both. I will present a recent controversy existing about the nature of the so-called orphan penumbra phenomenon originated form high spatial resolution studies that can only be solved by large-FOV data. The physical coupling between the spatial scales of the various solar phenomenon requires the use of high spatial resolution data (technologically limited to a small FOV) and context (i.e., synoptic) data that provides the complete picture. Thus, a better question is if the current existing programs in Solar Physics will be able to collaborate at an international level to ensure access to both types of data. Hopefully, the answer to this question will also be the one you are thinking: Yes.

Resolving Loops in the Solar Corona: Lessons from EIS, AIA, and Hi-C.

Abstract Author(s): David H Brooks

Institution(s): George Mason University

Presentation: S7-C-01

Abstract

Understanding the spatial scale of structures in the solar corona is fundamental to determining how it is heated to high temperatures. Recent observations and modeling of 2MK loops using Hinode/EIS have shown that the majority of loops are unresolved when observed at 1000km spatial scales. These studies suggest, however, that they are composed of only a few magnetic threads, and in some rare cases, are monolithic structures that are fully spatially resolved. Details of the models imply that an instrument with a spatial resolution of 200km or better is necessary to resolve most coronal loops, and the High Resolution Coronal Imager (Hi-C) achieved this performance on a rocket flight in July 2012. We use Hi-C data to measure the Gaussian widths of 91 loops observed in the solar corona and find a distribution that peaks at about 270km. We also use Atmospheric Imaging Assembly (AIA) data for a subset of these loops and find temperature distributions that are generally very narrow. These observations provide further evidence that loops in the solar corona are often structured at a scale of several hundred kilometers. This is within the achievable spatial resolution of Solar-C, but well above the spatial scale expected for many theoretical heating mechanisms.

New diagnostic tool for magnetic fields in low-*beta* plasma: CLASP

Abstract Author(s): Ryohko Ishikawa

Institution(s): National Astronomical Observatory of Japan

Presentation: S7-C-02

Abstract

The magnetic field measurements in low β regions (i.e. upper chromosphere and above) are essential for the understanding of its heating and dynamical activities. Unfortunately, the Zeeman effect does not give rise to measurable polarization signals from these regions because of the weak magnetic field strength and the larger Doppler broadening compared with the Zeeman splitting. The Hanle effect on the UV lines emitted from the transition region is expected to be a new diagnostic tool to overcome this difficulty. However, the way to infer magnetic fields with the Hanle effect is considerably different form that with the familiar Zeeman effect. In this talk, we present what information can (cannot) be reliably derived from the linear polarization signals of the hydrogen Lyman-α line as measured with CLASP (Chromospheric Lyman-Alpha Spectro-Polarimeter) sounding rocket experiment. We simulated the data analysis of CLASP by solving the inversion problem with a model atmosphere (Trujillo Bueno, Stepan, & Casini 2011). As a result of this investigation, we point out that the spectro-polarimetric observation of the UV lines if with other relevant observations indeed be a promising diagnostic tool to access these regions. Clear understanding of the information on magnetic fields available with the Hanle effect is also much needed for the concept design of SOLAR-C.

First Results of Coordinated Observations from Hinode, IRIS and New Solar Telescope

Abstract Author(s): Alexander Kosovichev, Wenda Cao, Phil Goode, Nicolas Gorceix, Lucia Kleint, Claude Plymate, John Varsik, Sergiy Shumko, Vasyl Yurchyshyn

Institution(s): Big Bear Solar Observatory, Big Bear Solar Observatory, Big Bear Solar Observatory , Big Bear Solar Observatory, LMSAL, Big Bear Solar Observatory, Big Bear Solar Observatory, Big Bear Solar Observatory, Big Bear Solar Observatory

Presentation: S7-C-03

Abstract

Most of the chromospheric structuring and dynamics is controlled by the underlying photospheric processes, associated with turbulent magnetoconvection, ubiquitous magnetic flux emergence, small-scale eruptions and acoustic events. The 1.6 m New Solar Telescope (NST) of Big Bear Solar Observatory offers a substantial improvement in ground-based high-resolution capabilities, and provides important support for the Hinode and IRIS missions. The primary goal of the coordinated observations is to obtain complementary data for investigations of photosphere-chromosphere links and drivers of the chromospheric dynamics. The NST observations are performed using the second-generation adaptive optics system AO-308, and three instruments: Broadband Filter Imagers (G-band and TiO), Visible Imaging Spectrometer (H-alpha), and Near InfraRed Imaging Spectropolarimeter (NIRIS). NIRIS provides high-cadence data in Fe I 1565 nm doublet which is the most Zeeman sensitive probe of magnetic fields in the deep photosphere, and in the He I 1083 nm multiplet for diagnostics of the upper chromosphere. We present initial results of the coordinated observations, and discuss properties of small-scale ejections in fibril magnetic structures.

Refining SOT/SP Measurements of Photospheric Magnetic Field By A Two-Step Deconvolution-Inversion Method

Abstract Author(s): Alberto Sainz Dalda, Mark Cheung, Michiel van Noort

Institution(s): Stanford-Lockheed Institute for Space Research

Presentation: S7-P-01

Abstract

We have implemented a simple, fast deconvolution technique for observations from the Solar Optical Telescope (SOT, Tsuneta et al 2008) onboard Hinode (Kosugi et al 2007). By performing Richardson-Lucy iterative deconvolution (Richardson 1972, Lucy 1974) on the polarization images one wavelength at a time, we remove the diffraction pattern of SOT from SP data before feeding them into a conventional inversion scheme (SIR, Ruiz Cobo & del Toro Iniesta 1992), which performs the inversion independently pixel-by-pixel. This is an alternative to the novel spatially-coupled inversion method of van Noort (2012), which operates on original SP data (i.e. images before deconvolution). The present two-step method bypasses the need for large shared-memory machines and each of the two steps can be feasibly performed even on laptops. Comparisons of inversion results from the two methods will be presented. Applications of the new technique to different photospheric regions (i.e. quiet Sun, plage, penumbra) and the impact of point-spread function removal on photospheric contrast and magnetic field measurements will be discussed.

Synthetic high-resolution prominence observations

Abstract Author(s): Stanislav Gunar, Petr Heinzel, Duncan H. Mackay, Ulrich Anzer

Institution(s): Astronomical Institute, Academy of Sci., Czech Rep., Astronomical Institute of the Academy of Sciences of Czech Republic, School of Mathematics and Statistics, University of St Andrews, UK, Max-Planck-Institut fur Astrophysik, Garching, Germany

Presentation: S7-P-02

Abstract

High-resolution observations of quiescent prominences obtained by the Hinode/SOT reveal a large amount of details of the prominence fine structures. Their analysis helps us to understand the structure of the magnetic field supporting the cool prominence material against the gravity and insulating it from the surrounding hot corona.

The whole-prominence magnetic fields are currently studied by several authors employing the linear or non-linear force-free MHD simulations. These are able to produce realistic 3D configurations of the magnetic field which well corresponds to the general structure of the observed prominences/filaments. However, the commonly used technique of visualization of the fine structures located in the magnetic dips present in these magnetic field configurations does not allow for a direct comparison with the filtergram observations such as those by Hinode/SOT.

We use a 3D non-linear force-free field simulation to produce the whole-prominence magnetic field configuration and we fill selected magnetic dips by a realistic prominence plasma. This allows us to populate the simulated prominence with fine structures in accordance with the observed prominences. We than compute the synthetic hydrogen H-alpha radiation emerging from this 3D structure with any given line of sight. Such synthetic filtergrams are suitable for the direct comparison with the Hinode/SOT H-alpha images.

Useful methods for coalignment calibration; from the experiences of XRT calibration

Abstract Author(s): Keiji Yoshimura, David E. McKenzie

Institution(s): Department of Physics, Montana State University, Department of Physics, Montana State University

Presentation: S7-P-03

Abstract

Coalignment is a basic and important step for any analyses using multiple observation data from different instruments. We will present a coalignment calibration for the XRT data, which successfully achieves very precise coalignment. In particular, coalignment accuracy between XRT and SDO/AIA is often better than 1". While our primary goal was to provide an easy and precise coalignment method to all users of the XRT data, some of the methods we developed for our calibration are useful not only for the XRT data but also for other missions and future projects. We will present these methods and the results from them in our calibration. For example, in the cross calibration using SDO data, we utilized the 'local correlation tracking method' to derive some coefficients required for coalignment, and found that the roll angle difference between XRT and SDO changed on a 1-year cycle. This methodology is likely to be useful for many other pairs of imaging data sets.

Empirical Corrections for the Small Light Leak in Hinode XRT

Abstract Author(s): Steven H. Saar, Edward E. DeLuca, Patrick I. McCauley, Adam R. Kobelski

Institution(s): Harvard-Smithsonian Center for Astrophysics, SAO, SAO, Montsna State Univ.

Presentation: S7-P-04

Abstract

On May 9, 2012, the the straylight level of XRT on Hinode suddenly increased, consistent with the appearance of a pinhole in the entrance filter (possibly a due to a micrometeorite strike). The effect of this event is most noticable in the optical G band data, which shows an average of ∼30% light excess. Data in several of the X-ray filters is also affected, due to low sensitivity "tails" of their filter responses at visible wavelengths. Observations taken with the G band filter but with the visible light shutter (VLS) closed show a weak, slightly shifted, blurred image, revealing the leaked light. The intensity of the leak depends on telescope pointing, dropping strongly for images taken off-disk. By monitoring light levels in the corners of full-Sun Ti-poly filter images, we determine the the event occurred at ∼13:30 UT. We use pairs of images taken just-before and after the filter breach to directly measure the leakage in two affected X-ray filters (Al-mesh and Ti-poly). We then develop a model using a scaled, shifted, and smoothed versions of the VLS closed images to remove the contamination. We estimate the uncertainties involved in our proposed correction procedure.

IRIS data products and distribution

Abstract Author(s): Neal Eugene Hurlburt, Bart De Pontieu, James Lemen, C. Jake Wolfson, Jean-Pierre Wuelser, Charles Kankelborg, Ed DeLuca, Viggo Hansteen, Mats Carlsson, Rock Bush

Institution(s): Lockheed Martin ATC, Lockheed Martin ATC, Lockheed Martin ATC, Lockheed Martin ATC, Lockheed Martin ATC, Montana State University, Smithsonian Astrophysical Observatory, University of Oslo, University of Oslo , Stanford University

Presentation: S7-P-05

Abstract

The Interface Region Imaging Spectrograph generates a complex set of data products that the IRIS team has strived to deliver to the community in forms that are easy to find and use. We review the results of these efforts and invite the community to explore the data and tools.

All standard IRIS data products are based on calibrated images that are corrected for a variety of instrumental effects. The resulting products are incorporated into the Heliophysics Event Knowledgebase (HEK) as annotated data sets accessible through the HEK Coverage Registry (HCR). Annotations include descriptions of the data products themselves (pointing, field of view, cadence...) as well as references to coordinated observations from the Hinode mission and other observatories, and to solar events identified in the HEK Event Registry (HER). IRIS data products are available at the LMSAL and Stanford (JSOC) data centers in Palo Alto and the Hinode Data Center in Oslo. Portals that can help users to select data products include the LMSAL iSolsearch, the Virtual Solar Observatory and Helioviewer. Supporting analysis software is available in the IRIS branch of SolarSoft.

Detecting chromospheric magneto-acoustic body wave near the MBPs by using Mg II h&k lines

Abstract Author(s): Yoshiaki Kato, Jorrit Leenaarts, Tiago Pereira, Mats Carlsson, Viggo Hansteen, Bart De Pontieu

Institution(s): NAOJ, ITA, Univ. of Oslo, ITA, Univ. of Oslo, ITA, Univ. of Oslo, LMSAL

Presentation: S7-P-06

Abstract

NASA's Interface Region Imaging Spectrograph (IRIS) will open a new window to explore the chromospheric/coronal waves that are potentially energize the solar atmosphere. By using an imaging spectrograph covering the Mg II h&k lines as well as a slit-jaw imager centered at Mg II k onboard IRIS, we are capable to determine the nature of propagating magneto-acoustic waves just below the transition region. In this study, we compute the vertically emergent intensity of the Mg II h&k lines from a time series of snapshots of a two-dimensional RMHD simulation of a magnetic element in the solar atmosphere, and investigate the synthetic line profiles for detecting the slow magneto-acoustic body wave (slow mode) which become the slow shock at the lower chromosphere in the magnetic element. We find that the Doppler shift of the line core represent the velocity amplitude of the longitudinal magneto-acoustic body wave. The contribution function of the line core profile indicates the formation of Mg II h&k lines is associated with the propagating shocks and therefore the time evolution of the line core intensity represents the propagating shocks projected on the optical surface. We conclude that the synergy between the imaging spectrograph and the slit-jaw imager onboard IRIS is capable to determine the energy flux of slow modes in the magnetic element. We will discuss the comparison between the upcoming IRIS data and the simulations.

Analytical solution of the Hanle effect in view of CLASP and future polarimetric solar studies

Abstract Author(s): Motoshi Goto, Ryohko Ishikawa, Roberto Casini, Saku Tsuneta

Institution(s): National Institute for Fusion Science, National Astronomical Observatory of Japan, High Altitude Observatory, ISAS/JAXA

Presentation: S7-P-07

Abstract

We have solved a problem of the Hanle effect of the hydrogen Lyman-alpha line in an intuitive and straightforward way. The Stokes parameters derived are expressed as an analytical formula which makes possible a prompt analysis of the observation data taken in the CLASP (Chromospheric Lyman-Alpha SpectroPolarimeter) project. Furthermore, since the analytical solution facilitates incorporation of the effect into any simulation model of the solar atmosphere, this result should have a general significance for future solar research projects such as SOLAR-C. Atoms in the solar atmosphere are excited by an anisotropic radiation field, which gives rise to unequal population distribution over the magnetic sublevels, the so-called atomic polarization, and the subsequent radiation emission is polarized. If there exists a magnetic field inclined from the direction normal to the solar surface at the same time, the polarization is relaxed to some extent by the Hanle effect. The CLASP project aims at determining a magnetic field vector in the chromosphere and the transition region from the polarization status of the Lyman-alpha line. A complete numerical calculation of such collective effects of the atomic polarization and the Hanle effect has been demonstrated by the group of Trujillo Bueno [J.T. Bueno et al., ApJ, 738, L11 (2011)] based on the method formulated by Degl ' Innocenti and Landolfi [Polarization in Spectral Lines, Springer, 2004]. Although the present intuitive method omits several troublesome effects such as the quantum interaction among the fine structure states and the radiative transfer, the result shows satisfactory consistency with that of the complete calculation within the expected ranges of the magnetic field strength, that ensures a validity of the analytical solution for a practical use in CLASP.

UV spectropolarimeter design for precise polarization measurement with 0.1% accuracy

Abstract Author(s): Noriyuki Narukage, Frederic Auchere, Ryoko Ishikawa, Ryouhei Kano, Saku Tsuneta, CLASP team

Institution(s): ISAS/JAXA, IAS, NAOJ, NAOJ, ISAS/JAXA

Presentation: S7-P-08

Abstract

We propose a new ultra violet (UV) spectropolarimeter design with 0.1% accuracy in polarization measurement. For this precise measurement, the spectropolarimeter should have a high throughput for a good signal-to-noise ratio observation, and should suppress the spurious polarization caused by the intensity variation of the observation target, not to mention the spurious polarization caused by the instrument itself. Our designed spectropolarimeter utilizes a concave diffraction grating as both the spectral dispersion element and the beam splitter. Each diffracted beam (-1 and +1 order) is focused by a separate off-axis parabolic mirror. A polarization analyzer on each channel, at 90-degree angle from each other, allows simultaneous observation of two orthogonal polarization states. A rotating 1/2-wave plate at the upper stream of the grating determines and modulates the polarizations seen by the two channels. The ability of simultaneous observation of two orthogonal polarization states suppresses the spurious polarization caused by the intensity variation of the observation target. In order to minimize the difference in the aberrations between two channels that causes the spurious polarization, the grating is mounted at an angle-of-incidence of zero, which makes the two channels optically symmetric. All optical components except the waveplate are the reflective type ones that can be equipped with the high reflectivity coating for the high throughput. Our designed spectropolarimeter with the high reflectivity coating make the 0.1% polarization accuracy possible. The spectropolarimeter thus designed is currently under fabrication for the sounding rocket project of Chromospheric Lyman-Alpha SpectroPolarimeter (CLASP) that aims at the direct measurement of the magnetic fields in solar atmosphere with UV line for the first time.

Polarization of the Lyman-alpha line of hydrogen in multi-thread models of quiescent solar prominences

Abstract Author(s): Jiri Stepan, Stanislav Gunar

Institution(s): Astronomical Institute ASCR

Presentation: S7-P-09

Abstract

Recent multi-thread models of quiescent solar prominences have been able to successfully reproduce many of the observed features of the Lyman lines of hydrogen. These two-dimensional radiative transfer models have implicitly taken into account the role of magnetic fields in structuring of the prominence plasma and, consequently, in formation of the spectral lines. However, the emergent intensity profiles are not directly sensitive to the action of magnetic fields. Diagnostics of magnetic fields can only be done by observation, modeling, and interpretation of the spectropolarimetric data. In this work, we include the physics of scattering polarization and the Hanle effect into the existing 2D models. We study the sensitivity of the Lyman-alpha line polarization to the thermal structure of the prominence-corona transition region (PCTR) and to the presence of magnetic fields. The forthcoming sounding rocket experiment CLASP can take advantage of observing the linear polarization of the Lyman-alpha line in a quiescent prominence and it may provide a clue for quantitative diagnostics of the PCTR magnetic fields.

The Center for Advanced Solar Spectro-Polarimetric Data Analysis (CASSDA)

Abstract Author(s): Christian Bethge, Nazaret Bello-Gonzalez, Catherine Fischer, Johannes Loehner-Boettcher

Institution(s): Kiepenheuer Institute for Solar Physics

Presentation: S7-P-10

Abstract

CASSDA is a project at the Kiepenheuer Institute for Solar Physics in Freiburg which is funded by the Leibniz Gesellschaft. We are working in close collaboration with other institutes, who all share the goal to provide the solar community with spectroscopic and spectro-polarimetric data observed at the German solar telescopes. For this purpose, data pipelines and software tools are being developed to standardize data processing and formatting and to provide quick-look inversions for physical parameters. This facilitates access to data taken with the VTT and the new GREGOR telescope and fosters the use of these observations together with data from other ground-based and space-borne observing sites. The software developed and the knowledge gained will be highly valuable for future observing sites such as the ATST, in particular for the Visible Tunable Filter (VTF) due to its similarity to the Triple Etalon Solar Spectrometer (TESOS) at the VTT. We present an overview of the project and the current status.

The Solar EUV telescopes for the Arka mission

Abstract Author(s): Sergey Bogachev, Sergey Kuzin, Andrey Pertsov, Sergey Shestov, Alexey Kirichenko, Artem Ulyanov, Anton Reva

Institution(s): P.N.Lebedev Institute of the Russia Academy of Sciences

Presentation: S7-P-11

Abstract

The Arka is a new Russian solar mission intended to take high-resolution images of the sun in the extreme ultraviolet wavelengths. The Arka experiment was approved by the Russian Space Agency (RSA) in the end of 2010 as a part of the program “Small Explorers for Fundamental Space Researches”. The satellite for the mission will be built in the Lavochkin Association (a Russian aerospace company). The Lebedev Institute of the Russian Academy of Sciences is responsible for all the scientific equipment for the experiment.

The Arka will be equipped with 2 high-resolution Ritchey Chretien telescopes designed to collect images of the sun with approximately 150 km spatial resolution in the field of view of about 10?× 10?. The scientific results of the mission may have a significant impact on the theory of coronal heating and may help to clarify the physics of small scale solar structures and phenomena including oscillations of fine coronal structures as well as the physics of micro and nanoflares.

We want to present the technical details of the mission and discuss the preliminary scientific program. The start of the mission is scheduled for the end of 2015.

LEMUR/EUVST: the spectrograph for the Solar C mission

Abstract Author(s): Luca Teriaca, George A Doschek, Louise K. Harra, Clarence Korendyke, Udo Schuehle, Toshifumi Shimizu

Institution(s): Max Planck Institute for Solar System Reserch

Presentation: S7-P-12

Abstract

Understanding the complex and extremely dynamic environment of the solar outer atmosphere requires concerted, simultaneous solar observations from the visible to the vacuum ultraviolet (VUV) and soft X-rays, at high spatial resolution (between 0.1" and 0.3"), at high temporal resolution (on the order of 10 s, i.e., the time scale of chromospheric dynamics), with a wide temperature coverage (from 5000 K to several million K in order to cover the widely disparate regimes from the solar surface through the chromosphere and transition region to the corona during events such as flares), and the capability of measuring magnetic fields through spectropolarimetry. Simultaneous spectroscopic measurements, providing information on the thermodynamic state of the plasma over the entire temperature range, are crucially important.

LEMUR/EUVST is a large VUV telescope feeding a scientific payload of high-resolution imaging spectrographs and cameras. It consists of two major components: a VUV solar telescope with a 30-cm diameter mirror and a focal length of 3.6 m, and a focal-plane package composed of VUV spectrometers covering six carefully chosen wavelength ranges between 17 nm and 127 nm. The slit covers 280" on the Sun with 0.14" per pixel sampling. LEMUR/EUVST will obtain spectra at 200 km resolution over lines formed at practically all temperatures between 10000 K and 20 MK with high spectral and temporal resolution. Thus, it has the capability of increasing enormously or understanding of coronal structures and of the physical mechanism(s) that maintain them.

Solar Hyper-spectral Imaging Polarimeter (SHIP): A Novel Instrument Concept for Near-simultaneous Polarimetric Imaging of the Solar Corona

Abstract Author(s): Dibyendu Nandi, Nirmalya Ghosh, Ayan Banerjee, B Ravindra

Institution(s): CESSI, IISER Kolkata, Center of Excellence in Space Science India (CESSI), IISER Kolkata, Center of Excellence in Space Science India (CESSI), IISER Kolkata, Indian Institute of Astrophysics

Presentation: S7-P-13

Abstract

Magnetic field dynamics in the Sun's outer atmosphere, the solar corona, constitutes the final critical stages in the chain of events that eventually leads to solar activity mediated forcing of the heliospheric environment through the generation of space weather. In the solar corona, loop dynamics heats and maintains the million degree solar corona, and rapid restructuring fed by flux emergence, magnetic instabilities and reconnection leads to coronal mass ejections. Constraining the topology and dynamics of coronal magnetic fields is therefore of fundamental importance. However, this has remained an outstanding challenge in the field of solar and space physics. While several theoretical techniques have been proposed to model coronal fields, it is not evident how accurate they are and routine observations of coronal field continue to elude us. Here we describe a novel optoelectronic instrument concept, which combining together three fundamental pillars of observational astronomy, namely, imaging, spectroscopy and polarimetry, is envisaged to perform near-simultaneous polarimetric imaging of the solar corona in the near future.

Our Gateway to the Magnetism of the Chromosphere-Corona Transition Region

Abstract Author(s): Javier Trujillo Bueno, Luca Belluzzi, Jiri Stepan

Institution(s): Instituto de Astrofisica de Canarias

Presentation: S7-P-14

Abstract

It is through spectropolarimetry that Hinode and ground-based telescopes have strongly contributed to improve our empirical knowledge on solar magnetic fields. However, the quantitative information we have is mainly restricted to the visible surface layers of the Sun (the photosphere). This is very regrettable because many of the most challenging and enduring problems in solar and stellar physics arise from magnetic processes taking place in the outer atmospheric regions (chromosphere, transition region and corona). To diagnose the physics of the outer solar atmosphere we need direct measurements of the magnetic field and this can only be achieved through remote sensing of the polarization of the spectral line radiation emitted by the solar plasma structure under investigation. The strongest allowed lines originating in the upper solar chromosphere and transition region are in the far ultraviolet (FUV) and extreme ultraviolet (EUV) regions of the solar spectrum. Spectropolarimetric measurements in such lines (e.g., Mg II h&k, H I Ly-alpha, He II Ly-alpha, etc.) can only be done from space, and they represent virgin territory. In this theoretical contribution we study the magnetic sensitivity of such resonance lines, showing also the pros and cons with respect to other spectral lines that can be observed from the ground (e.g., Ca II H&K, etc.). The results of our radiative transfer simulations in given models of the solar chromosphere are of interest for the planning of future space missions (e.g., the instrumentation of Jaxa's Solar-C telescope), and suggest that vacuum ultraviolet spectropolarimetry is a key gateway to the magnetism of the outer solar atmosphere.

Hinode-7
Session 7: Future Problems and Observations

Attempts for high spatial resolution at Hida observatory and future coordination with Hinode

Abstract Author(s): Kiyoshi Ichimoto, Yoshikazu Nakatani, Tomoko Kawate, Satoru Ueno, Masashi Yamaguchi, Masaoki Hagino, Goichi Kimura, Noriaki Miura

Institution(s): Hida observatory, Kyoto University, Kyoto University , Kyoto University , Kyoto University , Kyoto University , Kyoto University , Kitami Institute of Technology

Presentation: S7-P-15

Abstract

The Domeless Solar Telescope (DST) at Hida observatory is a vacuum tower telescope with the diameter of entrance aperture of 60cm. DST can provide dataset for the dynamic solar phenomena highly complementary to the SOT/ Hinode with a set of flexible high dispersion spectrograph and filtergraphs. Although the optical system of DST is aimed for achieving the diffraction limited angular resolution, observed images are significantly degraded due to the atmospheric seeing in nominal condition. To overcome the seeing effect, we developed a new adaptive optics system and a post-fact image processing package using the speckle masking algorithm, with which it becomes possible to attain a comparable spatial resolution with SOT with higher probability than before. We will demonstrate the high resolution imaging data obtained by DST with these new features, and discuss possible coordinated observations with Hinode.

Magnetic field and electric field of a surge with a spectropolarimetric observation in HI Paschen lines

Abstract Author(s): Tetsu Anan, Roberto Casini, Kiyoshi Ichimoto

Institution(s): Kwasan and Hida observatory

Presentation: S7-P-16

Abstract

HINODE discovered dynamical nature in chromosphere where magnetic pressure is higher than gas pressure and details of magnetic structure in photosphere where the gas pressure is higher than the magnetic one. Magnetic field structure in chromosphere is a key information to understand the heating and dynamical phenomena in the magnetic atmosphere. In order to study the magnetic field of chromospheric jets, we observed the full Stokes spectra of the Paschen series of neutral hydrogen in a surge that took place at the solar limb on May 5, 2012. For the observations, we used the spectropolarimeter of the Domeless Solar Telescope at Hida observatory, Japan. Inversion of the Stokes spectra taking into account the effect of magnetic field on the energy structure and polarization of the hydrogen levels (including the Hanle effect and level-crossing effects) elucidates the magnetic field approximately aligned with the visible structure of the surge. In addition to the magnetic field, the energy structure and the polarization of the hydrogen levels is sensitive to electric field through the Stark effect, electric Hanle effect (analogous effect with the Hanle effect by magnetic field), and the level-crossing effects. Since we found no definitive evidence of the polarization produced by the effect of electrics field, we derived upper limits of electric field felt by neutral atom moving across the magnetic field, and conclude that the velocity of the neutral atom perpendicular to the magnetic field was below the several percents of the velocity bulk plasma motion.

Development of a universal tunable filter for future space and ground observations

Abstract Author(s): Masaoki Hagino, Kiyoshi Ichimoto, Goichi Kimura, Yoshikazu Nakatani, Tomoko Kawate, Kazuya Shinoda, Yoshinori Suematsu, Hirohisa Hara, Toshifumi Shimizu

Institution(s): Kwasan Observatory, Kyoto University

Presentation: S7-P-17

Abstract

We have developed a new narrowband tunable filter to observe spectra and images of the solar chromosphere for future application to space (ex. Solar-C) and ground observations. Using Liquid Crystal Variable Retarders (LCVRs) as the tuning elements for wavelength and super achromatic half-wave plates, it is possible to make high speed tuning (about 0.1Sec), to exclude mechanical drives (and oil tank), and to cover a wide wavelength range (510-1100nm). This filter builds up with seven stages each consisting of a pair of calcites, LCVR, half wave plates and linear polarizer. The full width at half maximum (FWHM) of the filter transmission is about 0.025nm at 656.3nm. In this presentation, we will report performance and results of the first light of the filter by using the Domeless Solar Telescope at the Hida Observatory of the Kyoto University.

The magnetic and velocity field structure of the sunspot chromosphere

Abstract Author(s): Akihito Oi, Kiyoshi Ichimoto, Yukio Katsukawa, Yoshinori Suematsu

Institution(s): Kwasan and Hida Observatories, Kyoto University

Presentation: S7-P-18

Abstract

It has been known that supersonic flows toward a sunspot are common phenomena in a chromosphere above a sunspot. The flows are called an inverse Evershed flow, and have line-of-sight velocities of 10 to 20 km/s, in some cases over 50 km/s. It is necessary to obtain more knowledge on the phenomenon in terms of how magnetic field structures in the chromosphere drives the flow. In this study, we analyzed the chromospheric magnetic and velocity fields in the sunspot chromosphere utilizing precise polarimetric measurements and the Hanle effect. Recent developments of both observation technologies and theoretical modeling of the Hanle effect have allowed us to perform diagnostics of weak polarization signals in the chromosphere.

An Investigation of coronal mass ejections and EUV waves for space weather forecasting

Abstract Author(s): Shuhei Abe, Satoshi Nozawa

Institution(s): Ibaraki University, Ibaraki University

Presentation: S7-P-19

Abstract

Coronal mass ejections (CMEs) affect the terrestrial environment and technological infrastructure because they produce solar energetic particle events and geomagnetic storms. Extreme Ultraviolet (EUV) waves are large scale disturbances propagating over a significant fraction of the solar surface, so they are closely related to CMEs. Therefore, the EUV waves have the potential to the used for space weather forecasting. We examined CMEs and EUV waves using SOHO, STEREO and SDO associated with 176 major flares (M class and above) that occurred during 2010 June 12 $\sim$ 2012 June 14. We found that 75 of that 176 flares were associated with both CMEs and EUV waves, while 83 lacked both. Although we could not determine the associations of the the remaining 18 (or 10%) flares confidently, there is a clear one-to-one correspondence between CMEs and EUV waves. Since approximately half of the major flares are not associated with the CMEs, space weather alerts issued by only the flare information will be false half the time. Therefore, the EUV waves are useful tool to improve the space weather forecasting. On the other hand, the correlation between CME and EUV wave velocities is poor. The correlation is only 0.31. Therefore, the EUV wave velocities are not sufficient proxy of the CME Velocities. However, there is a possibility that the correlation may improve by including parameter that EUV wave acceleration. We will discuss how to measure the EUV waves velocities and estimate the CME velocities from the observation of flares and EUV waves.

Study of automatic observation system for compact solar telescope

Abstract Author(s): Kento Suto, Satoshi Nozawa

Institution(s): Ibaraki University, Ibaraki University

Presentation: S7-P-20

Abstract

The understanding of solar physics is indicated for astrophysics phenomena. Therefore, research of solar activity is important to observation of the sun for any measurement. Ground-based solar telescope is very useful, but the telescope cannot work when it is cloudy and night. So, consecutive observation from fixed position is very difficult and automatic observation system cannot be made sufficiently. We plan that automatic observation system set up from a number of positions. Our system is aimed for full automatic system for observation of the sun. Additionally the system automatically is taken sun image. We use the CCD camera on board the equatorial telescope. We control the equatorial telescope by astronomical simulation software and PC display. We developed software due to automatic observation system through the use of those. This system is monitor of the sun, and capture images day after day. In solar activity observations, it is important to focus on the active regions on the sun and detect sudden phenomena after all images are saved the selection the image by two pattern, sudden event or quiet sun. So, we can observation every day by this system, we allocate lightweight and low cost system at various position. We have a lot of problem, for example, this system still cannot track the sun. That is necessity option like solar tracking mode of Domeless Solar Telescope (DST) at hida. We will discuss problem of that system and outlook on that system.

Coordinated observations for High School Students as Hinode EPO Activity

Abstract Author(s): Kentaro Yaji

Institution(s): National Astronomical Observatory in Japan

Presentation: S7-P-21

Abstract

As one of education and public outreach(EPO) activities of Hinode, we have performed coordinated observations with high school students, public observatories and science museums, every year since 2010. The goals are that they have interests in Hinode data and compare their own data with Hinode data. They study Hinode data as references of their data and obtain new solar knowledge, which make their motivation higher on their activities. The students have a presentation on the observation results at a science contests. As other topic, students practice teaching materials developed with use of the coordinated data. In such way, the coordinated observations have played a important role as Hinode EPO.

In this presentation, we review the observation results especially in 2013 and assess them. Additionally, we would comment EPO towards Solar-C.

Development of the Mobile Spectrograph for Educational Observation

Abstract Author(s): Naoaki Mouri, Yuri Kato, Yumi Hibino, Kenichi Otsuji, Takashi Sakae, Akihito Oi, Kiyoshi Ichimoto, Masaoki Hagino, Reizaburou Kitai

Institution(s): Meisei University, Meisei University, Meisei University, National Astronomical Observatory of Japan, Urawanishi High School, Kyoto University, Kyoto University, Kyoto University, Kyoto University

Presentation: S7-P-22

Abstract

We built a new mobile spectrograph to be used for solar observations for educational purpose in high school. The spectrograph consists of a slit of our own composition, a grating (1200 grooves/mm, blaze angle optimized for 1micron) made by the Edmund Optics, and a 76 mm aperture refractive telescope. We obtained solar full disk spectroheliogram in He 1083 nm line on 18 August 2013 with the spectrograph. In this presentation, we will report performance and results of the first light of the spectrograph. Additionally, temperature distribution in chromosphere beneath coronal holes will be discussed by comparing our infrared spectroheliogram, H-alpha full disk images obtained by the SMART at the Hida Observatory of the Kyoto University, magnetograms taken by the SOT/Hinode and X-ray images taken by XRT/Hinode.

Participants

shuhei abe	*Ibaraki University*
Loren Acton	*Montana State University*
Kyo L. Akita	*Osaka Gakuin Univ.*
Tetsu Anan	*Kwasan and Hida observatory*
Patrick Antolin	*Centre for mathematical Plasma Astrophysics, Department of Mathematics, KU Leuven*
Inigo Arregui	*Instituto de Astrofisica de Canarias*
Ayumi Asai	*Kyoto University*
Frederic Auchere	*Institut d'Astrophysique Spatiale*
Guillaume Aulanier	*Observatoire de Paris, LESIA*
Deborah Baker	*UCL - MSSL*
Yumi Bamba	*STEL, Nagoya Univ.*
Luis Bellot Rubio	*Instituto de Astrofisica de Andalucia (CSIC)*
Arkadiusz Berlicki	*Astronomical Institute, Academy of Sciences of the Czech Republic*
Sergey A. Bogachev	*P.N.Lebedev Institute of the Russia Academy of Sciences*
Veronique Bommier	*LESIA, Observatoire de Paris*
Philippe A. Bourdin	*Max Planck Institute for Solar System Research*
David H Brooks	*George Mason University*
Allan Sacha BRUN	*AIM/CEA-Saclay*
Eric Buchlin	*Institut d'Astrophysique Spatiale, CNRS/Univ. Paris-Sud*
Paul S Cally	*Monash University*
Mats Carlsson	*Institute of Theoretical Astrophysics, University of Oslo*
Jongchul Chae	*Seoul National University*
Mark CM Cheung	*LMSAL*
Jonathan W Cirtain	*NASA*
John Leonard Culhane	*UCL Mullard Space Science Laboratory*
Sanja Danilovic	*Max Planck Institute for Solar System Research*
Jaime de la Cruz Rodriguez	*Uppsala University*
Ineke De Moortel	*University of St Andrews*
Bart De Pontieu	*LMSAL*
Edward E DeLuca	*Harvard-Smithsonian Center for Astrophysics*
Marc DeRosa	*Lockheed Martin Solar and Astrophysics Laboratory*
George A. Doschek	*Naval Research Laboratory*
Jaroslav Dudik	*RS Newton International Fellow*
Elena Dzifcakova	*Astronomical Institute Odrejov*
Frantisek Farnik	*Astronomical Institute AV CR*
Bernhard Fleck	*ESA*
Takatoshi Fukuoka	*Kyoto University*
Gabriel Giono	*NAOJ*
Thomas Peter Golding	*Institute of Theoretical Astrophysics, University of Oslo*
Boris Vilhelm Gudiksen	*Institute for theoretical astrophysics, University of Oslo*
Chloe Guennou	*Institut d'Astrophysique Spatiale*
Stanislav Gunar	*Astronomical Institute, Academy of Sci., Czech Rep.*
Yuko Hada	*Kyoto University*
Masaoki Hagino	*Kyoto University*
Michael Hahn	*Columbia University*
Iain G Hannah	*University of Glasgow*
Viggo Haraldson Hansteen	*Institute of Theoretical Astrophysics*
Juan Hao	*National Astronomical Observatories, Chinese Academy of Sciences*
Hirohisa Hara	*National Astronomical Observatory of Japan*
Louise Harra	*UCL-MSSL*
Petr Heinzel	*Astronomical Institute*
Andrew Stephen Hillier	*Kwasan Observatory, Kyoto University*
Hideyuki Hotta	*University of Tokyo*
Kiyoshi Ichimoto	*Hida observatory, Kyoto University*
Yusuke Iida	*ISAS/JAXA*
Haruhisa Iijima	*The University of Tokyo*
Shinsuke Imada	*Solar-Terretrial Environment Laboratory, Nagoya University*
Takako T Ishii	*Kwasan and Hida Obs., Kyoto-U.*

Shin-nosuke Ishikawa	*NAOJ*
Ryohko Ishikawa	*National Astronomical Observatory of Japan*
Kazumasa Iwai	*Nobeyama Solar Radio Observatory, National Astronomical Observatory of Japan*
Miho Janvier	*Lesia - Observatoire de Paris*
Vincent Joulin	*IAS*
Jan Jurcak	*Astronomical Institute AS CR*
Anjali John Kaithakkal	*SOKENDAI, NAOJ*
Takafumi Kaneko	*Department of Earth and Planetary Science, The University of Tokyo*
Ryouhei Kano	*National Astronomical Observatory of Japan*
Megumi Kasuga	*University of tokyo*
Yoshiaki Kato	*NAOJ*
Yukio Katsukawa	*National Astronomical Observatory of Japan*
Akito D. Kawamura	*Kwasan Observatory, Kyoto Univ.*
Tomoko Kawate	*Kyoto University*
Pradeep Kumar Kayshap	*Aryabhatta Research Institute of Observational Sciences (ARIES)*
Graham Stewart Kerr	*University of Glasgow*
Naomasa Kitagawa	*The Univ. of Tokyo*
Reizaburo Kitai	*Kyoto University*
Irina N. Kitiashvili	*Stanford University*
Lucia Kleint	*LMSAL / BAER Institute*
Ken Kobayashi	*UAHuntsville*
Adam Robert Kobelski	*Montana State University*
Alexander Kosovichev	*Big Bear Solar Observatory*
Masahito Kubo	*National Astronomical Observatory of Japan*
Elena Gennadievna Kupriyanova	*Central Astronomical Observatory at Pulkovo of the RAS*
Hiroki Kurokawa	*Kwasan & Hida Obseravatories, Kyoto University*
Kanya Kusano	*Solar-Terrestrial Environment Laboratory, Nagoya University*
Andreas Lagg	*Max Planck Institute for Solar System Research*
Kyoung-Sun Lee	*ISAS/JAXA*
Hwanhee Lee	*Kyung Hee University*
James R Lemen	*Lockheed Martin Solar and Astrophysics Lab*
Birgit Lemmerer	*IGAM-Kanzelhoehe Observatory Institute of Physics, University of Graz*
Ying Li	*Nanjing University*
Jun Lin	*Yunnan Astronomical Observatory*
Hsiao-Hsuan Lin	*Institute of Theoretical Astrophysics, University of Oslo*
Bruce William Lites	*HAO/NCAR*
David Long	*UCL/MSSL*
Hiroyuki Maehara	*Kiso Observatory, Institute of Astronomy, School of Science, The University of Tokyo*
rafael manso sainz	*instituto de astrofisica de canarias*
Youhei Masada	*Department of Computational Science, Kobe University*
Helen E Mason	*University of Cambridge*
Satoshi Masuda	*Solar-Terrestrial Environment Laboratory, Nagoya University*
Yuki Matsui	*Univ. of Tokyo*
Ram Ajor Maurya	*Seoul National University*
David E. McKenzie	*Montana State University*
Fusa Miyake	*Nagoya University*
Richard Morton	*Northumbria University*
Shin'ichi Nagata	*Kyoto University*
Takashi Nakabo	*STEL, Nagoya University*
Noriyuki Narukage	*ISAS/JAXA*
Lei Ni	*Yunnan Astronomical Observatory*
Keisuke Nishida	*Kyoto University*
Naoto Nishizuka	*National Astronomical Observatory of Japan*
Nariaki V. Nitta	*Lockheed Martin Advanced Technology Center*
Daisaku Nogami	*Kyoto University*
Yuta Notsu	*Kyoto University*
Shota Notsu	*Department of Astronomy, Kyoto University*
Satoshi Nozawa	*Ibaraki University*
Akihiro Ohkawa	*Ibaraki University*
Akihito Oi	*Kwasan and Hida Observatories, Kyoto University*

Joten Okamoto	*ISAS/JAXA*
Kosovare Olluri	*Institute of Theoretical Astrophysics, UiO*
Ada Ortiz-Carbonell	*Institute of Theoretical Astrophysics, University of Oslo*
Kenichi Otsuji	*National Astronomical Observatory of Japan Solar Observatory*
Etienne Pariat	*LESIA, CNRS, Observatoire de Paris*
Hyungmin Park	*Seoul National University*
Tiago M. D. Pereira	*Institute of Theoretical Astrophysics, University of Oslo*
Hardi Peter	*Hardi PETER*
Isabell Piantschitsch	*Universitatsplatz 5, 8010 Graz, Austria*
Valentin M Pillet	*National Solar Observatory*
Rui F. Pinto	*LESIA, Observatoire de Paris & AIM/SAp, CEA Saclay*
Eric R Priest	*St Andrews University*
Laurel Anne Rachmeler	*Royal Observatory of Belgium*
Bhavna Rathore	*Institute for theoritical astrophysics, Universitet i oslo*
Kathy Reeves	*Smithsonian Astrophysical Observatory*
Anton Reva	*Lebedev Physical Institute*
Luc Rouppe van der Voort	*University of Oslo*
Fatima Rubio da Costa	*Stanford University*
Steven H. Saar	*Harvard-Smithsonian Center for Astrophysics*
Taro Sakao	*ISAS/JAXA*
Nobuharu Sako	*The Graduate University for Advanced Studies (SOKENDAI)*
Takashi Sakurai	*National Astronomical Observatory of Japan*
Masafumi Sano	*Kyoto University*
Ryugo Sato	*Ibaraki university*
Sabrina L Savage	*NASA / MSFC*
Antonia Stefanova Savcheva	*Smithsonian Astrophysical Observatory*
Daniel Wolf Savin	*Columbia University*
Shinpei Sawada	*Ibaraki University*
Goran B. Scharmer	*Institute for Solar Physics of Stockholm University*
Carolus J Schrijver	*Lockheed Martin Advanced Technology Center*
Sergiy Shelyag	*Monash Centre for Astrophysics, Monash University, Australia*
Yuandeng Shen	*Kwasan Observatory*
Kazunari Shibata	*Kwasan and Hida Observatories, Kyoto University*
Takuya Shibayama	*Kyoto University*
Toshifumi Shimizu	*ISAS/JAXA*
Daikou Shiota	*Solar-Terrestrial Environment Laboratory, Nagoya University*
Daishi Shukuya	*STEL, Nagoya University*
Hakon Skogsrud	*Institute of Theoretical Astrophysics, University of Oslo*
Yoshiaki Sofue	*U. Tokyo & Meisei U.*
Oskar U. Steiner	*Kiepenheuer-Institut*
Jiri Stepan	*Astronomical Institute ASCR*
David Orozco Suarez	*Instituto de Astrofisica de Canarias*
Takenori Suda	*Kyoto University*
Yoshinori Suematsu	*National Astronomical Observatory of Japan*
Kento Suto	*Ibaraki University*
Takeru Ken Suzuki	*Department of Physics, Nagoya University*
Takuya Takahashi	*Kyoto University*
Shinsuke Takasao	*Kyoto University*
Yuki Tanaka	*Kyoto University*
Theodore D Tarbell	*LMSAL*
akiko tei	*Department Of Astronomy, Kyoto University*
Luca Teriaca	*Max Planck Institute for Solar System Reserch*
Paola Testa	*Harvard-Smithsonian Center for Astrophysics*
Stefan Thonhofer	*Instituto de Astrofisica de Andalucia and University of Graz*
Alan M Title	*LMSAL*
Sanjiv Kumar Tiwari	*Max-Planck Institute for Solar System Research*
Shin Toriumi	*Department of Earth and Planetary Science, University of Tokyo*
Javier Trujillo Bueno	*Instituto de Astrofisica de Canarias*
Bruce Tadashi Tsurutani	*space plasma research institute*
Satoru UeNo	*Kyoto University*

Dominik Utz	*IGAM/Institute of Physics, Karl Franzens University Graz*
Michiel van Noort	*Max Planck Institute for solar system research*
Tijmen van Wettum	*Max Planck Institute for Solar System Research*
V. K. Verma	*Uttarakhand State Application Center*
Gregal Vissers	*Institute of Theoretical Astrophysics, Oslo*
Shuoyang Wang	*University of Tokyo*
Hiroko Watanabe	*Kyoto University*
Kyoko Watanabe	*ISAS/JAXA*
Tetsuya Watanabe	*National Astronomical Observatory, Japan*
Mark Weber	*Smithsonian Astrophysical Observatory*
Sven Wedemeyer	*University of Oslo*
Brian Thomas Welsch	*Space Sciences Laboratory, University of California, Berkeley*
David R. Williams	*UCL Mullard Space Science Laboratory*
Amy R Winebarger	*NASA MSFC*
Jean-Pierre Wuelser	*Lockheed Martin Solar & Astrophysics Lab*
Kentaro Yaji	*National Astronomical Observatory in Japan*
Masashi Yamaguchi	*Kyoto University*
Takaaki Yokoyama	*The University of Tokyo*
Keiji Yoshimura	*Department of Physics, Montana State University*
Peter R. Young	*George Mason University*
Hsiu-Shan Yu	*Center for Astrophysis and Space Sciences, University of California, San Diego*
P. C. Yuen	*Mullard Space Science Laboratory*
Vasyl Yurchyshyn	*NJIT/Big Bear Solar Observatory*